To the Graduate Council:

I am submitting herewith a thesis written by Joe M. Keeton entitled "Multivariable Control of a Binary Distillation Column." I have examined the final copy of this thesis for form and content and recommend that it be accepted in partial fulfillment of the requirements for the degree of Master of Science, with a major in Chemical Engineering.

Charles F. Moore, Major Professor

We have read this thesis
and recommend its acceptance:

Duane D Bruns

Accepted for the Council:

Vice Chancellor
Graduate Studies and Research

MULTIVARIABLE CONTROL OF A BINARY DISTILLATION COLUMN

A Thesis

Presented for the

Master of Science

Degree

The University of Tennessee, Knoxville

Joe M. Keeton

December 1981

ABSTRACT

This work compares the performance of several multivariable control strategies on the control of a simple binary distillation column. The study is based on a detailed nonlinear simulation of a 20 tray n-octane/n-pentane column.

An extensive analysis of the column was conducted to find its steady-state gains and to fit more sophisticated models (first order lag, second order lag) to it. The distillate and bottoms compositions were controlled by manipulating the distillate flowrate and the steam rate to the reboiler. A relative gain analysis was done to determine the best way to pair controller loops in a non-decoupled scheme. A v-canonical decoupler and the different types of p-canonical decouplers were added and any improvement in response noted. Various degrees of decoupler element sophistication (steady-state, lead-lag, etc) were also examined. New-variable techniques were investigated, and steady-state singular value decomposition was used in a more advanced control scheme. Finally, the results were discussed and compared to highlight the advantages and disadvantages of each control method.

TABLE OF CONTENTS

LIST OF TABLES

LIST OF FIGURES

FIGURE PAGE

FIGURE PAGE

FIGURE PAGE

LIST OF SYMBOLS

A	Process gain matrix
c	Controlled variable
G	Process transfer function matrix
G(s)	Laplace transfer function relating process input to output
$G_{ij}(s)$	Transfer function relating jth input to ith output
H	Decoupler matrix
K	Steady-state gain
m	Manipulated variable
R	Set point
s	Laplace variable
S	Separation factor
U,V	Unitary matricies
x_B	Bottoms composition
x_D	Distillate composition
ζ	Damping ratio
θ	Dead time
λ	Relative gain
Σ	Matrix of singular values
τ	Time constant
ω	Undamped natural frequency

CHAPTER I

INTRODUCTION AND BACKGROUND

This work investigates and compares various multivariable control strategies applied to a binary distillation column.

Distillation is an important unit operation in the process industries and is one which classically exhibits a strong interaction between the top and bottom product composition control loops. In most cases a conventional single input single output approach cannot be implemented which will satisfactorily control both ends of the column. Commonly the approach is to select one end to control and let the other end float with changing process conditions. It is becoming more and more apparent that such simple practices are energy inefficient. It has been shown (15) that a minimum of energy is consumed by a distillation column when both distillate and bottoms compositions are controlled to their set points. The classical control of only one product has been preferred to the more complicated dual composition control stragegies while energy has been relatively inexpensive. With the increasing cost of energy, however, and the estimate that distillation consumes 40% of the energy used in a chemical plant (16) it becomes advantageous to spend more money on a sophisticated control scheme.

The multivariable studies presented in this work are based on a nonlinear simulation of a 20 tray column with a feed consisting

of 50% n-octane and 50% n-pentane. This system was chosen because it is simple yet exhibits the interaction problems typical of more complex industrial systems. Also, column response data were available (35) on which to base the dynamic modeling. A schematic diagram of the column, with some available valves and sensors, is shown in Figure 1.

The work presented in this thesis is based on two parts: modeling the system and using these models in various control schemes.

Modeling

Work done in 1963 by Moczeck, Otto, and Williams (18) on a large, high purity column indicates that fitting the responses to a second order lag plus dead time model would prove very favorable. For various different operating conditions most data could be fit using a one or two time constant transfer function plus dead time. Latour (13) obtained essentially the same conclusion as that of Moczeck, Otto, and Williams when he showed that a transfer function of the form

$$G(s) = \frac{Ke^{-\theta s}}{(1+\tau_1 s)(1+\tau_2 s)} \qquad \text{Eq. 1}$$

was generally adequate to describe a variety of chemical engineering processes, including distillation. In 1969 Koppel and Aiken (12) suggested a somewhat different transfer function form for general processes -- the sum of n first order lags with a common dead time.

$$G(s) = e^{-\theta s} \sum_{i=1}^{n} \frac{K_i}{(1+\tau_i s)} \qquad \text{Eq. 2}$$

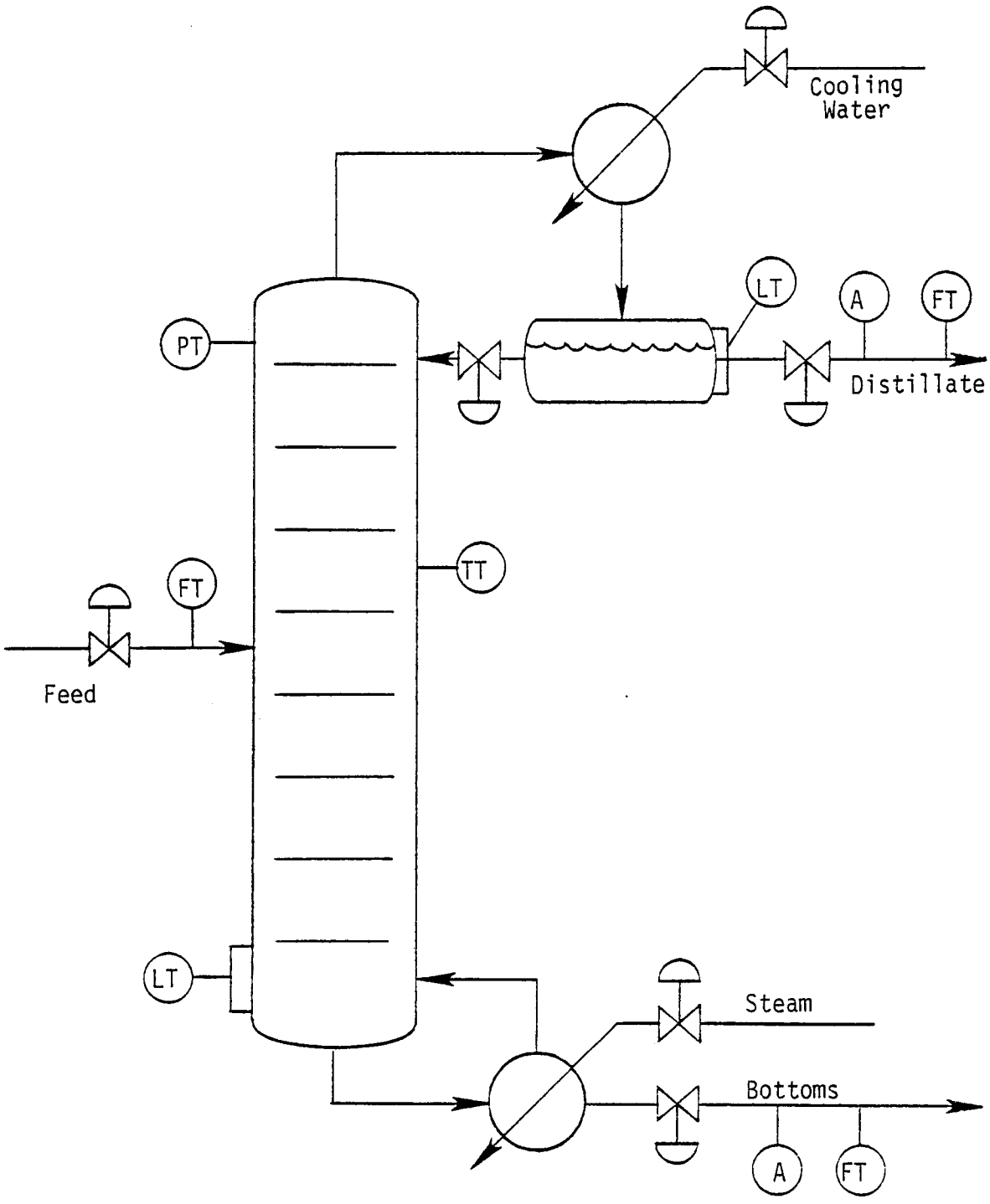

FIGURE 1. SCHEMATIC COLUMN SIMULATION.

Each of these modeling schemes, plus an under-damped second order lag of the form

$$G(s) = \frac{Ke^{-\theta s}}{1 + 2\zeta s/\omega + s^2/\omega^2} \qquad \text{Eq. 3}$$

were used in this study.

Control Methods

The second part of the work involved actual control of the column. The existing literature on distillation column control is based essentially on three schemes: p-canonical decoupling, v-canonical decoupling, and a non-decoupled scheme.

The simplest method in terms of implementation is the non-decoupled scheme. This involves only the pairing of controller loops. The idea of allowing the interaction, and not compensating for it with a decoupler, was proposed by Mesarovic (17) and later discussed in depth by Finkelstein (4). Niederlinski (19) considers two systems: what he calls an interacting (non-decoupled) and a non-interacting scheme (decoupled). He derives the disturbance transfer functions for each and calculates the deviation ratio, defined as the deviation with control divided by the deviation without control. He concludes that for the kind of interaction common to distillation columns, the non-decoupled scheme should result in superior disturbance attenuation. He then uses an example from Rosenbrock (25) to illustrate his point by tuning the PI controllers using the Zeigler-Nichols method, but does not go further in terms of tuning parameter optimization.

The decision having been made to use a non-decoupled scheme, the question then becomes how to pair the loops. The distillate composition can in theory be controlled by any of the following: the distillate flowrate, the reflux rate, the bottoms flowrate, or the steam rate to the reboiler. The same is true for control of the bottoms composition.

For a 2x2 system, either m_1 or m_2 can be manipulated to control c_1 and the other can be manipulated to control c_2. This is demonstrated in Figures 2 and 3.

To aid in the pairing decision, Bristol (1) developed the relative gain array. Not only can the relative gains tell which input variables to manipulate to control which output variables, but it can also give some indication of the degree of success the pairing is likely to have. A general 2x2 block diagram is shown in Figure 4. Shinskey (27) demonstrated the relative gain array derivation for a 2x2 system. The array consists of the relative gains, λ_{ij}, defined by

$$\lambda_{ij} = \frac{(\partial c_i/\partial m_j)_m}{(\partial c_i/\partial m_j)_c} \qquad \text{Eq. 4}$$

where c_i is the ith controlled variable and m_j is the jth manipulated variable. The subscripts m and c indicate holding all other manipulated and controlled variables constant, respectively. It is easy enough to do step tests holding all other manipulated variables constant. It is a much greater problem to do a step test holding all other <u>controlled</u> variables constant. To get around

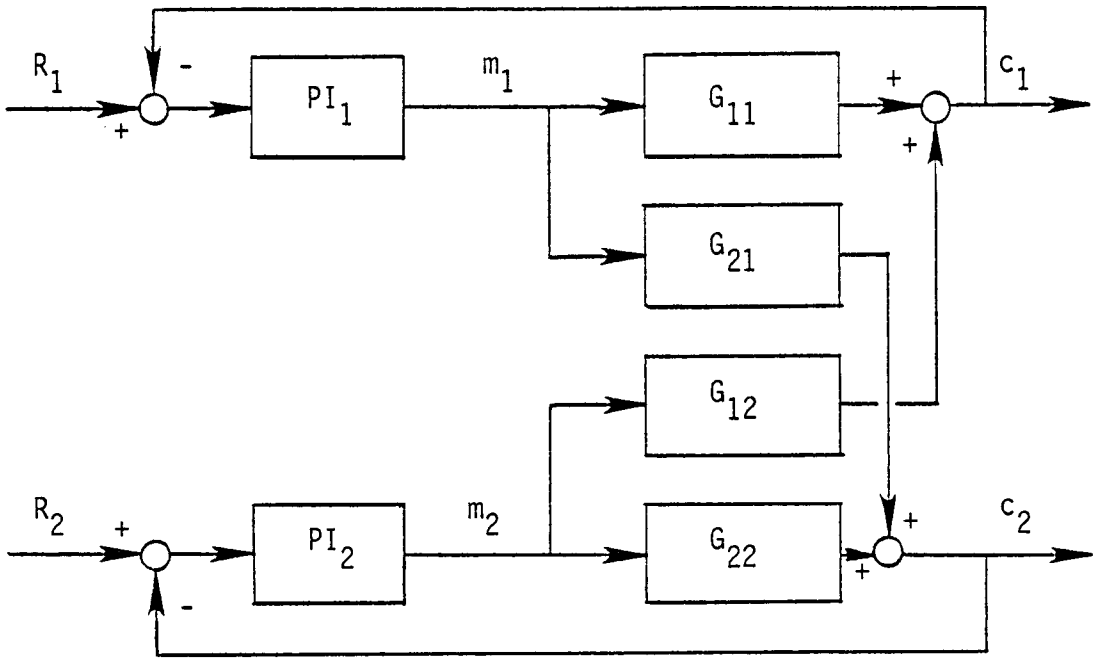

FIGURE 2. FORWARD CONTROLLER LOOP PAIRING.

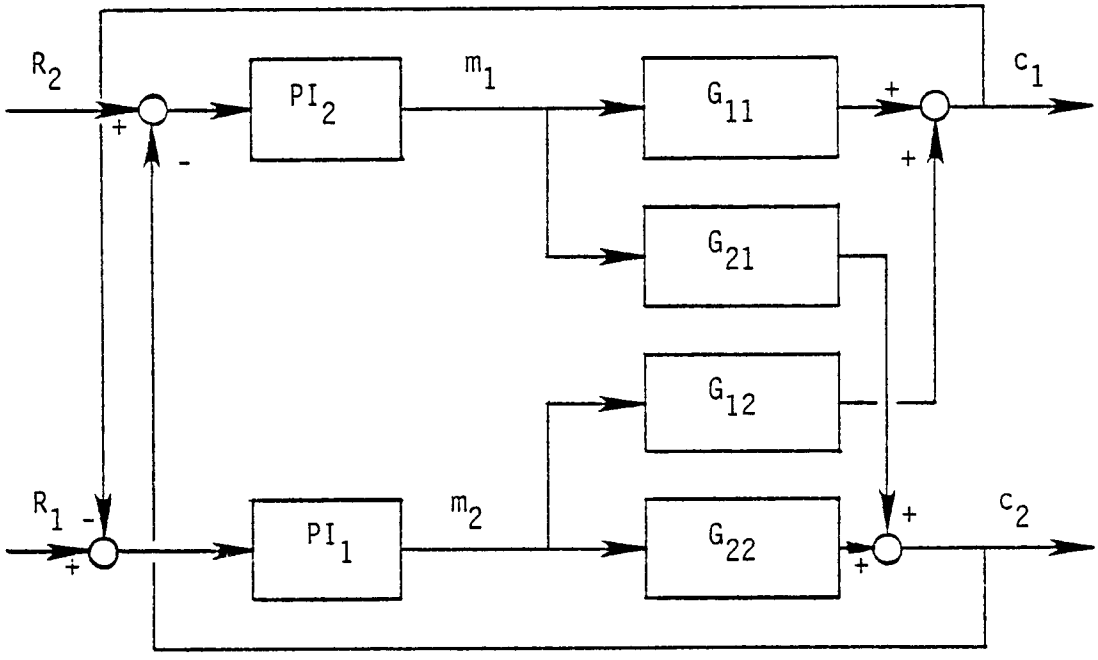

FIGURE 3. REVERSE CONTROLLER LOOP PAIRING.

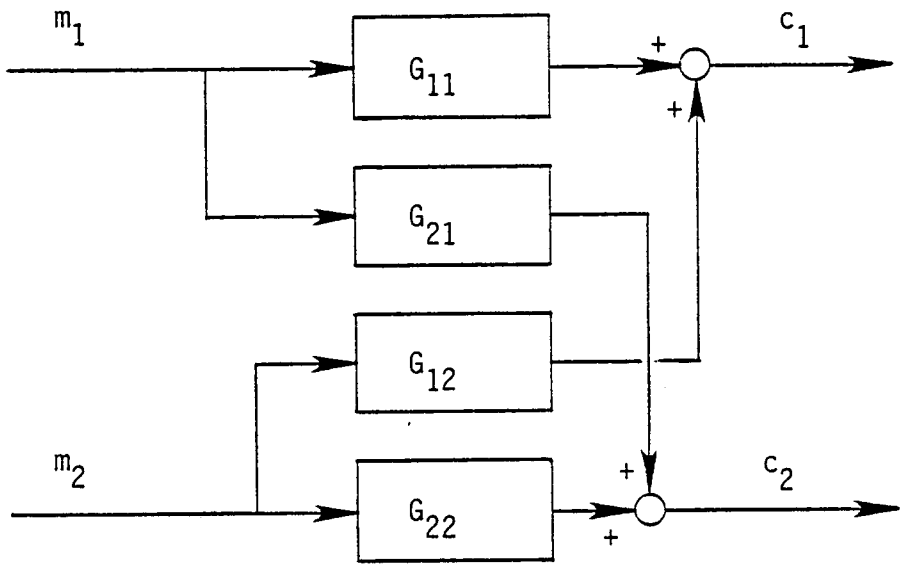

FIGURE 4. GENERAL 2X2 MULTIVARIABLE PROCESS.

this difficulty, Shinskey suggests determining the p-canonical representation of the system, which would be done by performing step tests and fitting the constants in equations 5 and 6.

$$c_1 = K_{11}\, m_1 + K_{12}\, m_2 \qquad \text{Eq. 5}$$

$$c_2 = K_{21}\, m_1 + K_{22}\, m_2 \qquad \text{Eq. 6}$$

The numerator of the relative gain is then given by

$$\left.\frac{\partial c_1}{\partial m_1}\right|_{m_2} = K_{11} \qquad \text{Eq. 7}$$

and the denominator is found by substituting for m_2 in equation 5 to yield

$$c_1 = K_{11}\, m_1 + K_{12}\, \frac{c_2 - K_{21}\, m_1}{K_{22}} \qquad \text{Eq. 8}$$

from which

$$\left.\frac{\partial c_1}{\partial m_1}\right|_{c_2} = K_{11} - \frac{K_{12}\, K_{21}}{K_{22}} \qquad \text{Eq. 9}$$

The relative gain is then given by:

$$\lambda_{11} = \frac{1}{1 - K_{12}\, K_{21}/K_{11}\, K_{22}} \qquad \text{Eq. 10}$$

One of the interesting and useful properties of the relative gain array is that the elements of the rows and columns sum to 1.0. In a 2x2 system, once λ_{11} has been found, the rest of the array is

predetermined by

$$\lambda_{22} = \lambda_{11} \qquad \text{Eq. 11}$$

and

$$\lambda_{12} = \lambda_{21} = 1 - \lambda_{11} \qquad \text{Eq. 12}$$

Once the array has been calculated, the variables should be paired to give the largest absolute values on the diagonal. How close the off-diagonal elements are (in absolute value) to the diagonal elements is a measure of the degree of interaction and thus a measure of the success a method is likely to have.

Another method of system analysis is the singluar value decomposition presented by Klema and Laub (11) and applied to azeotropic distillation columns by Downs and Moore (3). The SVD involves decomposing the gain matrix, A, into three matrices

$$A = U\Sigma V^T \qquad \text{Eq. 13}$$

where U and V are both unitary matrices, and Σ is a diagonal matrix containing the singular values, σ_i. The ratio of $\sigma_{max}/\sigma_{min}$ is the condition number, a measure of the difficulty of controlling the multivariable process. U and V are both orthonormal matrices which measure the degree of interaction and can be interpreted using a coordinate rotation.

The most prevalent non-interacting multivariable control method is p-canonical decoupling (2, 5, 6, 8, 10, 14, 27, 33, 35).

The first work done in this area was by Freeman (5, 6) and Kavanagh (8, 9) who, working independently, published papers outlining synthesis procedures using matrix notation and p-canonical models. Waller (33) gives a fairly general discussion of the types of matrix decouplers discussed here. In the p-canonical scheme the process matrix, G, is multiplied by a decoupling matrix, H, to achieve a system which looks to the individual control loops like a diagonal (non-interacting or decoupled) process. Figure 5 is a general block diagram representation of this system. The resulting diagonal matrix, D, is given by the equation:

$$G\,H = D \qquad \text{Eq. 14}$$

The only restriction on D is that the off-diagonal elements be zero. At least three different methods have been proposed to choose diagonal elements. Zalkind (36) suggests forcing the diagonal elements to 1 so that the effective matrix is

$$G\,H = D = \begin{bmatrix} 1 & 0 \\ 0 & 1 \end{bmatrix} \qquad \text{Eq. 15}$$

For reference purposes this approach will be called "perfect decoupling". If the modeled process contains lag elements then some of the elements of H will contain pure leads which are physically impossible to implement. Therefore, this scheme can be used if the process model, G, is steady-state only. Zalkind makes the comment: "The non-interacting controller network usually carries too much load, leaving the conventional controllers with nothing to do".

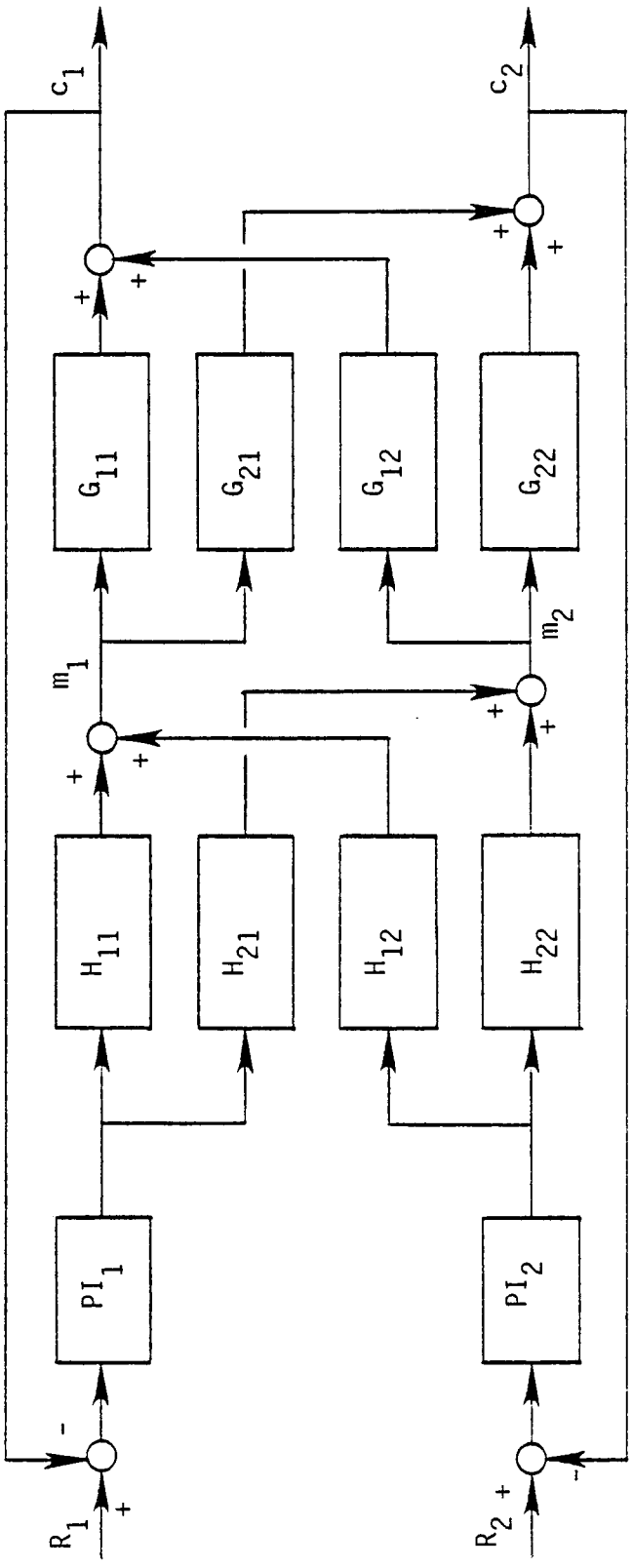

FIGURE 5. P-CANONICAL DECOUPLER WITH CONTROLLERS.

Luyben (14) introduces the term "ideal decoupling" to describe the result if the diagonal elements of D are set to their corresponding elements in G, so that the effective matrix is:

$$G\,H = D = \begin{bmatrix} G_{11} & 0 \\ 0 & G_{22} \end{bmatrix} \qquad \text{Eq. 16}$$

Waller comments that this leads to rather complicated expressions for the elements of H which may at times be impossible to implement. In general, H is given by:

$$H = \frac{1}{G_{11}\,G_{22} - G_{12}\,G_{21}} \begin{bmatrix} G_{22}\,D_{11} & -G_{12}\,D_{22} \\ -G_{21}\,D_{11} & G_{11}\,D_{22} \end{bmatrix} \qquad \text{Eq. 17}$$

For the ideal decoupling case, D_{11} would be set to G_{11} and D_{22} would be set to G_{22}.

A more logical choice would be to set some of the elements in H (Waller, Zalkind, Luyben). Luyben introduces the term "simplified decoupling" to describe the resulting system if the diagonal elements of H are set to 1. The system is then completely specified as:

$$G\,H = \begin{bmatrix} G_{11} & G_{12} \\ G_{21} & G_{22} \end{bmatrix} \begin{bmatrix} 1 & -\frac{G_{12}}{G_{11}} \\ -\frac{G_{21}}{G_{22}} & 1 \end{bmatrix}$$

$$= \begin{bmatrix} G_{11} - \frac{G_{12}\,G_{21}}{G_{22}} & 0 \\ 0 & G_{22} - \frac{G_{12}\,G_{21}}{G_{11}} \end{bmatrix} \qquad \text{Eq. 18}$$

Luyben (14) and Waller (33) point out that the decoupling elements are easier to implement than in the first two schemes. Toijala and Fagervik (32) indicate another advantage of this method is that the decoupling elements, $-G_{12}/G_{11}$ and G_{21}/G_{22} are relatively independent of frequency for continuous distillation systems.

Waller points out that any two elements of H can be set to unity, so long as they are not in the same column. Thus, if dead time considerations make one of the elements of H in equation 18 impossible to implement, any of equations 19, 20, or 21 could be used.

$$H = \begin{bmatrix} 1 & 1 \\ \frac{-G_{21}}{G_{22}} & \frac{-G_{11}}{G_{12}} \end{bmatrix} \qquad \text{Eq. 19}$$

$$H = \begin{bmatrix} \frac{-G_{22}}{G_{21}} & \frac{-G_{12}}{G_{11}} \\ 1 & 1 \end{bmatrix} \qquad \text{Eq. 20}$$

$$H = \begin{bmatrix} \frac{-G_{22}}{G_{21}} & 1 \\ 1 & \frac{-G_{11}}{G_{12}} \end{bmatrix} \qquad \text{Eq. 21}$$

Shinskey (27) points out that there are two problems with the p-canonical decoupling scheme: initialization and constrained operation. Ideally, initialization of the two decoupler outputs to begin automatic control should occur without "bumping" the system. In reality, however, the initial values are not known.

Automatic control must begin and an error be detected. The error must then be compensated for through controller action. The second problem, constrained operation, is more serious. If one of the manipulated variables is constrained at some value, both output variables cannot be controlled. Using the matrix decoupling stragety the controller will attempt to maintain both variables at their setpoints by manipulating the unconstrained variable. Since this is impossible, the variable will eventually become saturated. Shinskey suggests that these problems can be avoided by utilizing the v-canonical decoupler shown in Figure 6. In this system the two decoupling terms have the effect of canceling the interaction terms of the process matrix. The main problem with the v-canonical decoupling scheme is the presence of the feedback loop formed by the two decouplers. The gain of this loop is the product of the two decoupler gains. If the process matrix, G, has an odd number of negative signs, the loop gain will be negative; if it has an even number, the loop gain will be positive, and therefore unstable.

If instabilities do exist due to feedback problems, a solution would be to eliminate one of the decoupling elements, leaving a partially decoupled system (Figure 7). The problem then arising would be which loop to decouple. The choice might be made on the basis of several considerations. One might be, which controlled variable is most important? In distillation, one of either the distillate or the bottoms is usually more important to maintain than the other. In that case the more important loop would be decoupled from the less important. Another consideration might be the

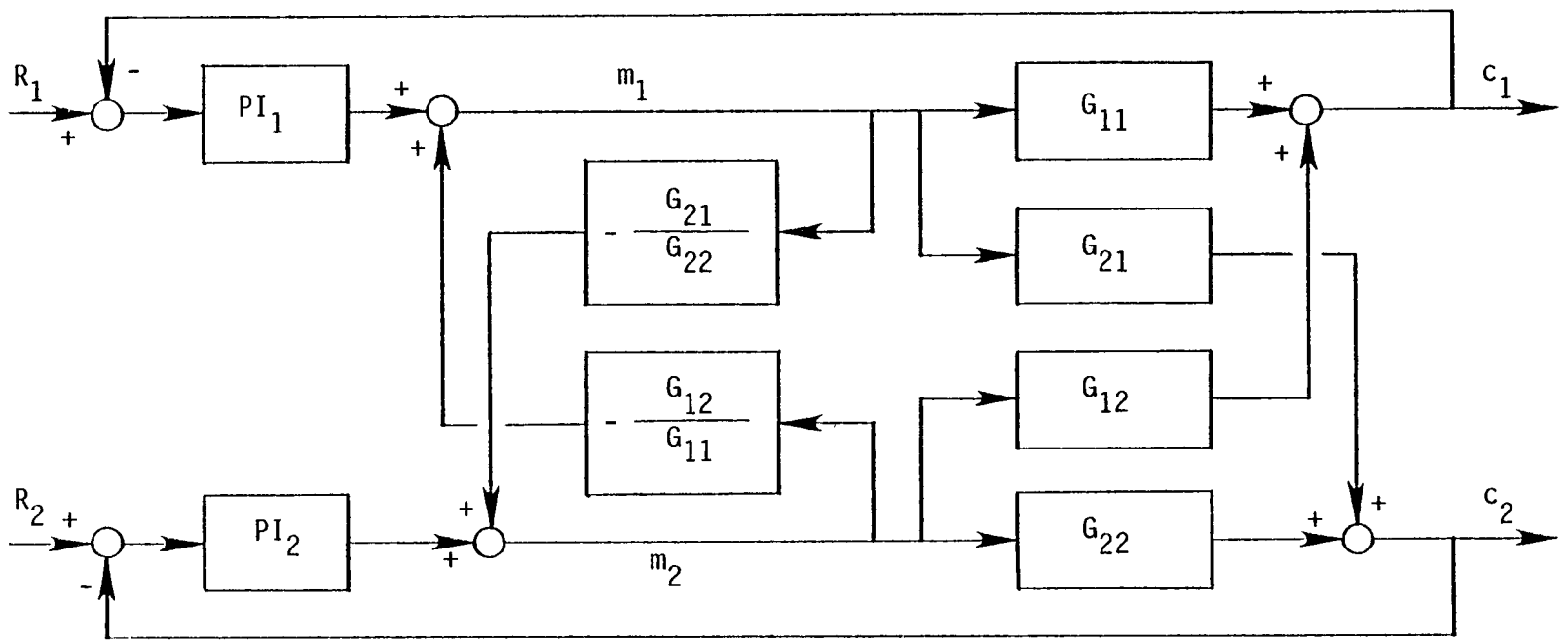

FIGURE 6. V-CANONICAL DECOUPLER WITH CONTROLLERS.

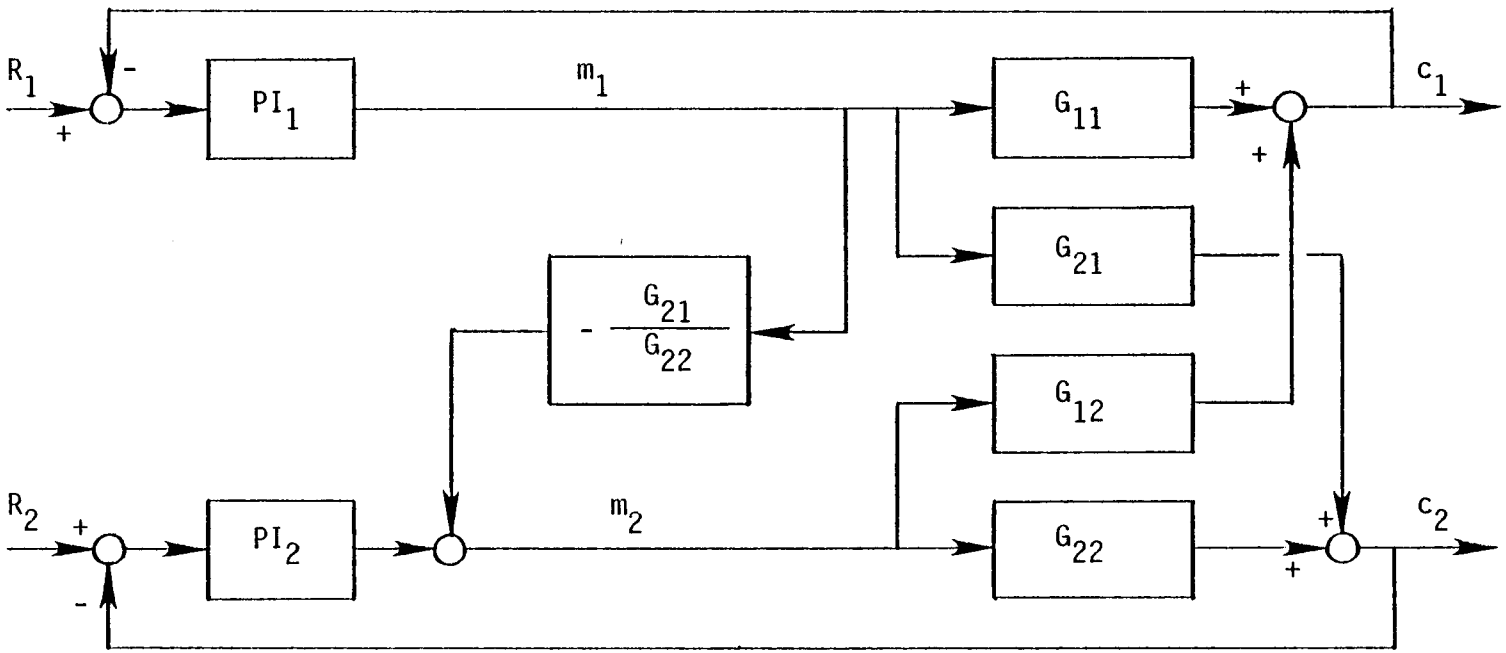

FIGURE 7. PARTIAL DECOUPLER WITH CONTROLLERS.

relative speed of response of the system. If one loop is quick-responding, it will not likely be affected by changes in the slow-responding loop, whereas the slow loop might be disturbed by changes in the other.

Another general method of dual composition control does not seek to decouple the system, but rather to define and control or manipulate new variables which do not interact. An example is the method proposed by Ryskamp (26), who suggests controlling the bottoms composition by manipulating the steam rate to the reboiler and controlling the distillate composition by manipulating, not the distillate flowrate, but the ratio of the distillate flowrate to the vapor rate up the column (almost a direct function of the steam rate to the reboiler). Ryskamp reports the successful implementation of this strategy on a range of towers.

Another example of these new variable techniques is a method proposed by Waltz (34), who suggests controlling the separation factor, S, rather than the bottoms composition. The separation factor is determined by equation 22.

$$S = \frac{x_D}{(1-x_D)} \quad \frac{(1-x_B)}{x_B} \qquad \text{Eq. 22}$$

in which x_D is the distillate composition and x_B is the bottoms composition. It has been suggested that S depends only upon the steam rate to the reboiler and is not significantly affected by changes in distillate flowrate. From equation 22 it is obvious that if both x_D and S are effectively controlled, then the bottoms composition will also be controlled.

McAvoy (16) did a relative gain array analysis on these two strategies. He concluded that Ryskamp's scheme is most appropriate for towers separating components with high relative volatilities into asymmetric product splits (for example, 99.9% pure distillate, but only 80% pure bottoms). He also found that Waltz's scheme worked well for most towers and was superior to Ryskamp's for towers separating components with low relative volatilities. Among other considerations, McAvoy points out that with Ryskamp's method, either of the two loops can be placed in manual without affecting the other loop. Controlling the separation factor, on the other hand, makes no sense if the distillate composition is not controlled. Thus the separation factor control loop can be put in manual without affecting the distillate composition loop. If the distillate composition control loop is put in manual, however, control of both compositions will be lost.

A more advanced control scheme (Klema, 11, Smith, 29,.30) utilizes the singular value decomposition for multivariable control. This method employs the principle that the process gain matrix, G, can be broken down (decomposed) into three matricies, the first and third being unitary, and the second being diagonal.

$$G = U\Sigma V^T \qquad \text{Eq. 23}$$

A useful property of unitary matricies is that their inverse is found by simply transposing them. Thus, if the process inputs are multiplied by $[U]^{-1} = U^T$ and the outputs by $[V^T]^{-1} = V$, the newly created inputs and outputs (called "structured variables" by Smith)

will be decoupled (see Figure 8). Two controllers could be put on the system at this point, but they would be manipulating and controlling the structured variables, not the real process variables. Also the set points would be in terms of the structured variables and operators would not readily be able to convert from the desired process set points to the required structured set points. If, through block diagram manipulation, the V matrix is brought around such that it operates on the error signals rather than the process outputs (Figure 9), the set points can then be in terms of real process variables.

Most of the previous decoupling elements were simple enough that full process transfer functions, including dynamics, could be used in the calculations. Finding the singular value decomposition involves finding the eigenvalues and eigenvectors of the process matrix such that, at this time, only the process gains can be included. As a result, the two loops are only independent in the steady state, and some interaction can be expected during the transient response.

Another advanced control method involves state variable feedback. This concept has been discussed by several authors, including Gilbert (7), Ogata (20), Pierini (22), Rekasius (24), and Slivinsky and Schultz (28). Work done by Rich, Law, and Weaver (23) demonstrated the application of state space theory to a one stage phase separator. Further work by Kleinpeter and Weaver (10) provided groundwork for

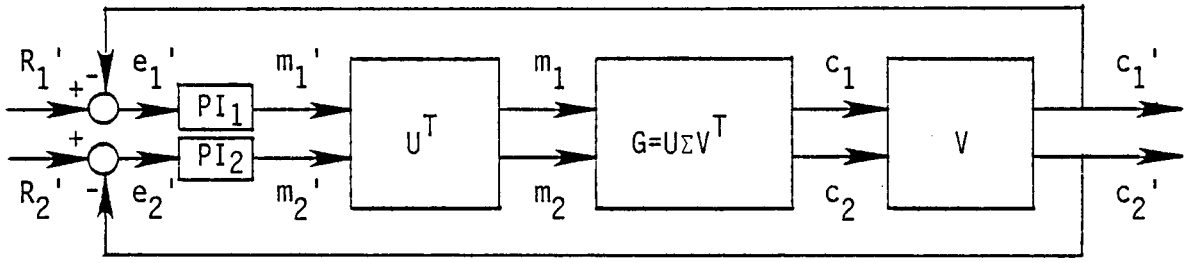

FIGURE 8. SVD CONTROLLER BEFORE BLOCK DIAGRAM MANIPULATION.

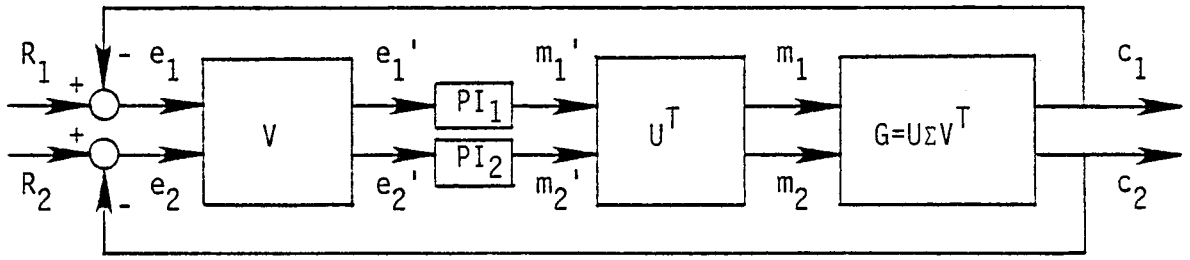

FIGURE 9. SVD CONTROLLER AFTER BLOCK DIAGRAM MANIPULATION.

applying feedforward and dynamic state variable decoupling to the separator. State variable feedback was not used in the present work, however.

Column Simulation

The column simulation used was a detailed non-linear version of a linear model reported by Weischedel and McAvoy (35). The column separates a 50% mixture of n-octane and n-pentane, which has a relative volatility of 2.17. 200 pounds of feed per hour is distilled in a 20 tray column, with feed on the tenth tray, into a distillate stream containing 95% n-pentane and a bottoms stream containing 5% n-pentane. The column specifications are shown in Table 1. Details of the linear model derivation are given in the paper by Weischedel and McAvoy. The nonlinear version consists of a separate steady-state model and dynamic model. The steady-state model is a nonlinear tray by tray calculation which assumes equimolar overflow and constant relative volatility. The dynamic model was empirically fit using data published by McAvoy and is driven by the steady-state model. A listing of the computer simulation and a more detailed discussion is presented in Appendix A.

TABLE 1

COLUMN SPECIFICATIONS

Diameter = 1.8 ft
Weir Height = 2.0 in
Weir Length = 1.26 ft
Tray Area = 2.32 ft^2
Pressure Drop per Plate = 0.0085 atm
Pressure at Reboiler = 1.0 atm
Reboiler Holdup = 10 times average tray holdup
Condenser Holdup = 10 times average tray holdup

CHAPTER II

PROCEDURE AND THEORETICAL DEVELOPMENTS

The general procedure, detailed more fully later in the chapter, was:

(1) The column was modeled using transfer functions with several levels of sophistication. Two or three models were picked that seemed to most represent the real system. These were later used in system analysis and to calculate decoupling elements.

(2) The best controller pairing was predicted, then controllers were added in a non-decoupled scheme.

(3) Several types of p-canonical decouplers were applied, including perfect decoupling, ideal decoupling, and simplified decoupling.

(4) A v-canonical decoupler was implemented, and then each of the decoupling elements was removed to give a partial decoupling scheme.

(5) Two new-variable schemes (Ryskamp's and Wlatz's) were employed.

(6) A singular value decomposition controller was used.

In order to compare these systems a single scenario was chosen. It was assumed that the column was initially operating at steady-state and a sudden change in feed composition disturbed the column operation.

The initial and final steady-state operation of the column is presented in Table 2.

TABLE 2

STEADY-STATE COLUMN OPERATION

	Initial	Final	
		no control	control
Feed Rate (lb/hr)	200	200	200
Feed Composition	0.50	0.55	0.55
Distillate Rate (lb/hr)	100	100	111.4
Distillate Composition	0.95	0.9718	0.95
Steam Rate (lb/hr)	258.28	258.28	265.68
Bottoms Composition	0.05	0.1282	0.05

For all control systems it was assumed that the first level column control was as shown in Figure 10. The various multivariable strategies were then connected to the column to manipulate the distillate flow and reboiler steam flow as shown in Figure 11.

For purposes of comparison of the various strategies a simple sum of the absolute error in both the top and bottom composition was computed for each run as in equation 24.

$$E = \Delta T \sum_{i=1}^{n} \left[|x_D - \hat{x}_D| + |x_B - \hat{x}_B| \right] \qquad \text{Eq. 24}$$

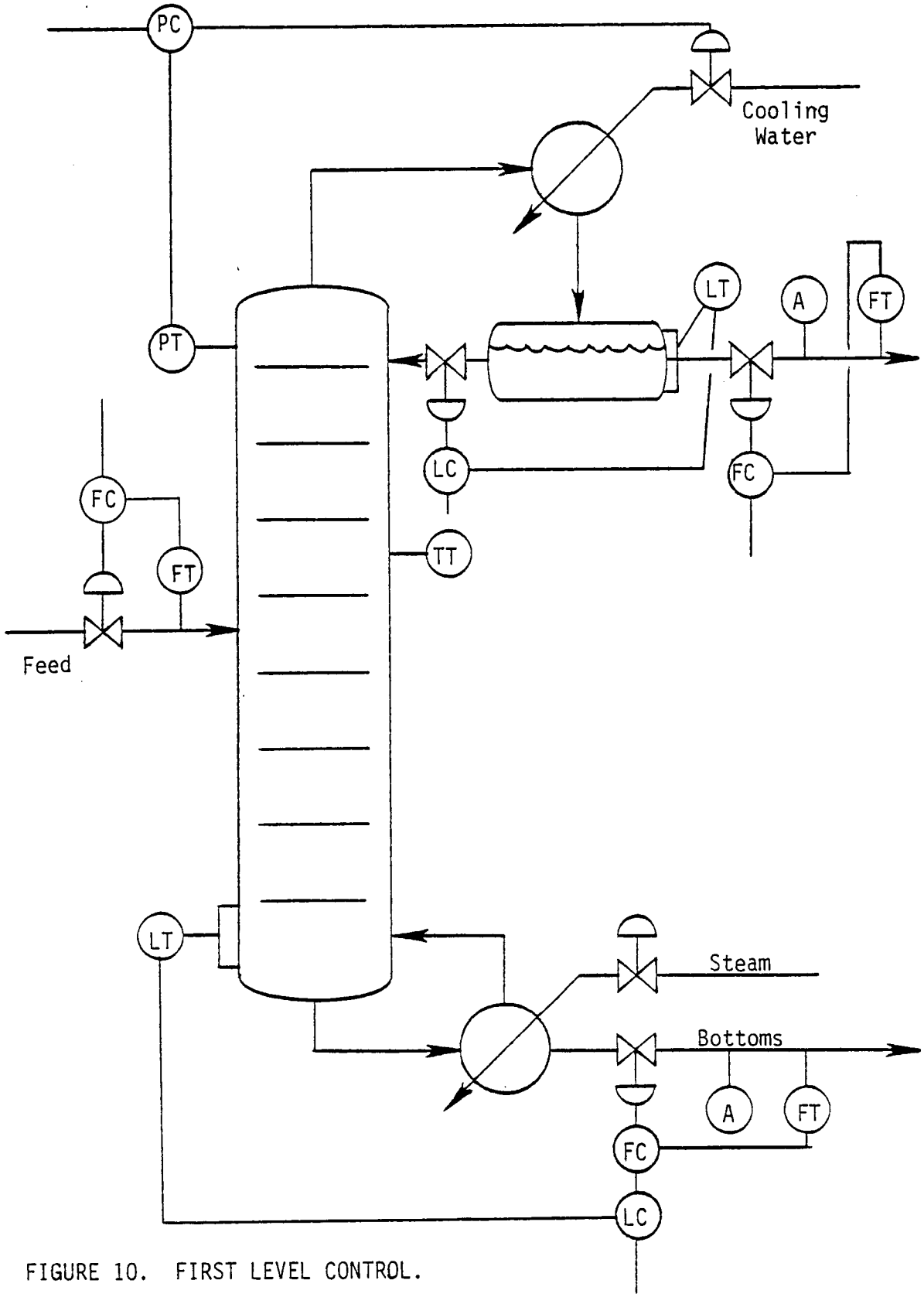

FIGURE 10. FIRST LEVEL CONTROL.

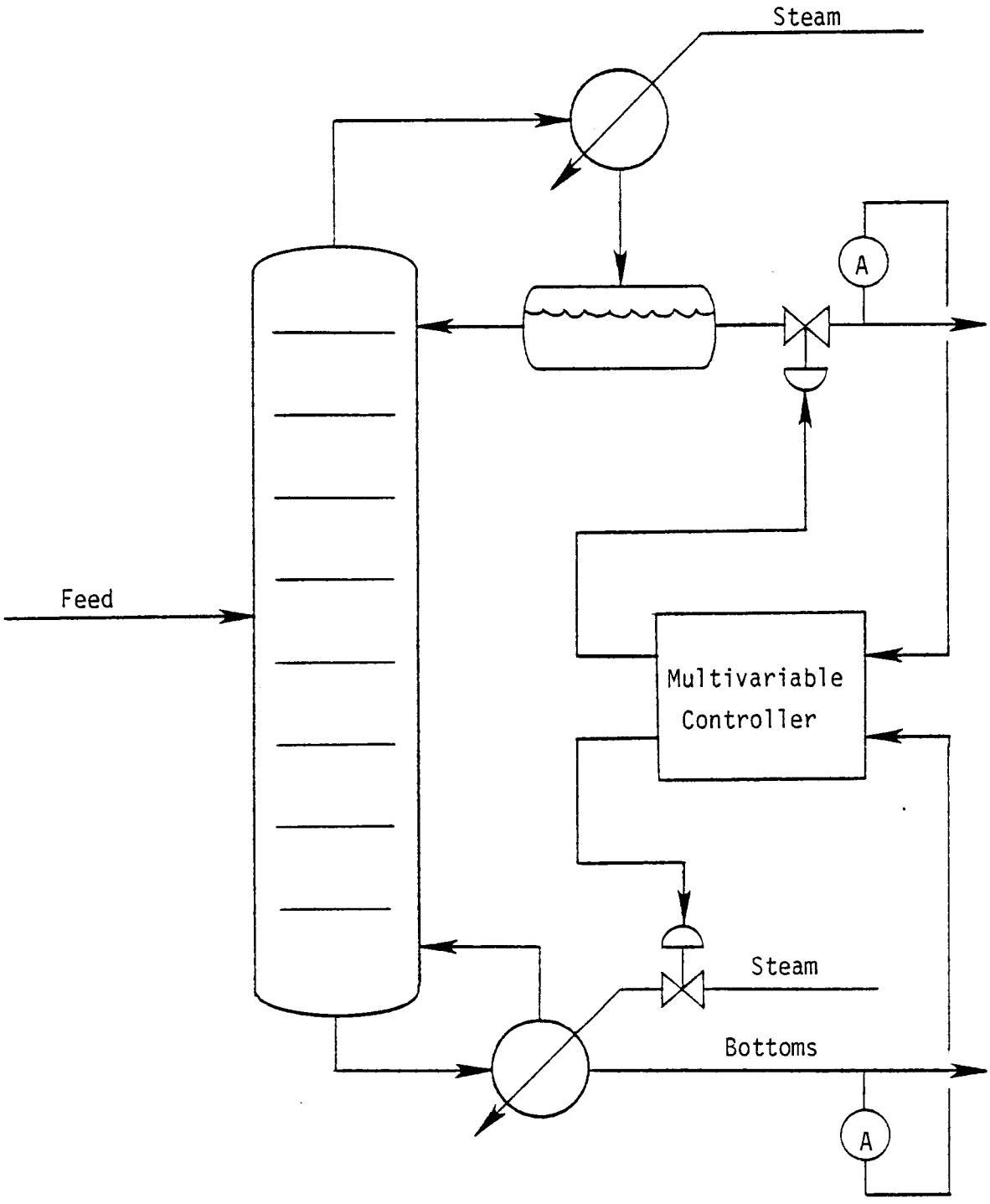

FIGURE 11. TOP LEVEL CONTROL.

where E = performance error

x_D = distillate composition

$\hat{x}_D$ = desired distillate composition

x_B = bottoms composition

$\hat{x}_B$ = desired bottoms composition

ΔT = integration time for the simulation (=0.1 min.)

n = iterations of the simulation (=2000)

Modeling

All the various multivariable strategies investigated are based on having linear dynamic models of the multivariable system. These were obtained in this study in much the same way they would be obtained in an actual process. Step tests were made on the simulation for both the steam rate and distillate rate and the dynamic responses in top and bottom composition were collected and analyzed to determine models of varying complexity.

Steady-State Models

The first, and simplest, model to fit to the data is steady-state. This simply uses the beginning and final values of the system to approximate its response. These experimental results are shown in Table 3.

Results from Table 3 were used to find:

$$\frac{\Delta x_D}{\Delta D} = -0.0054537 \qquad \frac{\Delta x_D}{\Delta G} = 0.00091622$$

$$\frac{\Delta x_B}{\Delta D} = -0.0033343 \qquad \frac{\Delta x_B}{\Delta G} = -0.00091622$$

TABLE 3

STEADY-STATE MODELING OF COLUMN

	Distillate Rate (lb/hr)	Steam Rate (lb/hr)	Distillate Composition (Weight Fraction)	Bottoms Composition (Weight Fraction)
Initial Value	100	258.28	0.9499973	0.05000274
First Run	110	258.28	0.8954603	0.01665959
Second Run	100	268.28	0.9591595	0.04084054
Change to First Run	+10	0	-0.054537	-0.03334315
Change to Second Run	0	+10	+0.0091622	-0.0091622

where D and G are the distillate and steam flowrates, respectively. It is interesting to note that $\Delta x_D/\Delta G$ is equal and of opposite sign from $\Delta x_B/\Delta G$. This is intuitively obvious from mass balance considerations. If the steam rate was the only thing changed (i.e. the distillate and bottoms rate both remain at 100 pounds per hour) and the feed composition is 0.5, then there had to be 100 pounds of n-octane per hour coming out in the steady state.

The steady-state approximations are shown alongside the real column responses in Figure 13.

First Order Lag Models

One step beyond modeling the system in the steady state was the use of first order lag models. The Laplace transfer function for a general first order lag looks like equation 25.

$$G(s) = \frac{K}{1+\tau s} \qquad \text{Eq. 25}$$

where K is the gain and τ the time constant. For a unit step input, the time response would look like equation 26.

$$x(t) = K(1 - e^{-t/\tau}) \qquad \text{Eq. 26}$$

Note that convenient use of Laplace transformations requires the initial value of the output to be zero, thus deviation variables had to be used. Equation 26 was fit to the real column data using a Pattern search routine (18). PATERN is a subroutine which finds the values of the parameters (in this case K and τ) which minimizes the COST (in this case the difference between the model response and

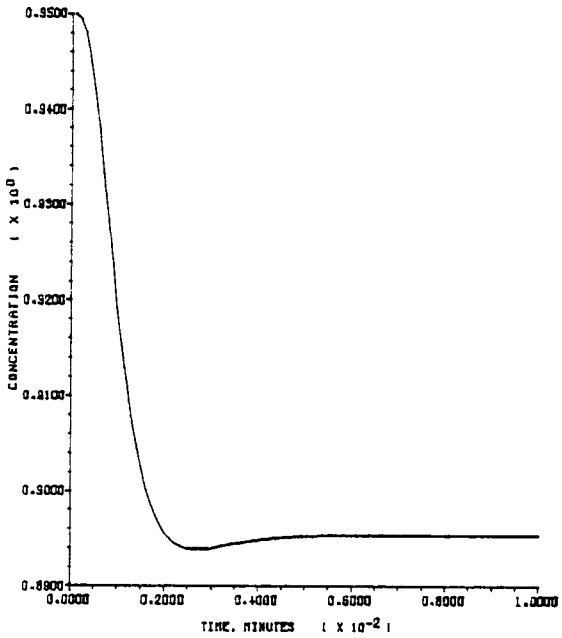

(a) Change in Distillate Composition With a Step Increase in Distillate Flow.

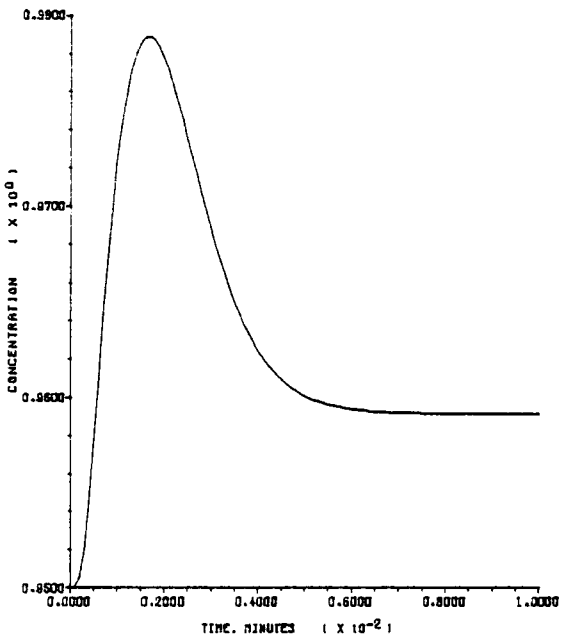

(b) Change in Distillate Composition With a Step Increase in Steam Flow.

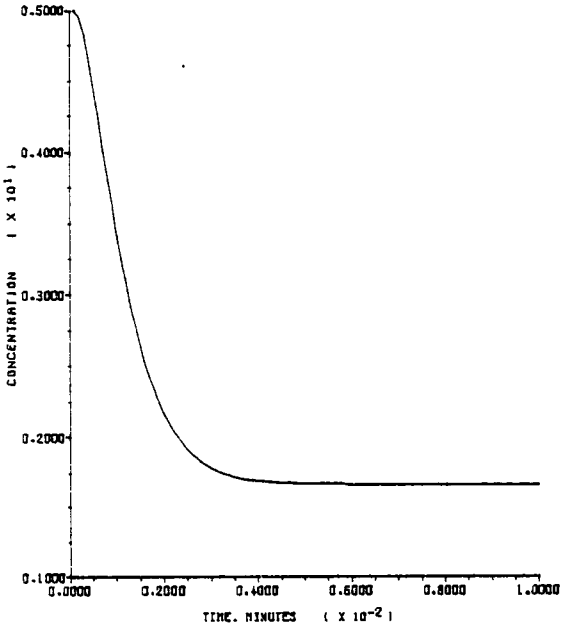

(c) Change in Bottoms Composition With a Step Increase in Distillate Flow.

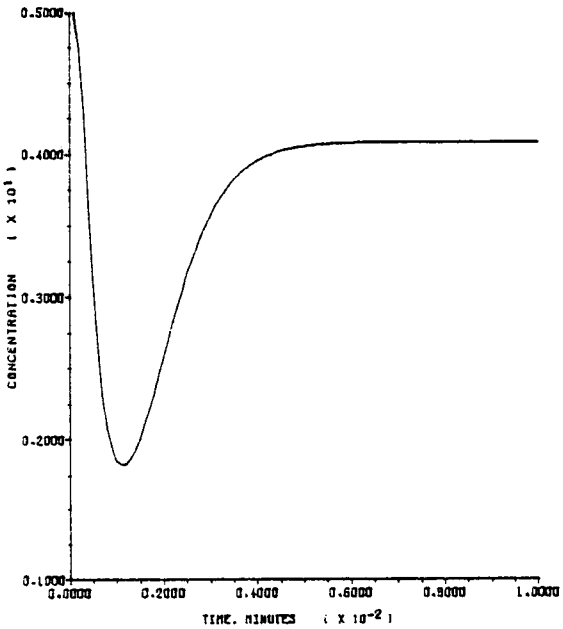

(d) Change in Bottoms Composition With a Step Increase in Steam Flow.

FIGURE 12. OPEN LOOP RESPONSES OF THE COLUMN.

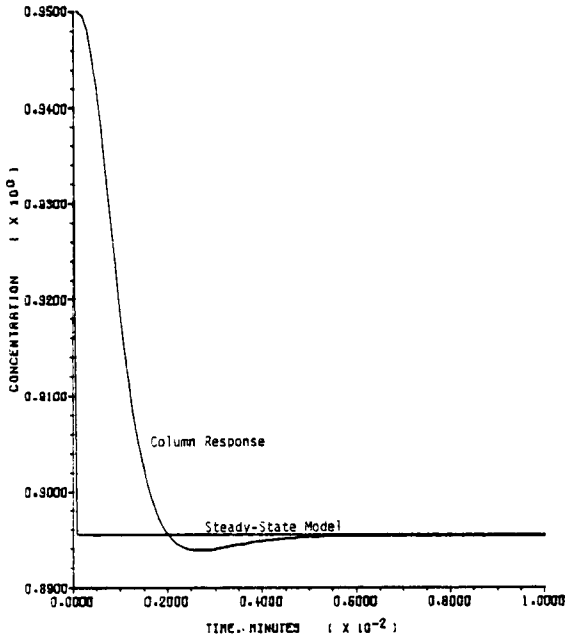

(a) Change in Distillate Composition With a Step Increase in Distillate Flow.

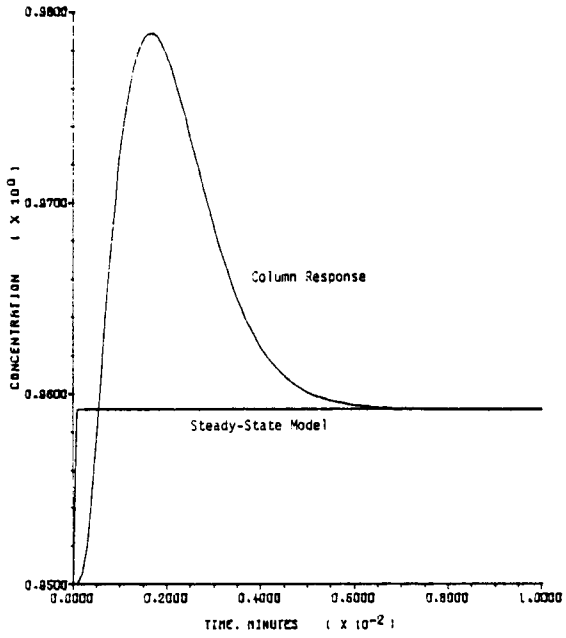

(b) Change in Distillate Composition With a Step Increase in Steam Flow.

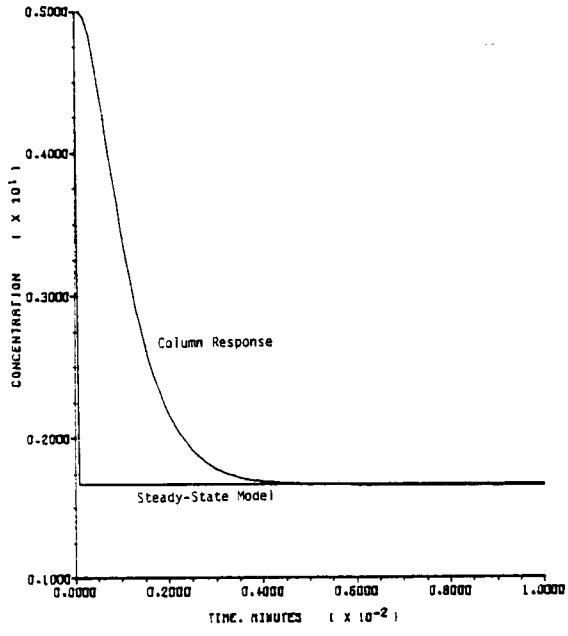

(c) Change in Bottoms Composition With a Step Increase in Distillate Flow.

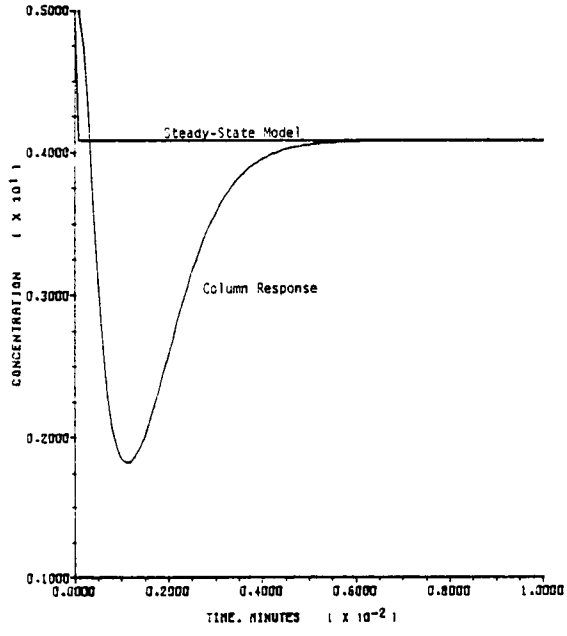

(d) Change in Bottoms Composition With a Step Increase in Steam Flow.

FIGURE 13. OPEN LOOP RESPONSES WITH STEADY-STATE MODELS.

the real column response). The results of the first order lag fit are given.

Response of x_D to D: $G_{11}(s) = \frac{-0.005454}{1+8.038s}$ Eq. 27

Response of x_D to G: $G_{12}(s) = \frac{0.000917}{1+2.96s}$ Eq. 28

Response of x_B to D: $G_{21}(s) = \frac{-0.003335}{1+11.07s}$ Eq. 29

Response of x_B to G: $G_{22}(s) = \frac{-0.000916}{1+1.82s}$ Eq. 30

The first order lag approximations are shown alongside the real column responses in Figure 14.

First Order Lag Plus Dead Time Models

One parameter which might be beneficial to add to the first order lag model would be dead time. Dead time would modify equation 25 to look like

$$G(s) = \frac{Ke^{-\theta s}}{1+\tau s} \qquad \text{Eq. 31}$$

where θ is the dead time. For a step input, the time response of a first order lag plus dead time model is described by equation 32.

$$x(t) = K[1-e^{-(t-\theta)/\tau}] \qquad \text{Eq. 32}$$

Again, a Pattern search routine was used to fit the parameters, and the results are given.

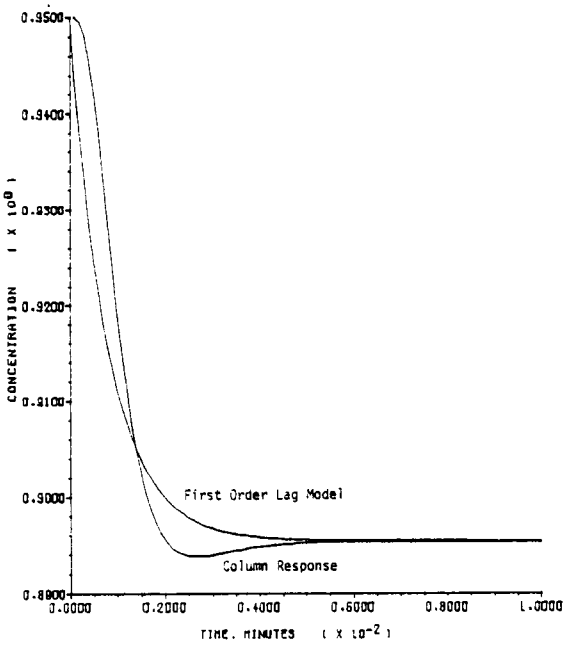

(a) Change in Distillate Composition With a Step Increase in Distillate Flow.

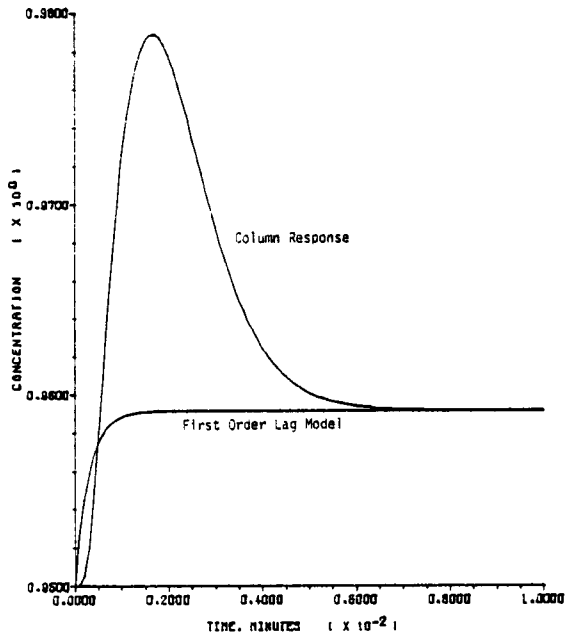

(b) Change in Distillate Composition With a Step Increase in Steam Flow.

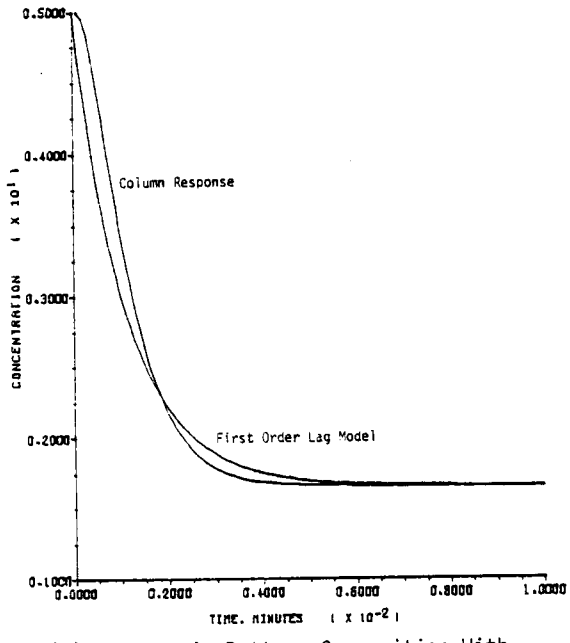

(c) Change in Bottoms Composition With a Step Increase in Distillate Flow.

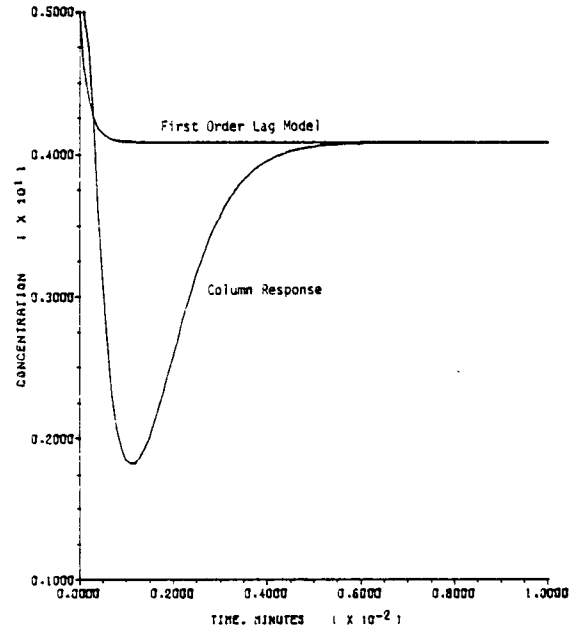

(d) Change in Bottoms Composition With a Step Increase in Steam Flow.

FIGURE 14. OPEN LOOP COLUMN RESPONSES WITH FIRST ORDER LAG MODELS.

Response of x_D to D: $G_{11}(s) = \frac{-0.005454\ e^{-5s}}{1+5.14s}$

Response of x_D to G: $G_{12}(s) = \frac{0.000917\ e^{-2s}}{1+1.96s}$

Response of x_B to D: $G_{21}(s) = \frac{-0.003334\ e^{-5s}}{1+7.92s}$

Response of x_B to G: $G_{22}(s) = \frac{-0.000916\ e^{-0s}}{1+1.82s}$

The first order lag plus dead time approximations are shown alongside the real column responses in Figure 15. By comparing Figures 14 and 15 it can be seen that little was gained in terms of model accuracy by adding dead time.

Over-Damped Second Order Lag Models

A step beyond modeling the column with first order lags was the use of over-damped second order lags. The Laplace transfer function for a general over-damped second order lag would look like equation 33.

$$G(s) = \frac{K}{(1+\tau_1 s)(1+\tau_2 s)} \qquad \text{Eq. 33}$$

For a step input, the time response of an over-damped second order lag depends upon the relation between τ_1 and τ_2.

$$x(t) = K\left[1 + \frac{\tau_1 e^{-t/\tau_1} - \tau_2 e^{-t/\tau_2}}{\tau_2 - \tau_1}\right] \quad \text{if } \tau_2 \neq \tau_1 \qquad \text{Eq. 34}$$

$$x(t) = K\left[1 - (1+t/\tau)e^{-t/\tau}\right] \quad \text{if } \tau_2 = \tau_1 \qquad \text{Eq. 35}$$

The Pattern search routine was used to fit the parameters, and the results are given.

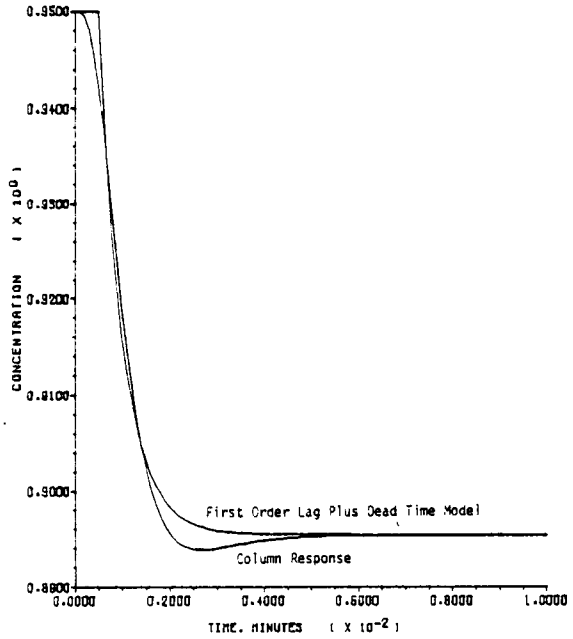

(a) Change in Distillate Composition With a Step Increase in Distillate Flow.

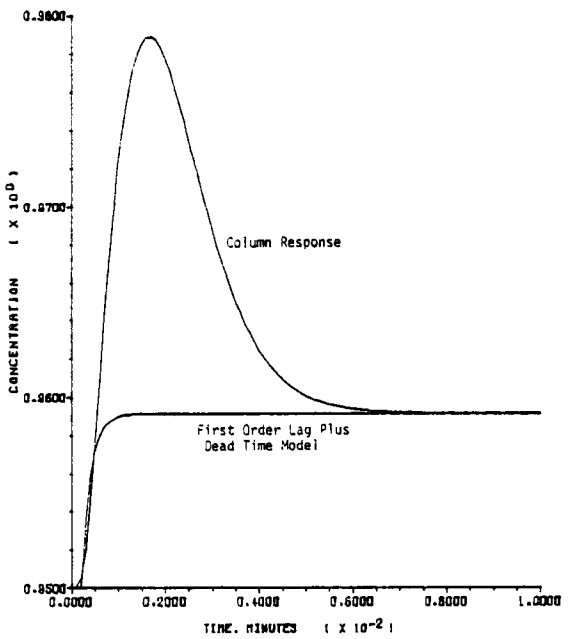

(b) Change in Distillate Composition With a Step Increase in Steam Flow.

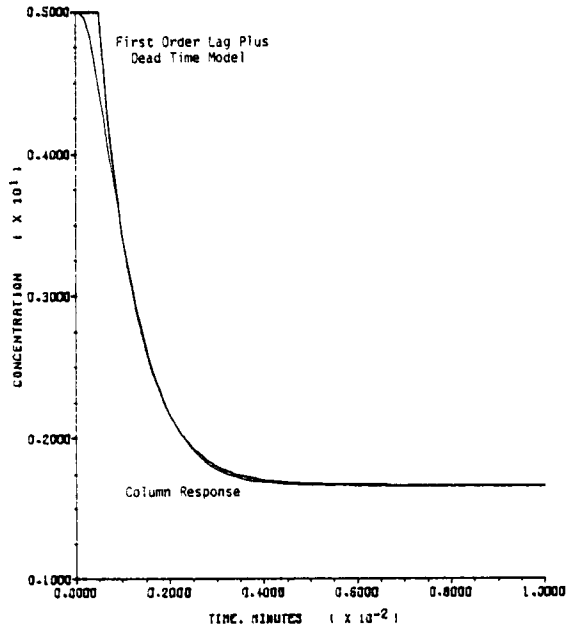

(c) Change in Bottoms Composition With a Step Increase in Distillate Flow.

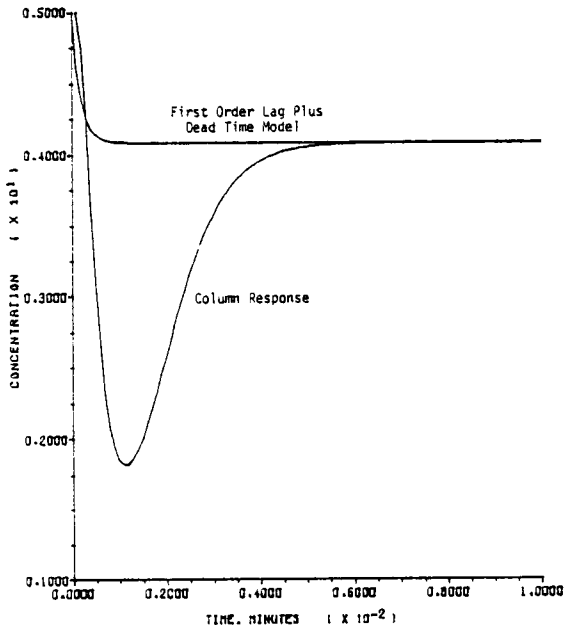

(d) Change in Bottoms Composition With a Step Increase in Steam Flow.

FIGURE 15. OPEN LOOP COLUMN RESPONSES WITH FIRST ORDER LAG PLUS DEAD TIME MODELS.

Response of x_D to D: $$G_{11}(s) = \frac{-0.005454}{(1+4.67s)(1+4.68s)}$$

Response of x_D to G: $$G_{12}(s) = \frac{0.000917}{(1+1.69s)(1+1.68s)}$$

Response of x_B to D: $$G_{21}(s) = \frac{-0.003334}{(1+6.05s)(1+6.07s)}$$

Response of x_B to G: $$G_{22}(s) = \frac{-0.000916}{(1+1.00s)^2}$$

The over-damped second order lag approximations are shown alongside the real column responses in Figure 16. By comparing Figures 14 and 16 it can be seen that the improvement of the over-damped second order lag model over the first order lag model was very slight.

Over-Damped Second Order Lag Plus Dead Time Models

Adding dead time to the over-damped second order lag models would not be likely to improve the model fits greatly, and by examining Figure 17, this can be seen to be the case. Figure 17 shows the over-damped second order lag plus dead time approximations alongside the real column responses. The best-fit approximations are:

Response of x_D to D: $$G_{11}(s) = \frac{-0.005455\ e^{6s}}{(1+0.03s)(1+4.17s)}$$

Response of x_D to G: $$G_{12}(s) = \frac{0.000917\ e^{-2s}}{(1+0.69s)(1+1.0s)}$$

Response of x_B to D: $$G_{21}(s) = \frac{-0.003334\ e^{-2s}}{(1+7.04s)(1+3.55s)}$$

Response of x_B to G: $$G_{22}(s) = \frac{-0.000916\ e^{-0s}}{(1+0.986s)(1+0.984s)}$$

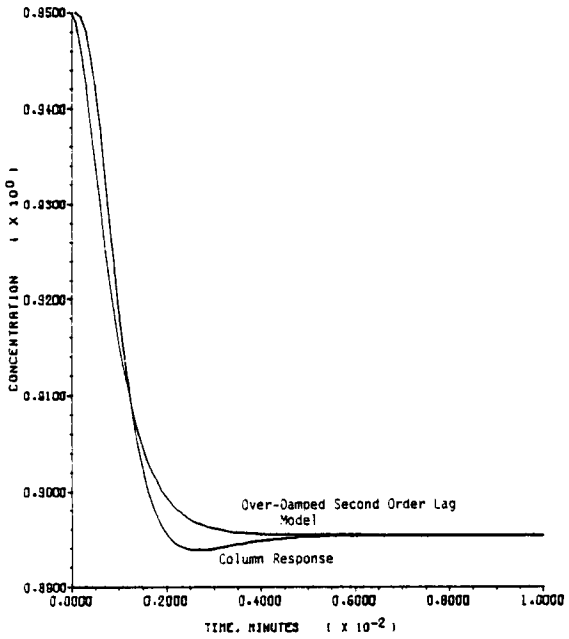

(a) Change in Distillate Composition With a Step Increase in Distillate Flow.

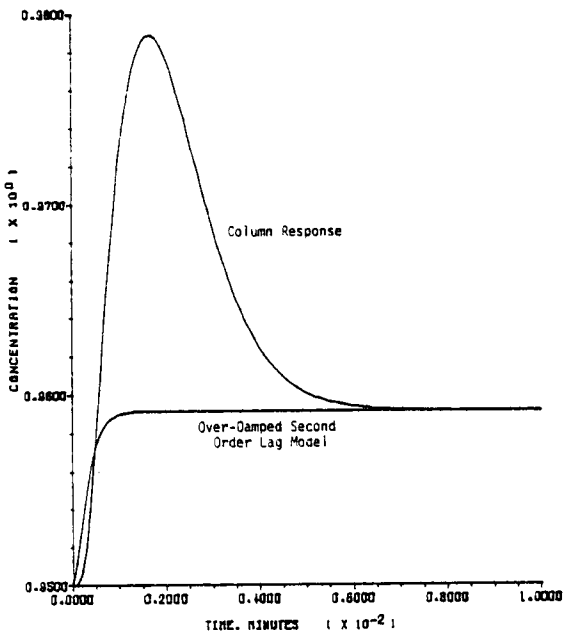

(b) Change in Distillate Composition With a Step Increase in Steam Flow.

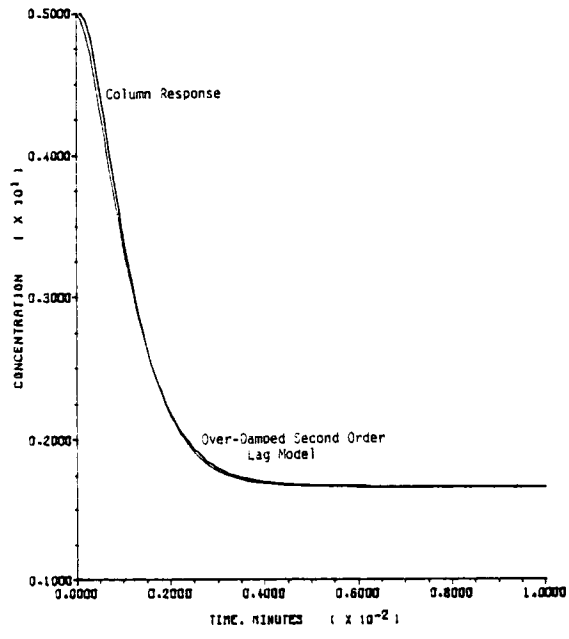

(c) Change in Bottoms Composition With a Step Increase in Distillate Flow.

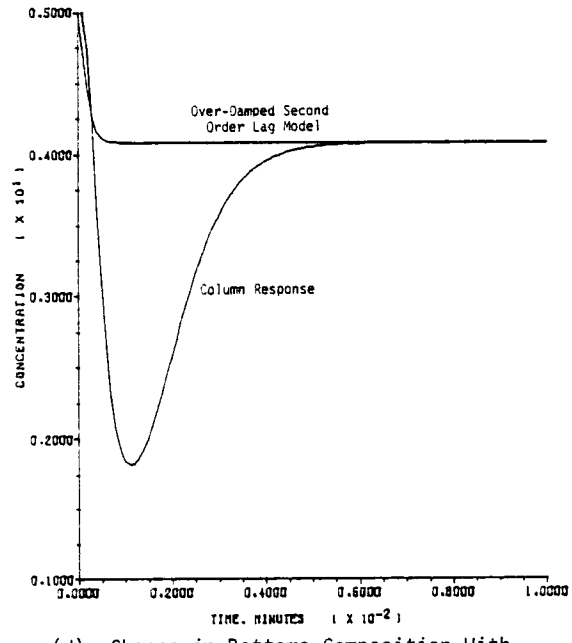

(d) Change in Bottoms Composition With a Step Increase in Steam Flow.

FIGURE 16. OPEN LOOP COLUMN RESPONSES WITH OVER-DAMPED SECOND ORDER LAG MODELS.

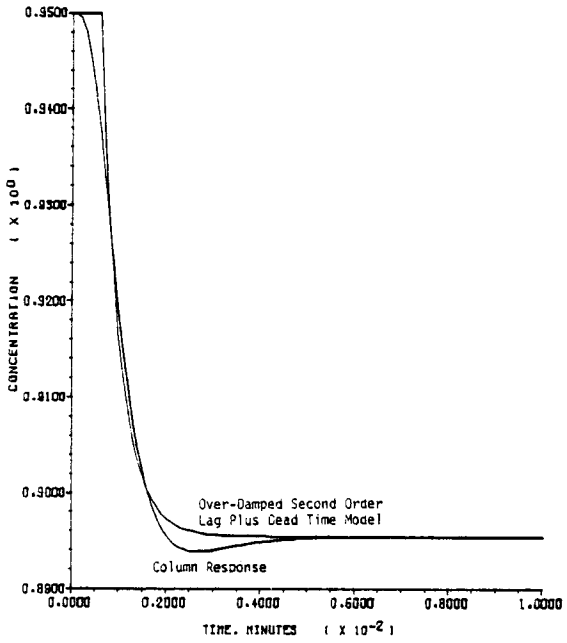

(a) Change in Distillate Composition With a Step Increase in Distillate Flow.

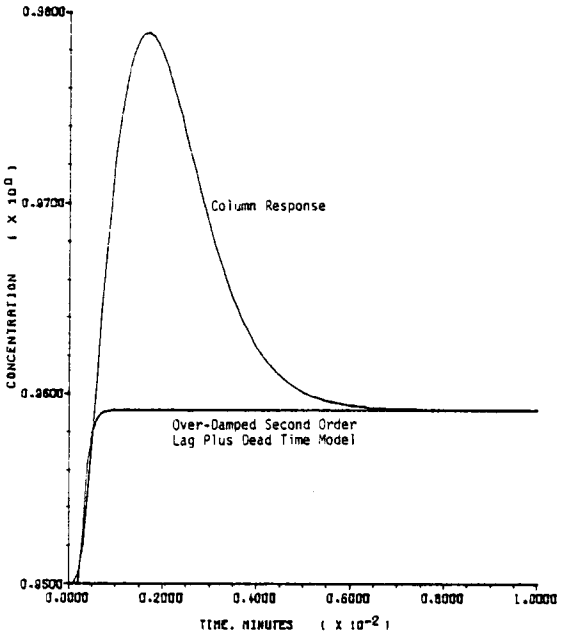

(b) Change in Distillate Composition With a Step Increase in Steam Flow.

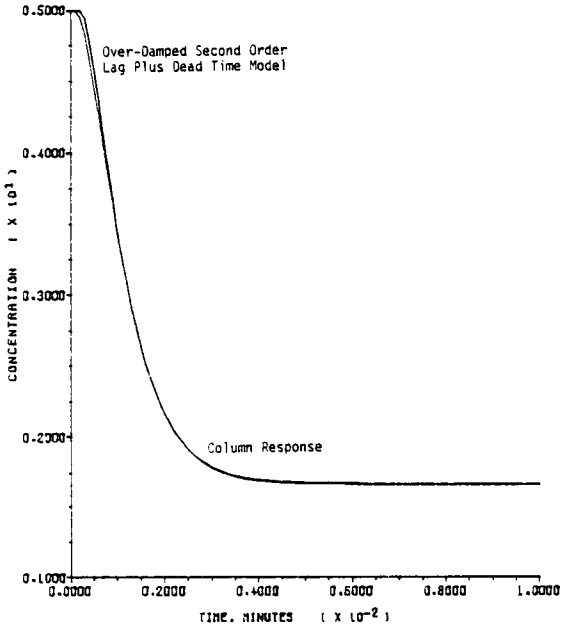

(c) Change in Bottoms Composition With a Step Increase in Distillate Flow.

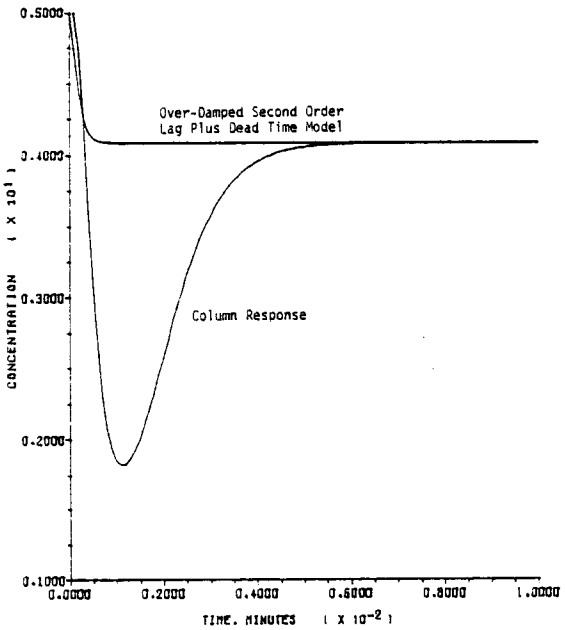

(d) Change in Bottoms Composition With a Step Increase in Steam Flow.

FIGURE 17. OPEN LOOP COLUMN RESPONSES WITH OVER-DAMPED SECOND ORDER LAG PLUS DEAD TIME MODELS.

Under-Damped Second Order Lag Models

It appeared that what would be necessary to improve the fit for the second and forth responses would be a model that could describe overshoot. Under-damped second order lag models can do this. The Laplace transfer function for a general under-damped second order lag looks like equation 36.

$$G(s) = \frac{K}{1+2\zeta s/\omega + s^2/\omega^2} \qquad \text{Eq. 36}$$

For a step input, the time response of an under-damped second order lag is given by equation 37.

$$x(t) = K\left\{1 - \frac{e^{-t\zeta\omega}\sin\left[\omega\sqrt{1-\zeta^2}\ t - \tan^{-1}\left(\frac{\sqrt{1-\zeta^2}}{-\zeta}\right)\right]}{\sqrt{1-\zeta^2}}\right\}$$

Again, a Pattern search routine was used to fit the parameters, and the results are given.

Response of x_D to D: $G_{11}(s) = \dfrac{-0.005454}{1+2(0.727)s/0.1668+s^2/(0.1668)^2}$

Response of x_D to G: $G_{12}(s) = \dfrac{0.000919}{1+2(0.2117)s/0.2816+s^2/(0.2816)^2}$

Response of x_B to D: $G_{21}(s) = \dfrac{-0.003334}{1+2(0.9421)s/0.1554+s^2/(0.1554)^2}$

Response of x_B to G: $G_{22}(s) = \dfrac{-0.000917}{1+2(0.1702)s/0.4335+s^2/(0.4335)^2}$

The under-damped second order lag approximations are shown alongside the real column responses in Figure 18. As was predicted, the second and fourth models did show some overshoot, thereby improving the fit over the first order lag models.

Under-Damped Second Order Lag Plus Dead Time Models

It was not thought that adding dead time to the under-damped second order lag models would provide a significant improvement. Figure 19, which shows the under-damped second order lag plus dead time approximations alongside the real column responses, shows this to be true. No real improvement is seen over the approximations in Figure 18. The best-fit approximations, as determined by a Pattern search routine, are given.

$$\text{Response of } x_D \text{ to D:} \quad G_{11}(s) = \frac{-0.005454\ e^{-2s}}{1+2(0.7436)s/0.2021+s^2/(0.2021)^2}$$

$$\text{Response of } x_D \text{ to G:} \quad G_{12}(s) = \frac{0.000978\ e^{29s}}{1+2(0.3251)s/0.0626+s^2/(0.0626)^2}$$

$$\text{Response of } x_B \text{ to D:} \quad G_{21}(s) = \frac{-0.003333\ e^{-2s}}{1+2(0.998)s/0.1893+s^2/(0.1893)^2}$$

$$\text{Response of } x_B \text{ to G:} \quad G_{22}(s) = \frac{-0.000916\ e^{-1s}}{1+2(0.1133)s/0.733+s^2/(0.733)^2}$$

Non-Decoupled Scheme

The relative gain array calculation, as described earlier, is very straight-forward to perform. It was first assumed that the distillate flowrate would be manipulated to control the distillate

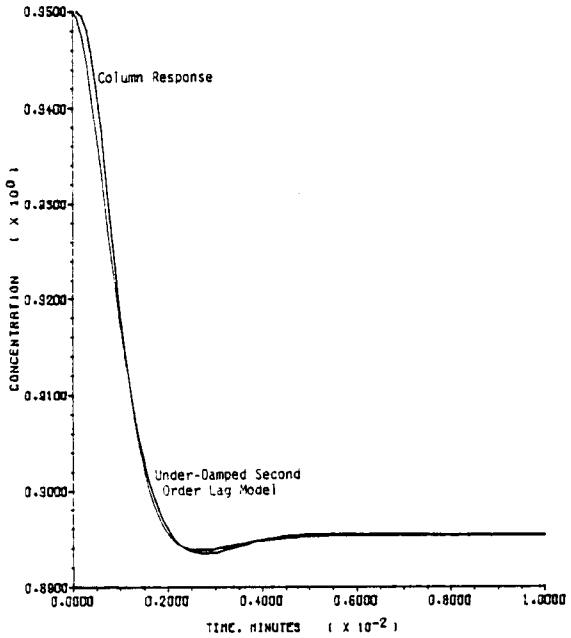

(a) Change in Distillate Composition With a Step Increase in Distillate Flow.

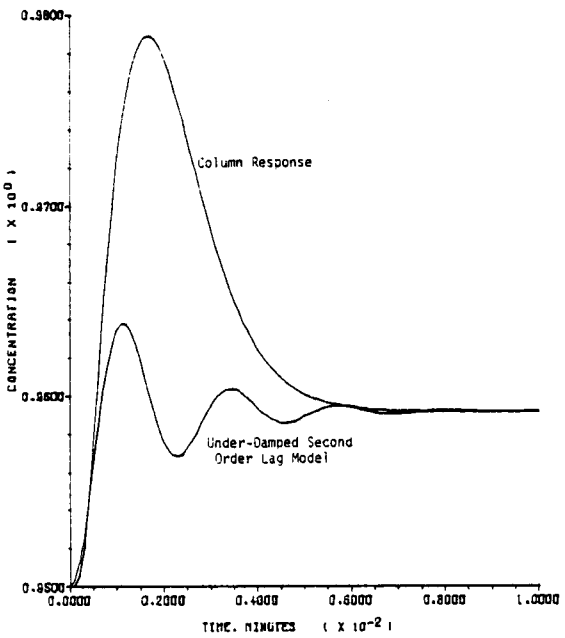

(b) Change in Distillate Composition With a Step Increase in Steam Flow.

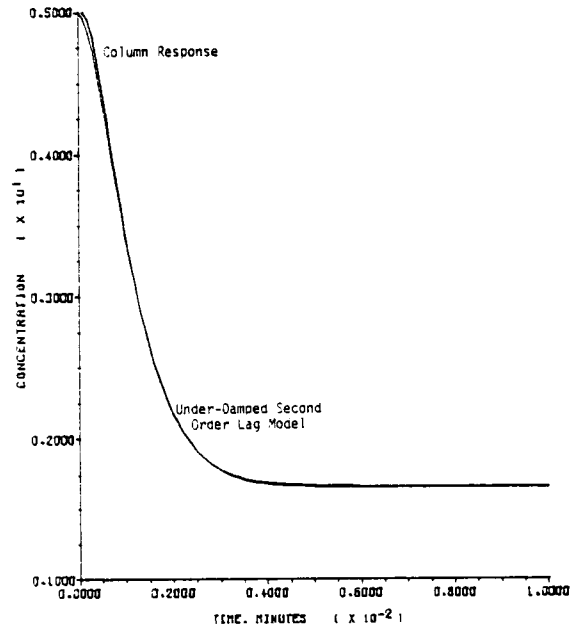

(c) Change in Bottoms Composition With a Step Increase in Distillate Flow.

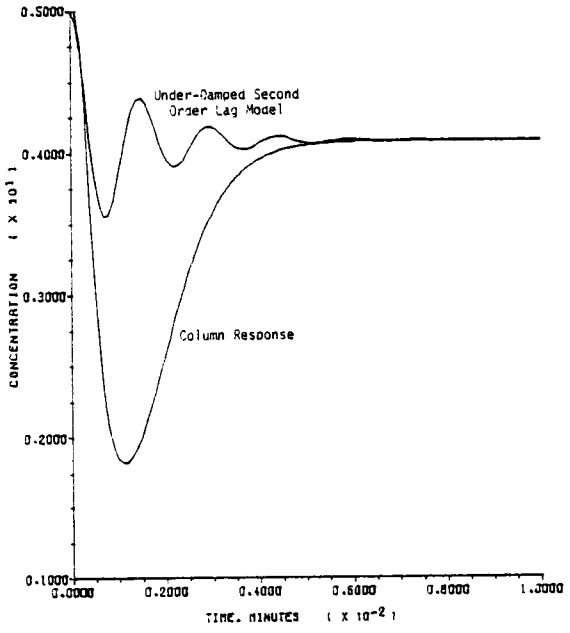

(d) Change in Bottoms Composition With a Step Increase in Steam Flow.

FIGURE 18. OPEN LOOP COLUMN RESPONSES WITH UNDER-DAMPED SECOND ORDER LAG MODELS.

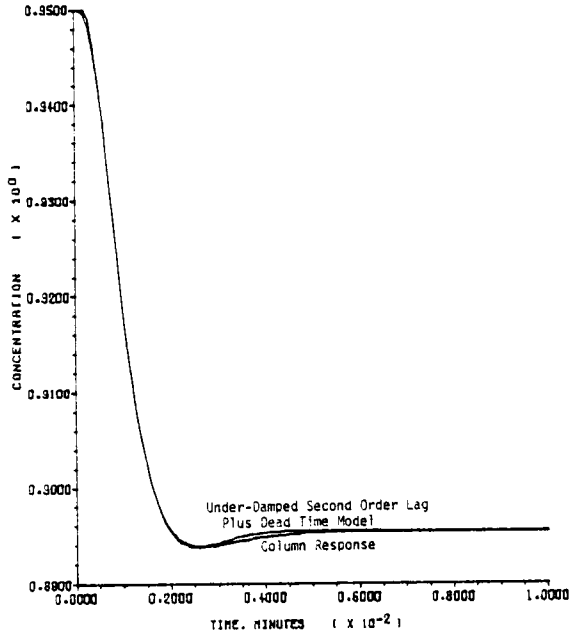

(a) Change in Distillate Composition With a Step Change in Distillate Flow.

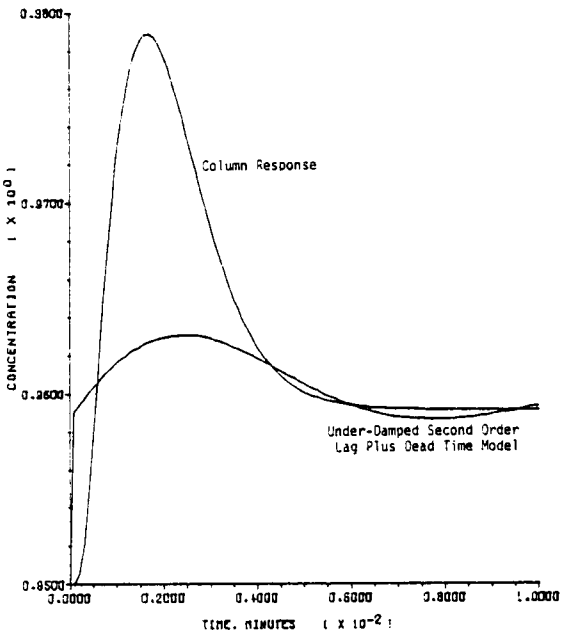

(b) Change in Distillate Composition With a Step Increase in Steam Flow.

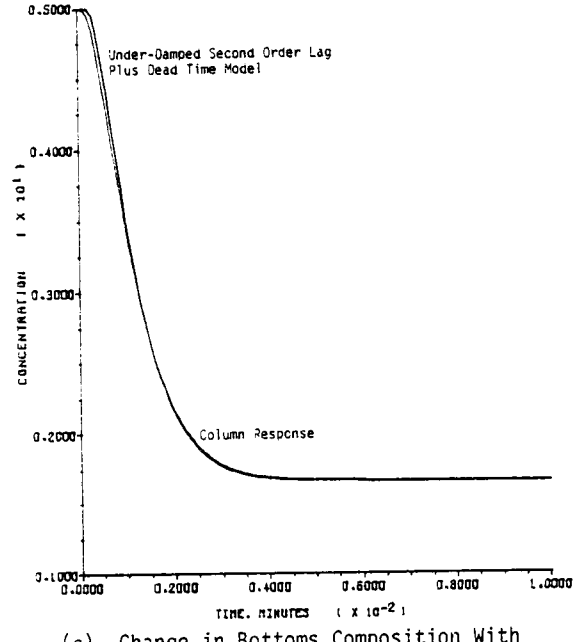

(c) Change in Bottoms Composition With a Step Increase in Distillate Flow.

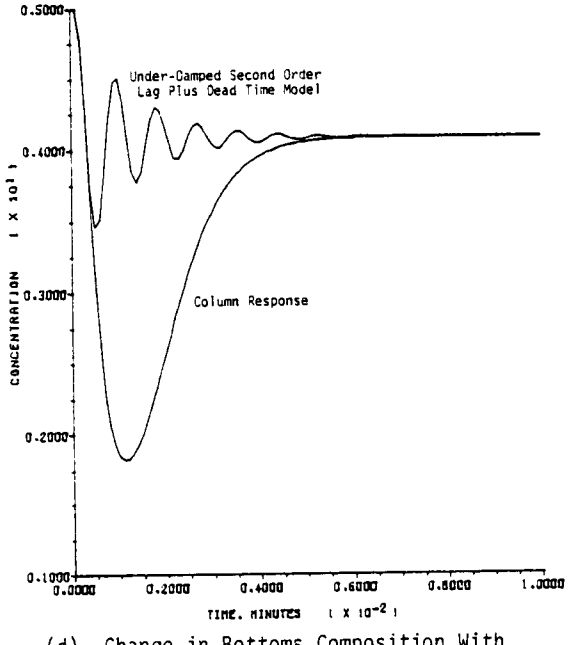

(d) Change in Bottoms Composition With a Step Increase in Steam Flow.

FIGURE 19. OPEN LOOP COLUMN RESPONSES WITH UNDER-DAMPED SECOND ORDER LAG PLUS DEAD TIME MODELS.

composition and the steam flowrate would be manipulated to control the bottoms composition. The process gain matrix then looked like equation 38.

$$\begin{bmatrix} -0.0054537 & 0.00091622 \\ -0.0033343 & -0.00091622 \end{bmatrix} \begin{bmatrix} D \\ G \end{bmatrix} = \begin{bmatrix} x_D \\ x_G \end{bmatrix} \qquad \text{Eq. 38}$$

These values were plugged into equation 10 to find that $\lambda_{11} = 0.62058$. By using equations 11 and 12, the array came out to be:

	x_D	x_B
D	0.62058	0.37942
G	0.37942	0.62058

As the largest relative gains came out on the diagonal, the assumed pairing was correct. If the distillate flowrate had been manipulated to control the bottoms composition and the steam rate manipulated to control the distillate composition, the relative gain array would have come out to be:

	x_B	x_D
D	0.37942	0.62058
G	0.62058	0.37942

which would have indicated a bigger interaction problem.

P-Canonical Decoupling Scheme

Four general p-canonical decouplers were examined: the perfect decoupler, ideal decoupler, and two simplified decouplers.

Expressions for the decoupling matrix, H, were derived by plugging into equation 17. For perfect decoupling, $D_{11} = D_{22} = 1$. This resulted in equation 39.

$$H_{\text{Perfect Decoupling}} = \begin{bmatrix} \frac{G_{22}}{(G_{11}\ G_{22} - G_{12}\ G_{21})} & \frac{-G_{12}}{(G_{11}\ G_{22} - G_{12}\ G_{21})} \\ \frac{-G_{21}}{(G_{11}\ G_{22} - G_{12}\ G_{21})} & \frac{G_{11}}{(G_{11}\ G_{22} - G_{12}\ G_{21})} \end{bmatrix} \quad \text{Eq. 39}$$

For ideal decoupling, $D_{11} = G_{11}$ and $D_{22} = G_{22}$. Plugging this into equation 17 yielded equation 40.

$$H_{\text{Ideal Decoupling}} = \begin{bmatrix} \frac{G_{11}\ G_{22}}{(G_{11}\ G_{22} - G_{12}\ G_{21})} & \frac{-G_{12}\ G_{22}}{(G_{11}\ G_{22} - G_{12}\ G_{21})} \\ \frac{-G_{11}\ G_{21}}{(G_{11}\ G_{22} - G_{12}\ G_{21})} & \frac{G_{11}\ G_{22}}{(G_{11}\ G_{22} - G_{12}\ G_{21})} \end{bmatrix} \quad \text{Eq. 40}$$

The expression for the decoupling matrix for simplified decoupling is given in equation 18.

$$H_{\text{Simplified Decoupling}} = \begin{bmatrix} 1 & \frac{-G_{12}}{G_{11}} \\ \frac{-G_{21}}{G_{22}} & 1 \end{bmatrix} \quad \text{Eq. 41}$$

Another of the simplified decouplers was used to demonstrate setting an off-diagonal element of H to one.

$$H_{\text{Alternate Simplified}} = \begin{bmatrix} \frac{-G_{22}}{G_{21}} & \frac{-G_{12}}{G_{11}} \\ 1 & 1 \end{bmatrix} \qquad \text{Eq. 42}$$

One basic question to this approach concerns the complexity of the models used in the design of the decouplers. Decouplers were developed for each of the three models considered using a Z-transform procedure to determine an appropriate difference equation as shown in Table 4. The coefficients in this table were used in equation 43 as a numerical simulation of the various decoupler elements.

$$m_n = a_1 u_n + a_2 u_{n-1} + a_3 u_{n-2} + b_1 m_{n-1} + b_2 m_{n-2} \qquad \text{Eq. 43}$$

In this equation the u's are the inputs and the m's the outputs, n is the current time step, and the a's and b's the constants from Table 4. As mentioned earlier, only steady-state decoupling elements could be used in the perfect decoupling scheme.

A listing of a sample decoupler simulation is given in Appendix A.

V-Canonical Decoupling Scheme

The full v-canonical decoupler was examined using both a steady-state and a first order process model to derive the decoupling matrix. Also, in case of instabilities with the full scheme, each decoupling element in turn was removed. The remaining partial decoupler was one derived from a first order process model.

TABLE 4

DIFFERENCE EQUATION COEFFICIENTS FOR P-CANONICAL DECOUPLERS

	a_1	a_2	a_3	b_1	b_2
Perfect Decoupling					
steady-state					
H_{11}	-113.792	-	-	-	-
H_{12}	-113.792	-	-	-	-
H_{21}	414.081	-	-	-	-
H_{22}	-677.384	-	-	-	-
Ideal Decoupling					
steady-state					
H_{11}	0.620619	-	-	-	-
H_{12}	0.104256	-	-	-	-
H_{21}	-2.2584	-	-	-	-
H_{22}	0.620619	-	-	-	-
first order					
H_{11}	0.7856	-1.5381	0.7528	1.9527	-0.9531
H_{12}	0.3585	-0.7094	0.3509	1.9527	-0.9531
H_{21}	-0.4701	.8990	-0.4298	1.9527	-0.9531
H_{22}	0.7856	-1.5381	0.7528	1.9527	-0.9531

TABLE 4 (Continued)

	a_1	a_2	a_3	b_1	b_2
Simplified Decoupling					
steady-state					
H_{11}	1	-	-	-	-
H_{12}	0.16800	-	-	-	-
H_{21}	-3.63919	-	-	-	-
H_{22}	1	-	-	-	-
first order					
H_{11}	1	-	-	-	-
H_{12}	0.44663	-0.44104	-	0.9668	-
H_{21}	-0.62572	0.59294	-	0.9910	-
H_{22}	1	-	-	-	-
u.d. second order					
H_{11} [1]	-	-	-	-	
H_{12}	0.47878	-0.94579	0.46711	1.9874	-0.9882
H_{21}	-0.46764	0.87532	-0.40938	1.9709	-0.9711
H_{22}	1	-	-	-	-
Alternate Simplified					
steady-state					
H_{11}	-0.274805	-	-	-	-
H_{12}	0.167987	-	-	-	-

TABLE 4 (Continued)

	a_1	a_2	a_3	b_1	b_2
H_{21}	1	-	-	-	-
H_{22}	1	-	-	-	-
first order					
H_{11}	-1.5961	1.5815	-	0.9465	-
H_{12}	0.44663	-0.44104	-	0.9668	-
H_{21}	1	-	-	-	-
H_{22}	1	-	-	-	-

The actual implementation of a v-canonical decoupler in the control of the column was accomplished as follows (see Figure 9): The distillate decoupler action from the last time step was operated upon by the decoupling element and added to the steam controller action from the present time step. The sum was the required steam flowrate change. Similarly, the steam decoupler action from the last time step was operated upon by the decoupling element and added to the distillate controller action from the present time step. The sum was the required distillate flowrate change.

It is obvious from Figure 6 that there was a very good possibility of having positive feedback within the decoupler itself. The Routh Stability Criterion (31) was useful at this point in predicting system stability. Through block diagram reduction the total system transfer function was derived and Routh analysis applied to it (see Reference 31 for details). The result was, for stability, that each of the following expressions had to be of the same sign:

1. $K_{22} K_{11} \tau_{21} \tau_{12} - K_{12} K_{21} \tau_{22} \tau_{11}$
2. $K_{22} K_{11} (\tau_{21} + \tau_{12}) - K_{12} K_{21} (\tau_{22} + \tau_{11})$
3. $K_{22} K_{11} - K_{12} K_{21}$

By examining the first order lag approximations to the column responses derived earlier in this chapter, it could be seen that all the time constants were positive and all the gains but one, K_{12}, were negative. Applying these facts to the expressions above, it was clear that they were <u>all</u> positive indicating a stable system.

It should be noted that the difference equation coefficients were the same as those in Table 4 under "Simplified Decoupling". The distinction between the v-canonical decoupler and the simplified p-canonical decoupler is that the decoupling terms acted upon the controller output in the p-canonical scheme whereas they act upon the previous decoupler outputs in the v-canonical scheme.

A listing of a sample v-canonical decoupling routine is given in Appendix A.

New Variable Schemes

Ryskamp's method basically involved manipulating G to control x_B and manipulating D/G to control x_D. The actual implementation of this scheme in the control of the column was accomplished as follows: The bottoms composition error was used to calculate the bottoms composition controller output which was sent directly to the column as the required change in steam rate. This was exactly as in the non-decoupled scheme. The distillate composition error, on the other hand, was used to calculate the distillate composition controller output which was sent to the column as D/G. This had to be multiplied by the current value of G before being used as the required change in distillate flowrate.

Waltz's method involved manipulating D to control x_D and manipulating G to control S, the separation factor, defined by equation 22. The implementation of Waltz's method was accomplished as follows: The distillate composition error was used to calculate the required change in distillate flowrate as in the non-decoupled scheme. The

bottoms composition, however, had to be combined with the distillate composition in an algorithm to determine S. The error in S was then used to calculate the required change in bottoms flowrate.

Listings of the controller routines for both Ryskamp's and Waltz's schemes are given in Appendix A.

SVD Controller

To implement the SVD controller it was necessary to calculate the singular value decomposition of the process gain matrix, given in equation 44.

$$A = \begin{bmatrix} -0.005454 & 0.0009162 \\ -0.003334 & -0.0009162 \end{bmatrix} \qquad \text{Eq. 44}$$

This calculation could have been performed by hand, calculating the eigenvalues and eigenvectors of the matricies formed by multiplying both AA^H and A^HA. The superscript H indicates the Hermitian transpose of the matrix. In the case where all the elements of A are real, this reduces to the simple transpose of the matrix. There are, however, very accurate numerical techniques for finding U, Σ, and V. One is contained in the IMSL Library. Using this method, the decomposition was computed and is given in equation 45.

$$A = U\Sigma V^T \qquad \text{Eq. 45}$$

$$U = \begin{bmatrix} -0.8582418 & 0.5132456 \\ -0.5132456 & -0.8582418 \end{bmatrix}$$

$$V = \begin{bmatrix} 0.9987796 & -0.04938975 \\ 0.04938975 & 0.9987796 \end{bmatrix}$$

$$\Sigma = \begin{bmatrix} 0.006399822 & 0 \\ 0 & 0.001258092 \end{bmatrix}$$

The matricies U and V are sometimes expressed in terms of a Givens Rotation, where U is a function of θ and V the same function of β.

$$U = \begin{bmatrix} \sin\theta & \cos\theta \\ -\cos\theta & \sin\theta \end{bmatrix} \qquad \text{Eq. 46}$$

$$V = \begin{bmatrix} \sin\beta & \cos\beta \\ -\cos\beta & \sin\beta \end{bmatrix} \qquad \text{Eq. 47}$$

For the distillation column gain matrix decomposition, $\theta = -59.12°$ and $\beta = 92.83°$.

The actual implementation of the SVD controller was accomplished as follows (see Figure 9). The distillate and bottoms compositions were compared to their respective set points and any error sent to the controller. The first step in the controller was to operate on the error signals using the V matrix which created "structured" error signals. These structured signals were then put through conventional PI controllers which created structured controller outputs. The structured outputs were then operated upon by the U^T matrix, which created the required changes in distillate and steam flowrates.

CHAPTER III

RESULTS AND DISCUSSION

Each of the control strategies described and developed in Chapter II were implemented on the distillation column simulation. In the cases where open loop tests were made, both controllers were put into manual. A step input of +10 lb/hr was made in the distillate flowrate and the system response noted. Starting with the initial values again, a step input of +10 lb/hr was made in the steam flowrate and the system response noted.

In the cases where closed loop tests were to be made, both controllers were put into automatic and a step feed composition disturbance (x_F = 0.50 at t=0, x_F = 0.55 at $t \geqq 1$) was made. Single-loop approximate controller parameters were found using the closed loop Zeigler-Nichols method, both loops were put on automatic control, and the tuning adjusted to give acceptable control. The closed loop Zeigler-Nichols method of tuning PI controller was designed for single input/single output systems. It involves setting the integral mode sensitivity to zero and increasing the proportional gain until sustained oscillation occurs. This value is called the Ultimate Gain and the period of this oscillation is called the Ultimate Period. The tuning parameters are then estimated to be as follows: Porportional Gain = 0.45 x Ultimate Gain, Integral Reset Time = 0.83 x Ultimate Period. As this method does not account for interaction with another

loop, some parameter adjustments were necessary. The resulting parameters were used as the initial values in a Pattern search for the optimum controller tuning. The cost criterion (the value which PATERN tried to minimize) was the integral absolute value of the error signals for 200 minutes for both the distillate and bottoms compositions. The minimum error for a given control strategy also affords some comparison of its effectiveness.

Non-Decoupled Scheme

Figure 2 has the distillate composition paired with the distillate flowrate and the bottoms composition paired with the steam rate to the reboiler. For reference purposes, this will be called "forward" pairing. Figure 3, on the other hand, has the distillate composition paired with the steam rate to the reboiler and the bottoms composition paired with the distillate flowrate. This will be called "backward" pairing.

For both pairing cases proportional plus integral controllers were appropriately added and tuned using the nonlinear regression Pattern search (21). The objective function in each case was a IAE (Integral Absolute Error) criteria based on equal weighting of top and bottom compositions (equation 24). The result of the optimizations are given.

Forward: $P_D = 837$, $I_D = 9.73$, $P_B = 55$, $I_B = 1.13$

Backward: $P_D = 784$, $P_B = 654$, $I_B = 2.93$

$IAE_{forward} = 0.307$ $\quad$ $IAE_{backward} = 2.72$

Note for the backward controller pairing, the Pattern search determined that a minimum IAE could be obtained by eliminating integral control in the distillate controller. This allowed some offset in the distillate composition, but reduced some oscillation in the system.

Figure 20 is a response of the system to a feed composition disturbance for both the forward and backward pairings using the controller tuning given here. In Figure 20a it can be seen that most of the increased error of the backward pairing over the forward is the offset of the distillate composition. In part b, it is seen that backward control actually allows less of an excursion (peak composition error) in the bottoms composition than the forward pairing, though the difference is much less than that in part a.

The distillate controller action (c) was about the same for the two pairings, but the bottoms controller action (d) was considerably less for the forward pairing than the backward.

Thus the relative gain array prediction of the best controller pairing was correct. Not only did the forward pairing give the best control, but it did so with less controller action.

P-Canonical Decoupler

Of the many process models determined in the beginning of Chapter II, it was decided to use the steady-state model and one other for deriving decoupling elements. To facilitate the decision of which model to use, each of the steady-state, first order lag, and under-damped second order lag were used to derive the simplified

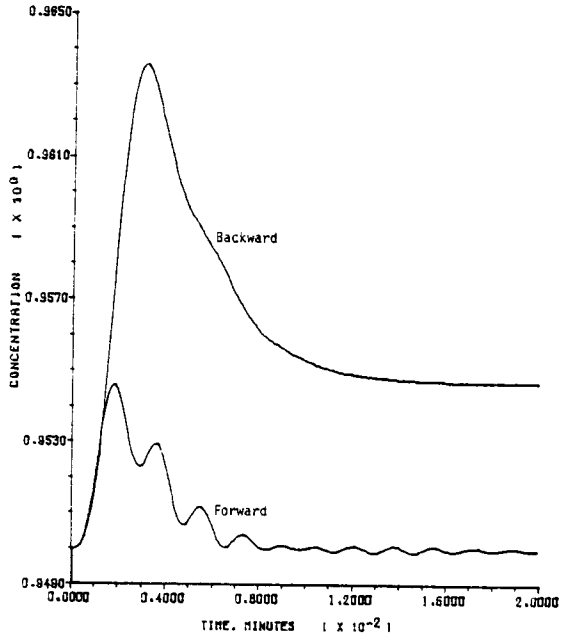

(a) Distillate Composition.

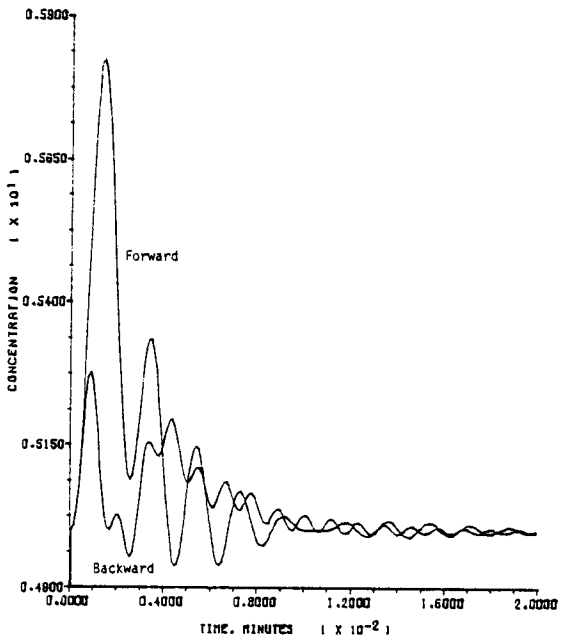

(b) Bottoms Composition.

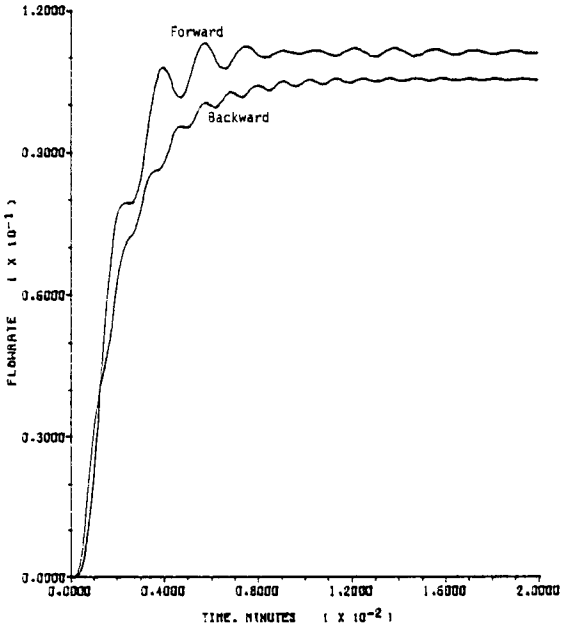

(c) Distillate Controller Action.

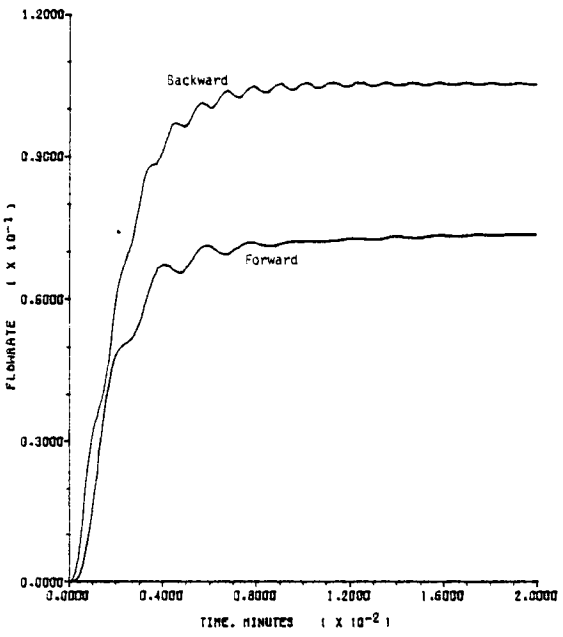

(d) Bottoms Controller Action.

FIGURE 20. FORWARD AND BACKWARD CONTROLLER PAIRING FOR NON-DECOUPLED SCHEME.

p-canonical decoupler elements. These simplified p-canonical decouplers were then attached to the column and open loop tests conducted to determine how well the systems were decoupled. The test results are shown in Figures 21, 22, and 23 for the steady-state, first order lag, and second order lag derived decoupling elements, respectively. In these figures, parts a and b were the distillate and bottoms composition responses to a step change in distillate controller output. According to theory the distillate composition (part a) should have changed during this test, but the bottoms composition (part b) should have been unaffected. Obviously, due to modeling inaccuracies this was not perfect. Similarly, parts c and d were the distillate and bottoms composition responses to a step change in bottoms controller output. Again, according to theory the bottoms composition (part d) should have changed during this test, but the distillate composition (part c) should have been unaffected. Thus, in judging the decouplers' effectiveness, Figures b and c were the important figures to examine.

For the steady-state derived decoupling elements, Figure 21 shows the system response. From part b, and an examination of the data which were plotted, it was determined that the peak bottoms composition excursion was 0.1072 and the final offset was 0.0063. When the bottoms controller output was changed, part c revealed a peak distillate composition excursion of 0.0195 and a final offset of 0.002.

Figure 22 shows the response when a simplified p-canonical decoupler using first order lag derived elements was applied. From

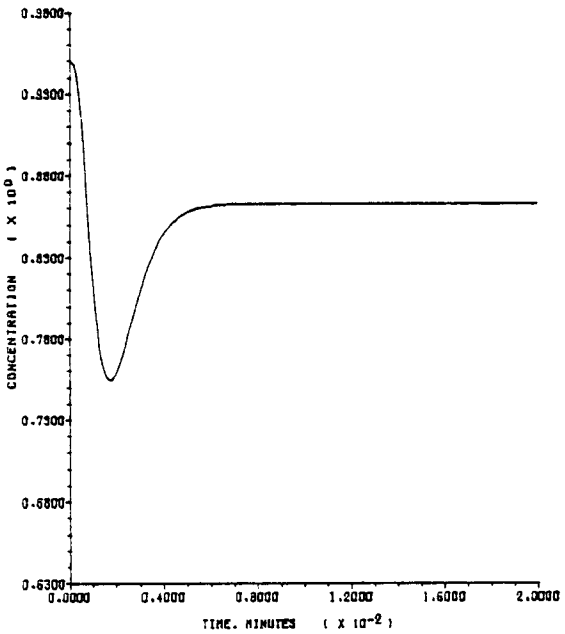

(a) Distillate Composition Response to a Step Increase in Distillate Controller Output.

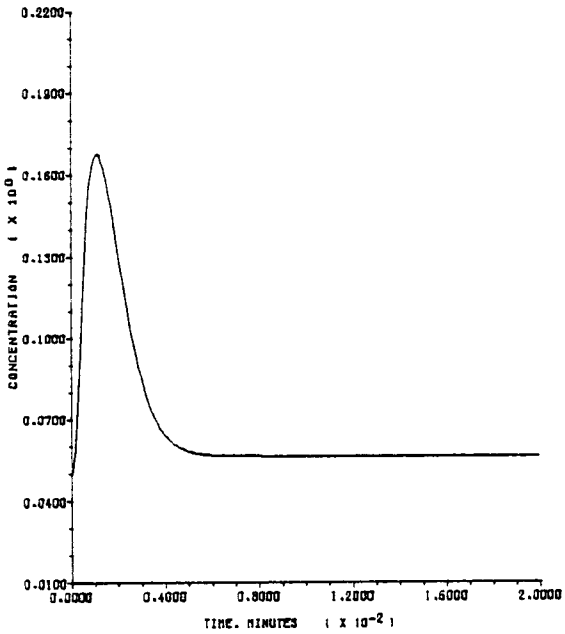

(b) Bottoms Composition Response to a Step Increase in Distillate Controller Output.

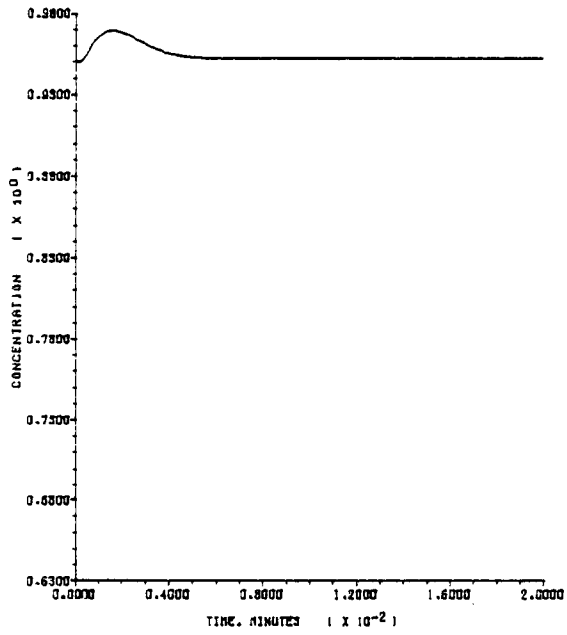

(c) Distillate Composition Response to a Step Increase in Bottoms Controller Output.

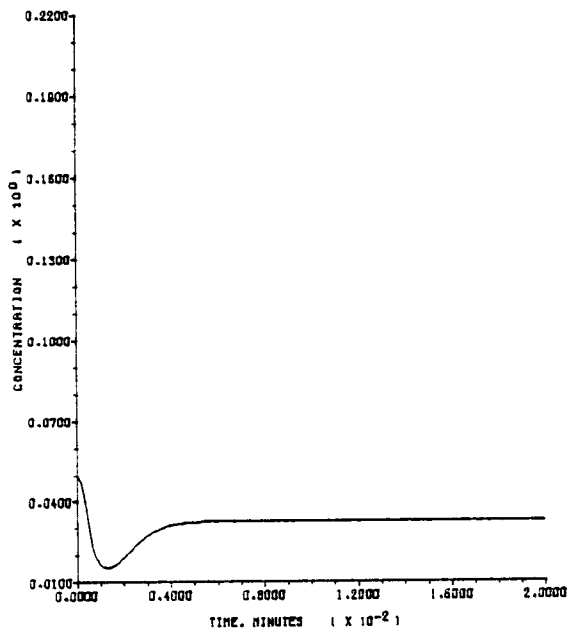

(d) Bottoms Composition Response to a Step Increase in Bottoms Controller Output.

FIGURE 21. OPEN LOOP SIMPLIFIED P-CANONICAL DECOUPLER WITH STEADY-STATE DERIVED ELEMENTS. BOTH CONTROLLERS IN MANUAL.

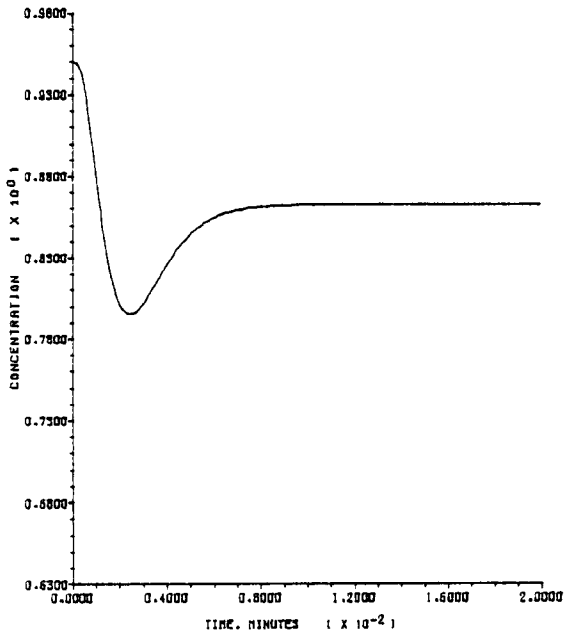

(a) Distillate Composition Response to a Step Increase in Distillate Controller Output.

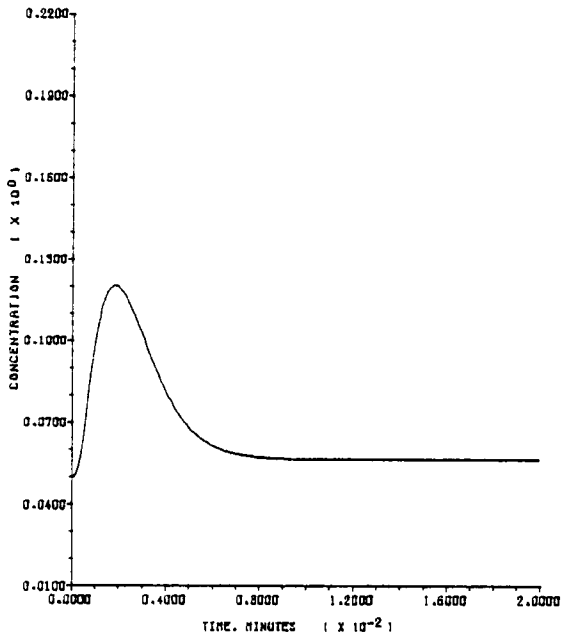

(b) Bottoms Composition Response to a Step Increase in Distillate Controller Output.

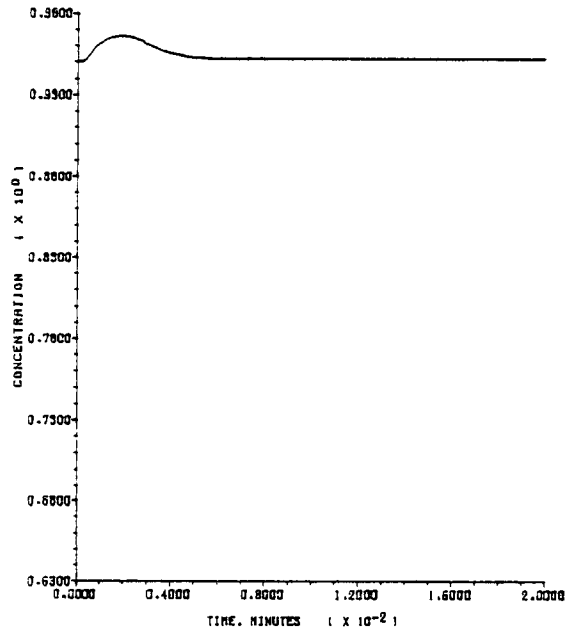

(c) Distillate Composition Response to a Step Increase in Bottoms Controller Output.

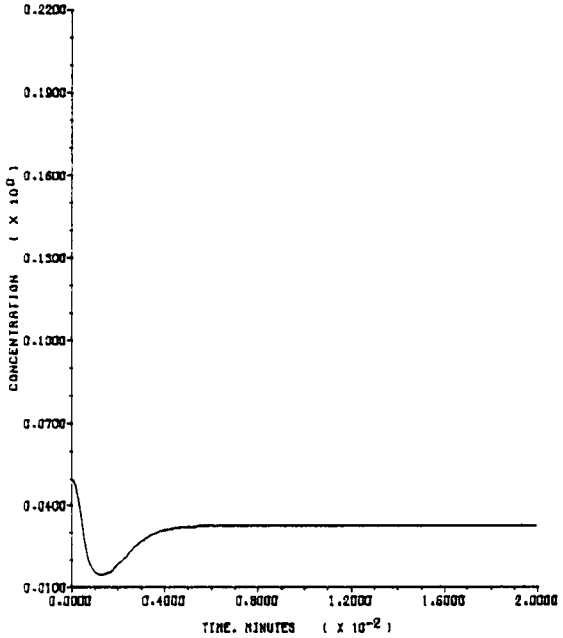

(d) Bottoms Composition Response to a Step Increase in Bottoms Controller Output.

FIGURE 22. OPEN LOOP SIMPLIFIED P-CANONICAL DECOUPLER WITH FIRST ORDER LAG DERIVED ELEMENTS.

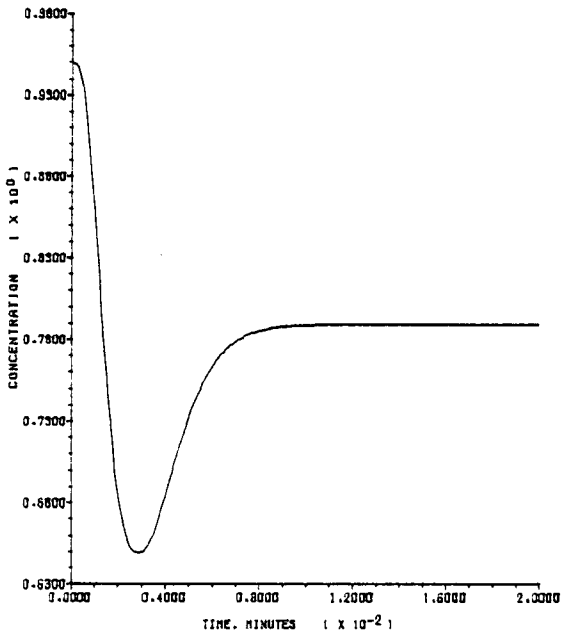

(a) Distillate Composition Response to a Step Increase in Distillate Controller Output.

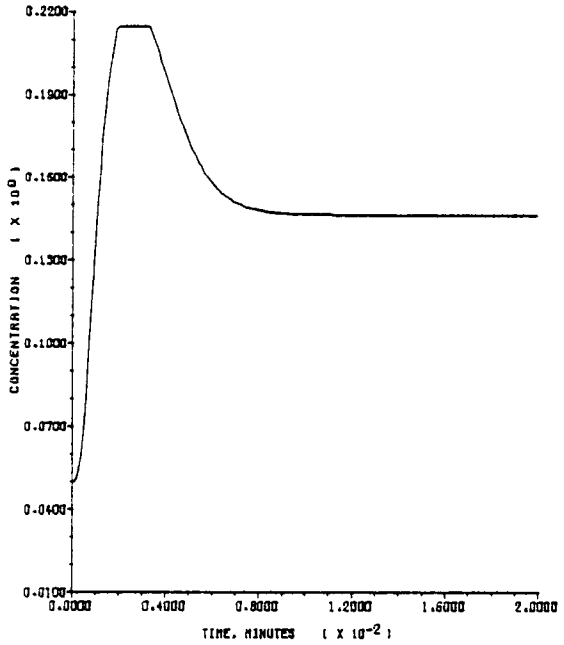

(b) Bottoms Composition Response to a Step Increase in Distillate Controller Output.

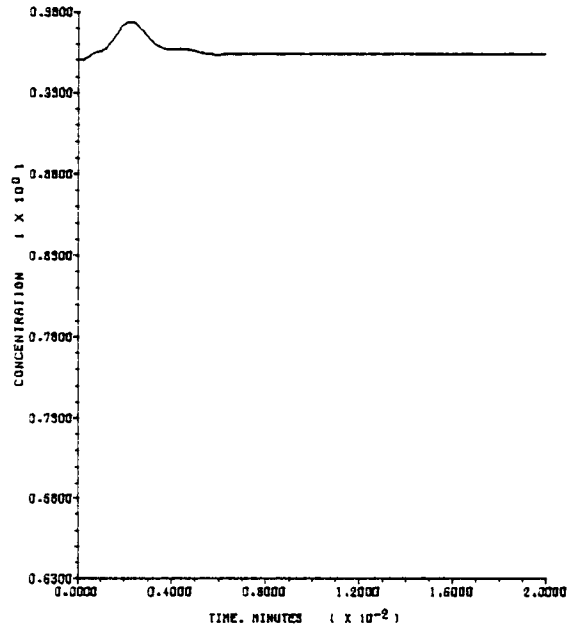

(c) Distillate Composition Response to a Step Increase in Bottoms Controller Output.

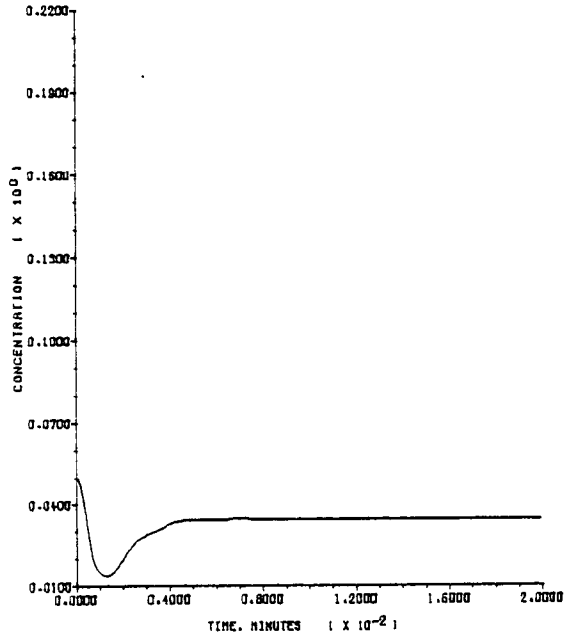

(d) Bottoms Composition Response to a Step Increase in Bottoms Controller Output.

FIGURE 23. OPEN LOOP SIMPLIFIED P-CANONICAL DECOUPLER WITH SECOND ORDER LAG DERIVED ELEMENTS.

part b it was determined that the peak bottoms composition excursion was 0.0704 and the final offset 0.0072. When the bottoms controller output was changed, part c showed a peak distillate composition excursion of 0.0136 and a final offset of 0.0025.

The response of the system when a simplified p-canonical decoupler with second order lag derived elements was added, is shown in Figure 23. When the distillate controller output was changed, part b showed that the peak bottoms composition excursion was 0.165 and the final offset 0.099. Part c showed the peak distillate composition excursion to be 0.024 and the final offset to be 0.005.

For ease of comparison these results are summarized in Table 5. This table shows several things. First, the steady-state derived elements give the least final offset. This would be expected because the steady-state derived decoupling elements are steady-state themselves and would not suffer from the complexities associated with dynamics. These steady-state elements do not show as good decoupling during the dynamic portion (indicated by the peak excursion). This, too, would be expected because design of the decoupling elements was based upon final values. The first order lag derived elements, as expected, showed improvement during the transient response (lower peak excursion), but also showed more final offset. The second order lag derived elements showed poor decoupling, either because of the very complex decoupling elements or because of the oscillatory nature of the models themselves.

TABLE 5

DECOUPLER ELEMENT COMPARISON

	Bottoms		Distillate	
	Peak Excursion	Final Offset	Peak Excursion	Final Offset
Steady-State	0.1072	0.0063	0.0195	0.0020
First Order Lag	0.0704	0.0072	0.0136	0.0025
Second Order Lag	0.1650	0.0990	0.0240	0.0050

In general it was felt that the best decoupling was achieved using first order lag derived elements.

Simplified Decoupler

Closed loop studies were conducted on the simplified p-canonical decoupler using two conventional proportional plus integral controllers. The proportional and integral modes were tuned using the Pattern search routine to reduce the combined IAE. The results are:

	Distillate Controller	Bottoms Controller
P	154.4	660.
I (min)	3.16	4.65

IAE = 0.305 min

The system response to a feed composition disturbance is shown in Figure 24.

It is interesting to note that this is just under the IAE for forward pairing in the non-decoupled scheme. The indication is that little improvement was added by decoupling the system using a simplified matrix decoupler with steady-state derived elements.

Next, the loop was closed around the column with a first order lag derived simplified p-canonical decoupler. The controller proportional gains and integral reset times were optimized using a Pattern search and the results given.

P_D = 181. P_B = 389.

I_D = 68.3 min. I_B = 40.1 min.

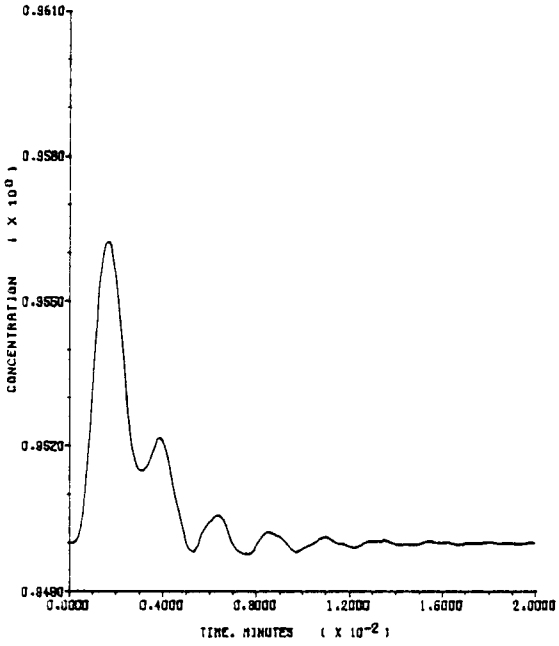

(a) Distillate Composition.

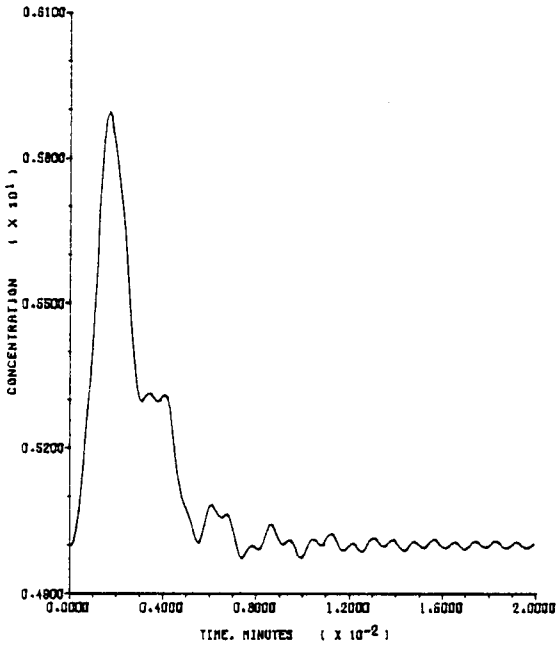

(b) Bottoms Composition.

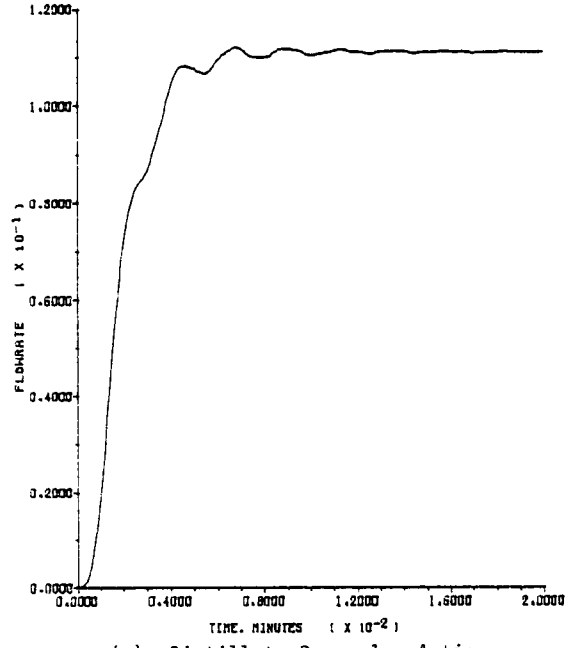

(c) Distillate Decoupler Action.

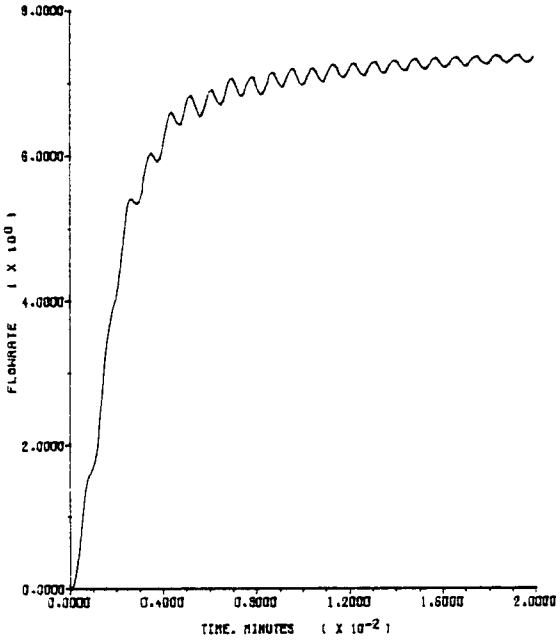

(d) Bottoms Decoupler Action.

FIGURE 24. CLOSED LOOP SIMPLIFIED P-CANONICAL DECOUPLER WITH STEADY-STATE DERIVED ELEMENTS. RESPONSE TO FEED COMPOSISION DISTURBANCE.

Figure 25 shows the closed loop response of this system to a feed composition disturbance. The IAE corresponding to these controller parameters was 0.5803 minutes, close to twice as much as for the steady-state derived decoupling elements.

Ideal Decoupling

Ideal p-canonical decoupling elements were derived using the first order lag process model. This ideal decoupler was then attached to the column and open loop tests conducted to determine how effectively the system interaction was canceled. The test results are shown in Figure 26. This is like Figures 21 - 23 in that parts a and b were distillate and bottoms composition responses to a step change in distillate controller output and parts c and d were distillate and bottoms composition responses to a step change in bottoms controller output. Again, according to decoupling theory, parts b and c should exhibit no interaction. From part b it was determined that the peak bottoms composition excursion was 0.045 and the final offset 0.004. When the bottoms composition controller output was changed, part c showed a peak distillate composition excursion of 0.018 and a final offset of 0.005.

The loop was then closed around the column with first order lag derived ideal p-canonical decoupler. The controller proportional gains and integral reset times were optimized using a Pattern search and the results given.

$P_D = 276.$ $\qquad$ $P_B = 473.$

$I_D = 60.53$ min. $\qquad$ $I_B = 34.78$ min.

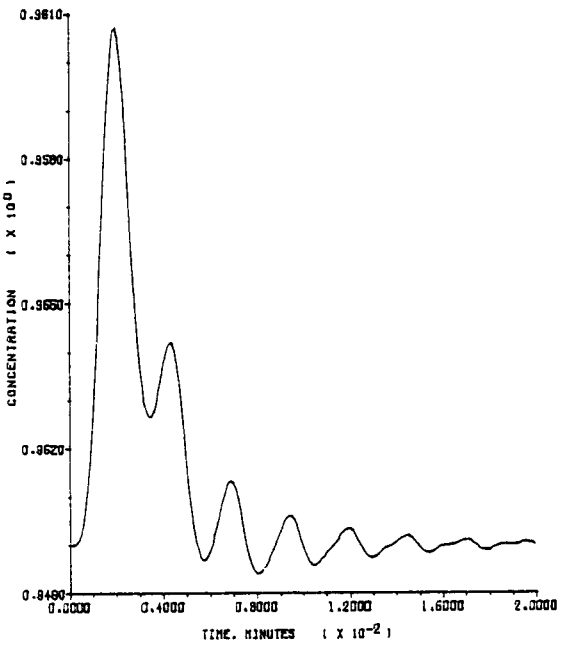

(a) Distillate Composition.

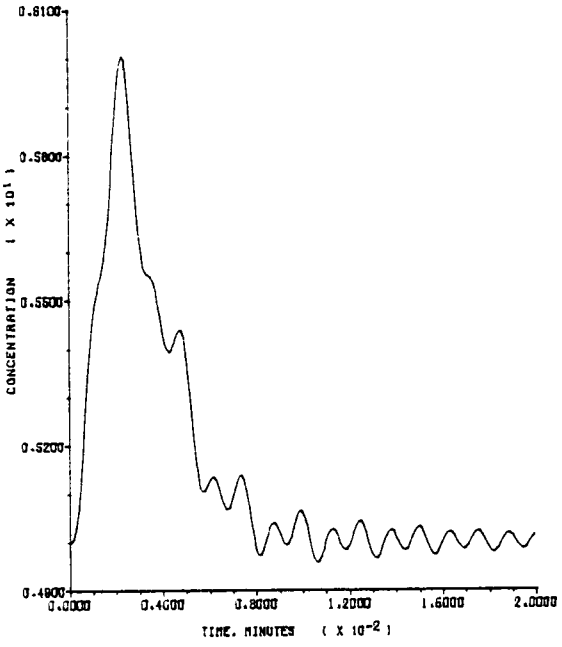

(b) Bottoms Composition.

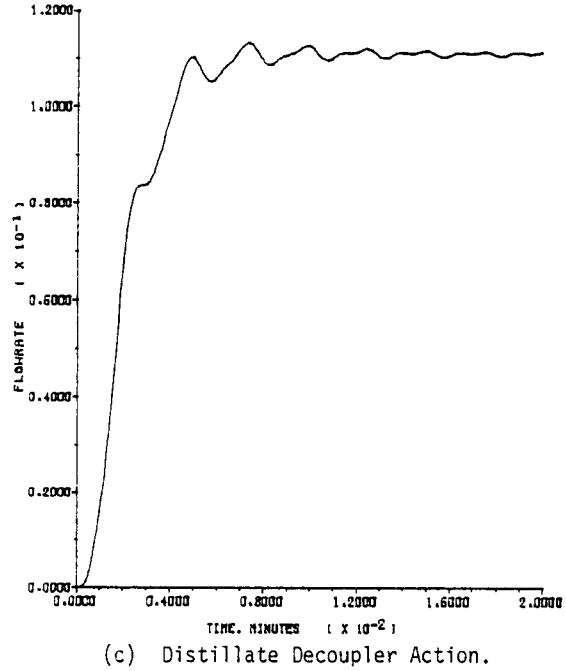

(c) Distillate Decoupler Action.

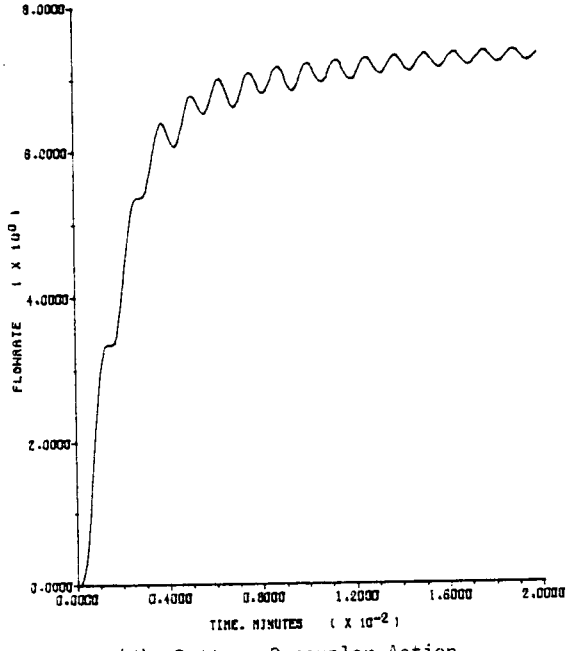

(d) Bottoms Decoupler Action.

FIGURE 25. CLOSED LOOP SIMPLIFIED P-CANONICAL DECOUPLER WITH FIRST ORDER LAG DERIVED ELEMENTS.

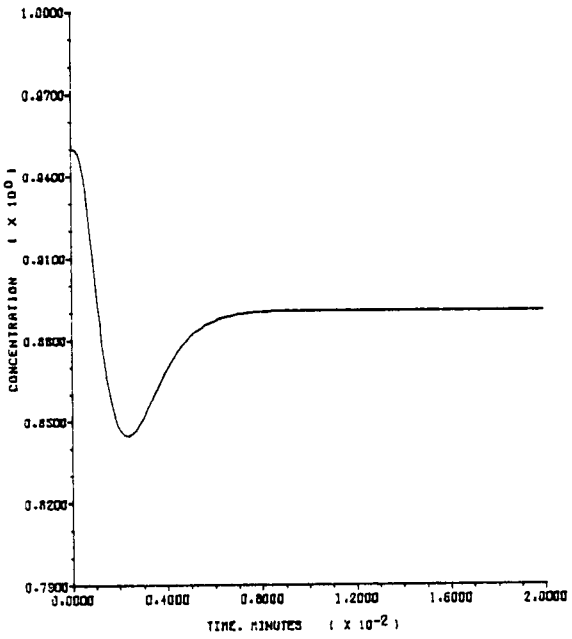

(a) Distillate Composition Response to a Step Increase in Distillate Controller Output.

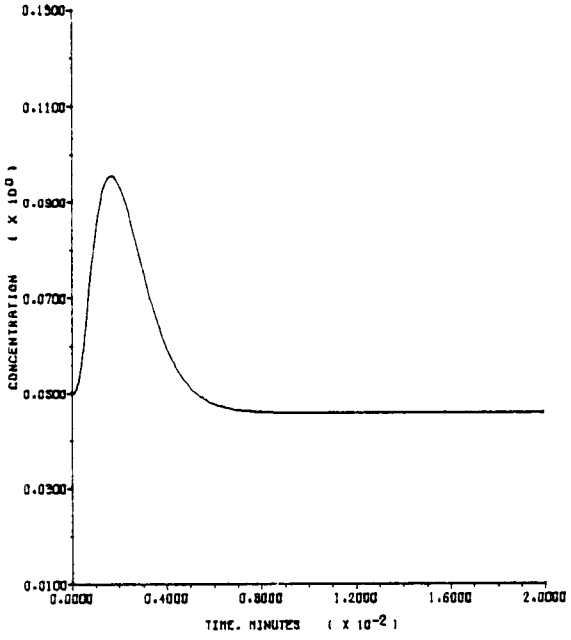

(b) Bottoms Composition Response to a Step Increase in Distillate Controller Output.

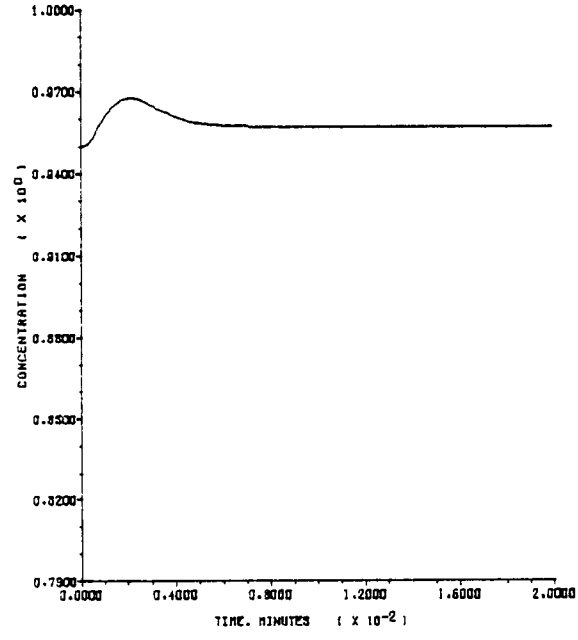

(c) Distillate Composition Response to a Step Increase in Bottoms Controller Output.

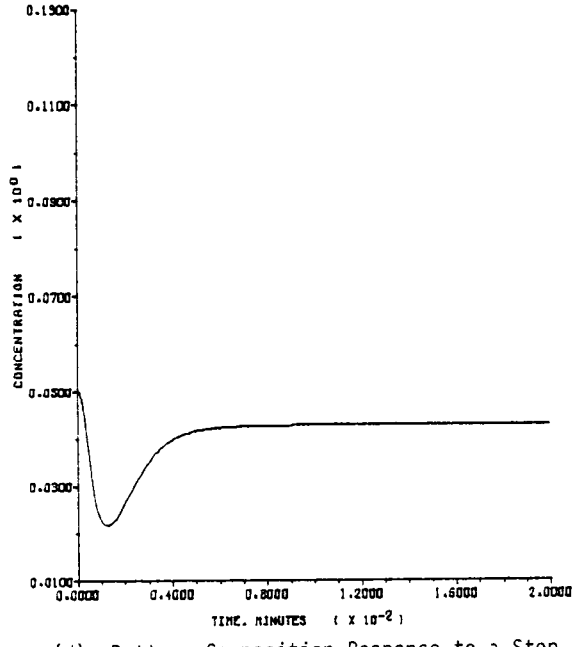

(d) Bottoms Composition Response to a Step Increase in Bottoms Controller Output.

FIGURE 26. OPEN LOOP IDEAL P-CANONICAL DECOUPLER WITH FIRST ORDER LAG DERIVED ELEMENTS.

Figure 27 shows the closed loop response of this system to a feed composition disturbance. The error corresponding to these controller parameters was 0.757 minutes.

Alternate Simplified Decoupling

An alternate simplified p-canonical decoupling strategy was tried, in which H_{21} was set equal to 1 rather than H_{11}. Decoupling elements were first derived using the first order lag process model. This simplified decoupler was attached to the column and open loop tests conducted to determine how effectively the process interaction was canceled. The test results are shown in Figure 28. Again, according to theory, parts b and c should exhibit no interaction. From part b it was determined that the peak bottoms composition excursion was 0.026 and the final offset 0.007. When the bottoms composition controller output was changed, part c showed a peak distillate composition excursion of 0.018 and a final offset of 0.002.

The loop was then closed around the column and decoupler. The controller proportional gains and integral reset times were optimized using a Pattern search and the results given.

$P_D = -211.$ $\quad P_B = 391.$

$I_D = 20.89$ min. $\quad I_B = 46.27$ min.

Figure 29 shows the closed loop response of this system to a feed composition disturbance. The IAE corresponding to these controller parameters was 0.6111 minutes.

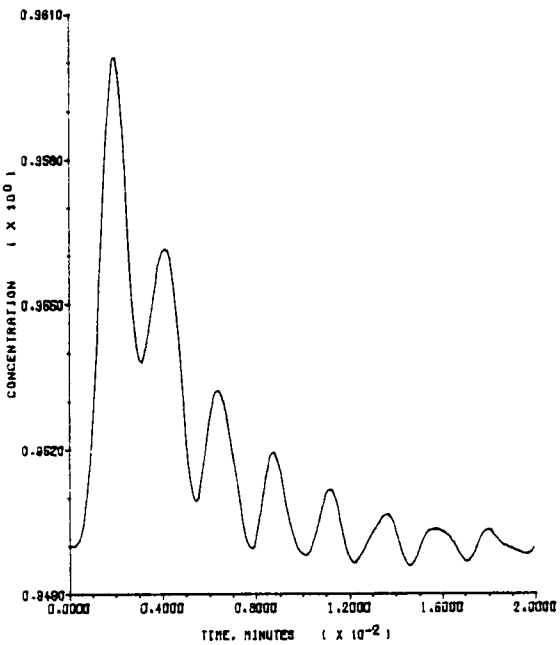

(a) Distillate Composition.

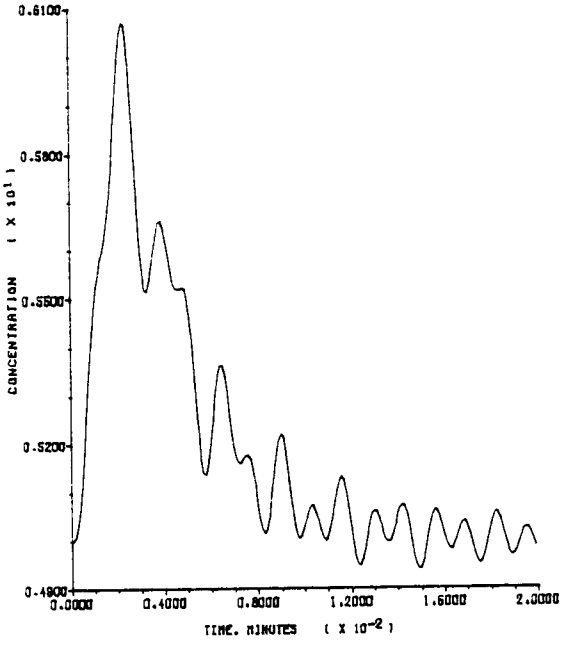

(b) Bottoms Composition.

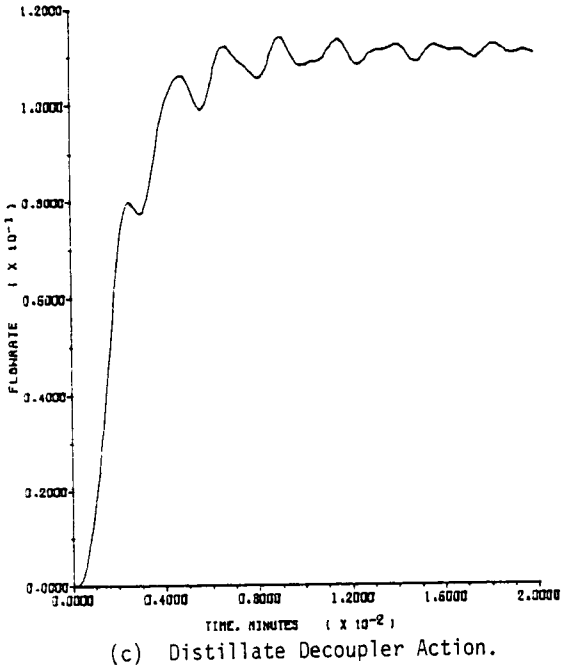

(c) Distillate Decoupler Action.

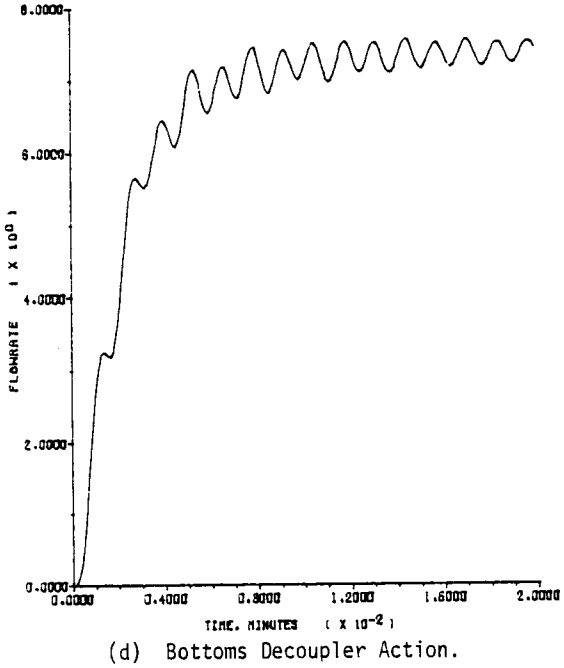

(d) Bottoms Decoupler Action.

FIGURE 27. CLOSED LOOP IDEAL P-CANONICAL DECOUPLER WITH FIRST ORDER LAG DERIVED ELEMENTS.

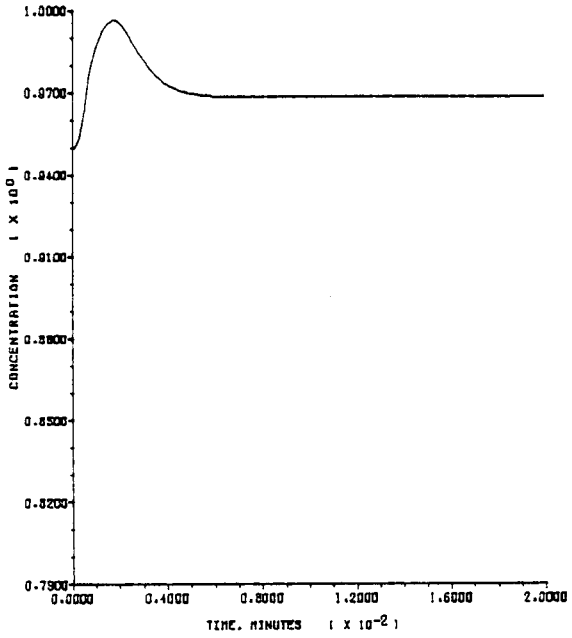

(a) Distillate Composition Response to a Step Increase in Distillate Controller Output.

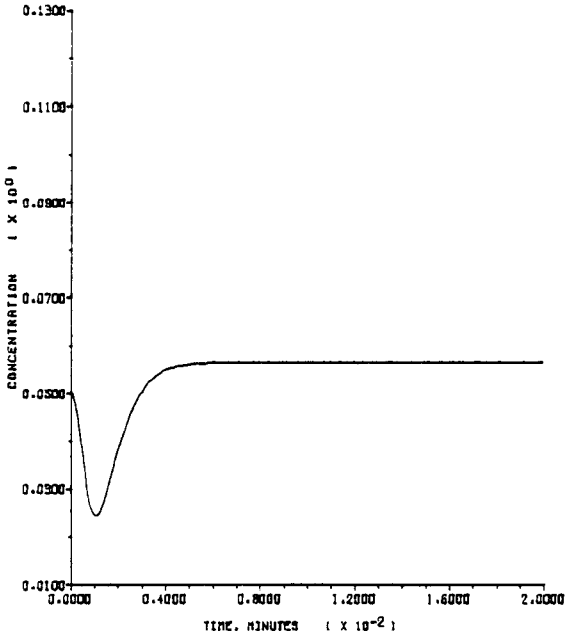

(b) Bottoms Composition Response to a Step Increase in Distillate Controller Output.

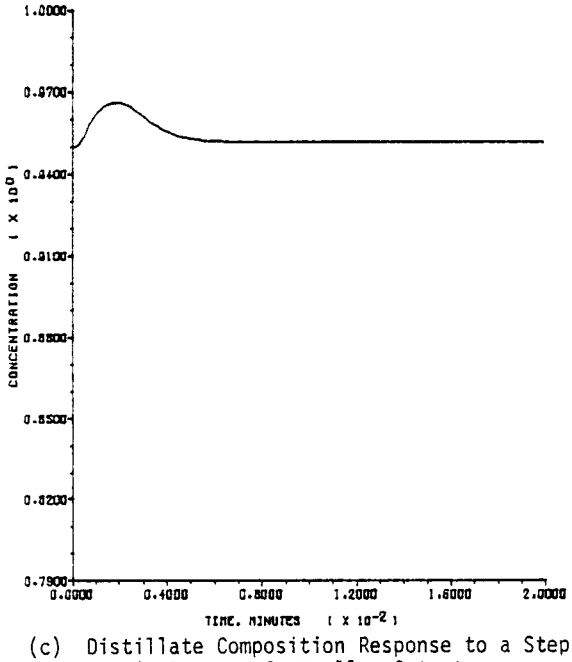

(c) Distillate Composition Response to a Step Increase in Bottoms Controller Output.

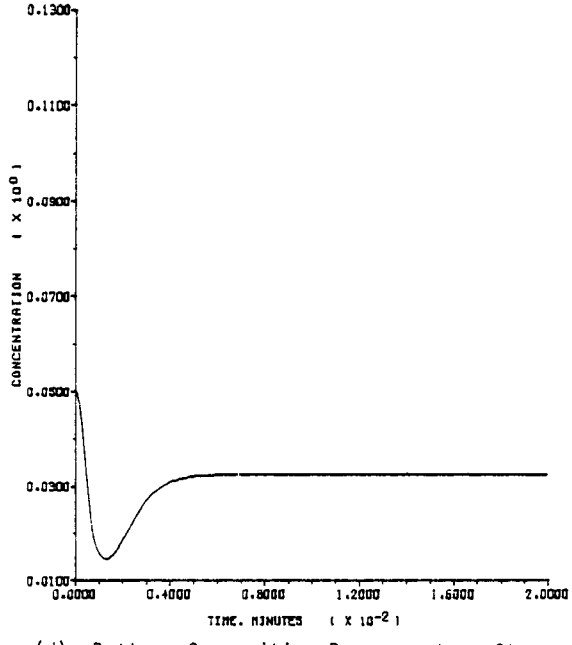

(d) Bottoms Composition Response to a Step Increase in Bottoms Controller Output.

FIGURE 28. OPEN LOOP ALTERNATE SIMPLIFIED P-CANONICAL DECOUPLER WITH FIRST ORDER LAG DERIVED ELEMENTS.

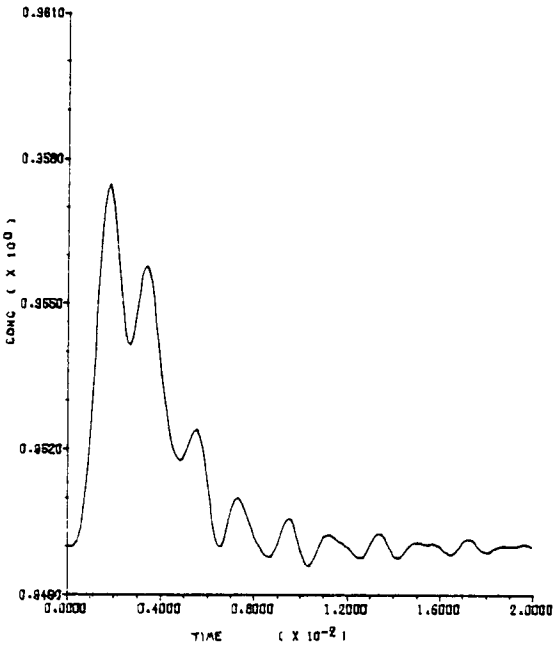

(a) Distillate Composition.

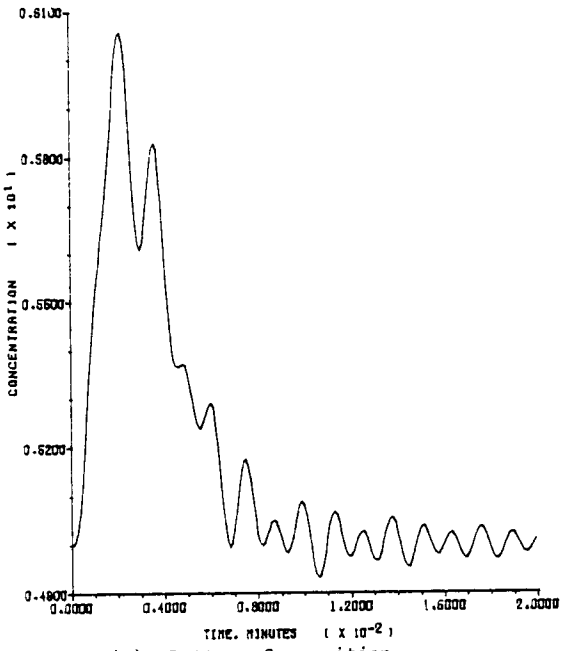

(b) Bottoms Composition.

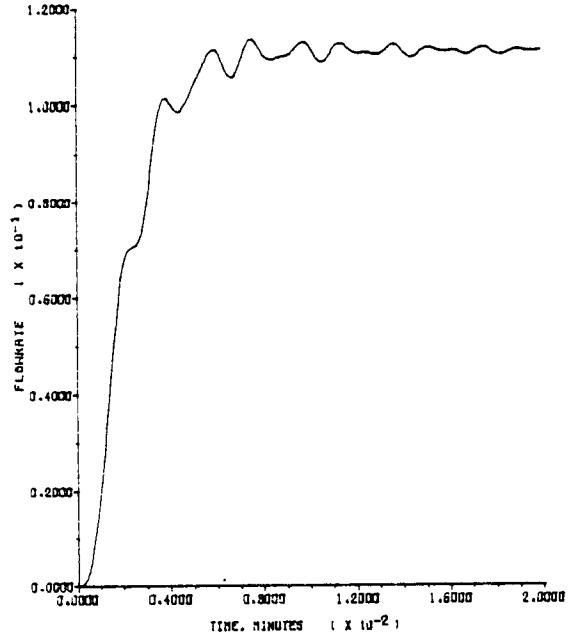

(c) Distillate Decoupler Action.

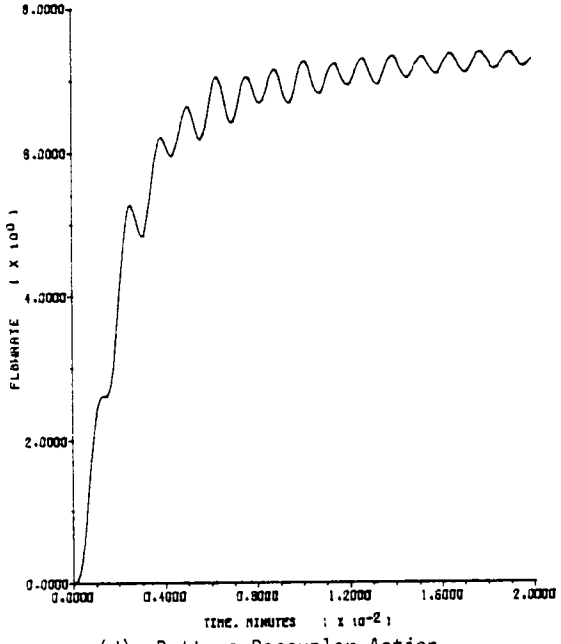

(d) Bottoms Decoupler Action.

FIGURE 29. CLOSED LOOP ALTERNATE SIMPLIFIED P-CANONICAL DECOUPLER WITH FIRST ORDER LAG DERIVED ELEMENTS.

It should be noted that steady-state derived elements were also used in each of the types of p-canonical decouplers described here. All the open loop responses had the same shape though different magnitudes. This being the case, all the closed loop responses looked identical to Figure 24; only the magnitudes of the optimum controller parameters changed.

V-Canonical Decoupler

The primary problem area for the full v-canonical decoupler was the possibility of decoupler instabilities. It was predicted in Chapter II, however, that no stability problems would be encountered for the column under consideration. To test this prediction the open-loop decouplers were examined.

Full V-canonical Decouplers

V-canonical decoupling elements were first derived using the steady-state process model. The decoupler was attached to the column and open loop tests conducted to determine how effectively the system interaction was canceled. The test results are shown in Figure 30. Like the previous open loop figures, parts a and b were distillate and bottoms composition responses to a step change in distillate controller output, and parts c and d were distillate and bottoms composition responses to a step change in bottoms controller output. According to theory, parts b and c should show no interaction. From part b it was determined that the peak bottoms composition excursion was 0.073 and the final offset 0.001. When the bottoms composition

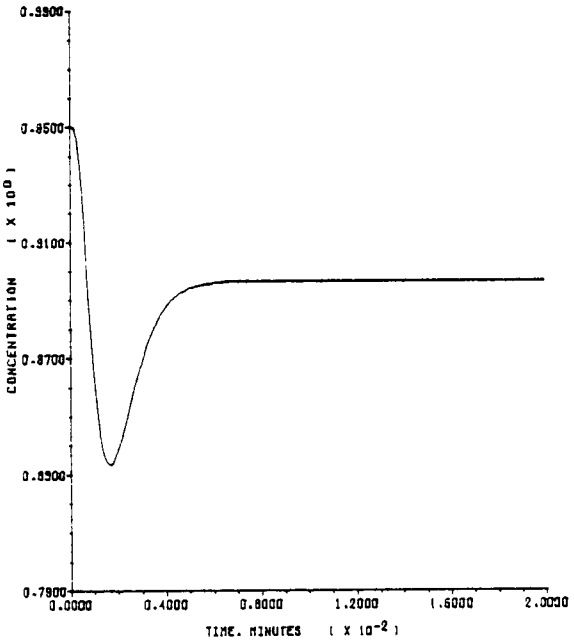

(a) Distillate Composition Response to a Step Increase in Distillate Controller Output.

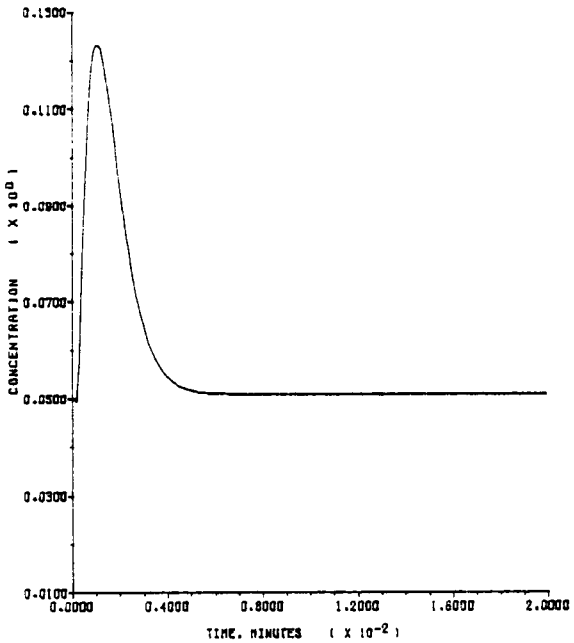

(b) Bottoms Composition Response to a Step Increase in Distillate Controller Output.

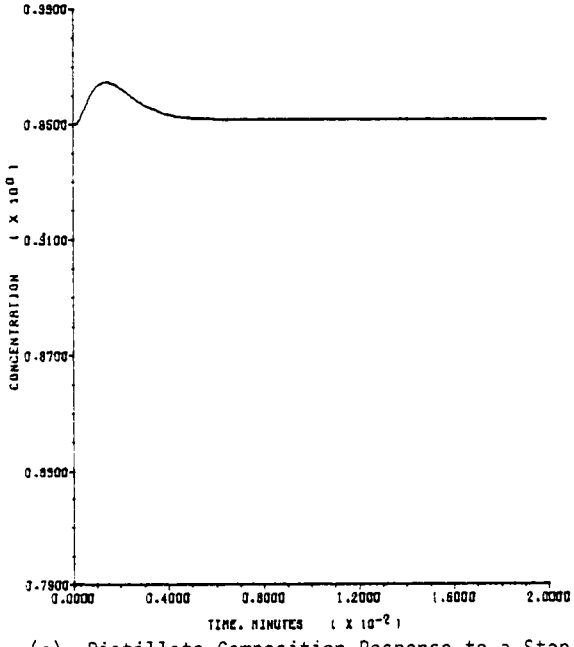

(c) Distillate Composition Response to a Step Increase in Bottoms Controller Output.

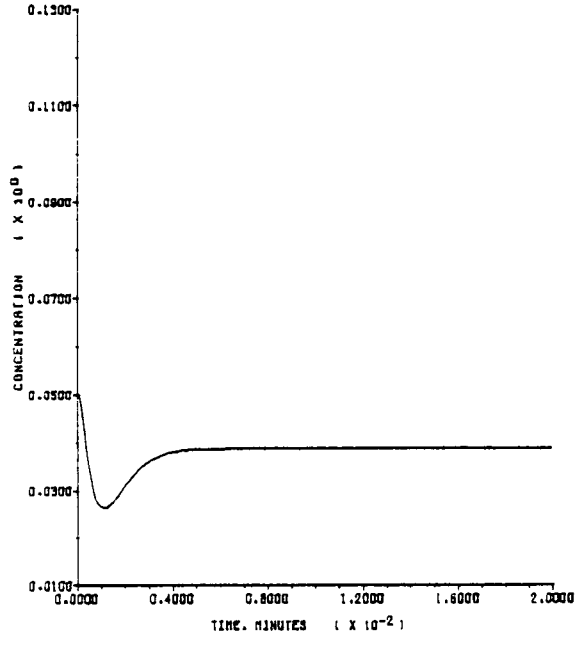

(d) Bottoms Composition Response to a Step Increase in Bottoms Controller Output.

FIGURE 30. OPEN LOOP V-CANONICAL DECOUPLER WITH STEADY-STATE DERIVED ELEMENTS.

controller output was changed, part c showed a peak distillate composition excursion of 0.016 and a final offset of 0.002.

The loop was then closed around the column with a steady-state derived v-canonical decoupler. The controller proportional gains and integral reset times were optimized using a Pattern search and the results given.

$P_D = 1001.$ $\quad P_B = 1517.$

$I_D = 5.21$ min. $\quad I_B = 3.495$ min.

Figure 31 shows the closed loop response of this system to a feed composition disturbance. The IAE corresponding to these controller parameters was 0.173 minutes, a significant improvement over any strategy examined thus far.

V-canonical decoupling elements were then derived using the first order lag process model. This decoupler was attached to the column and open loop tests conducted to determine how effectively the process interaction was canceled. The results are shown in Figure 32. According to theory, parts b and c should exhibit no interaction. From part b it was determined that the peak bottoms composition excursion was 0.053 and the final offset 0.001. When the bottoms composition controller output was changed, part c showed a peak distillate composition excursion of 0.020 and a final offset of 0.002.

The loop around the column and decoupler was then closed. The controller proportional gains and integral reset times were optimized using a Pattern search and the results given.

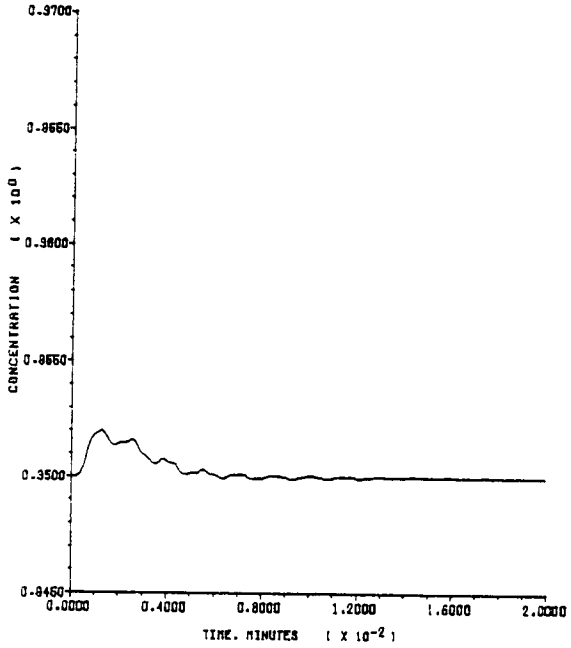

(a) Distillate Composition.

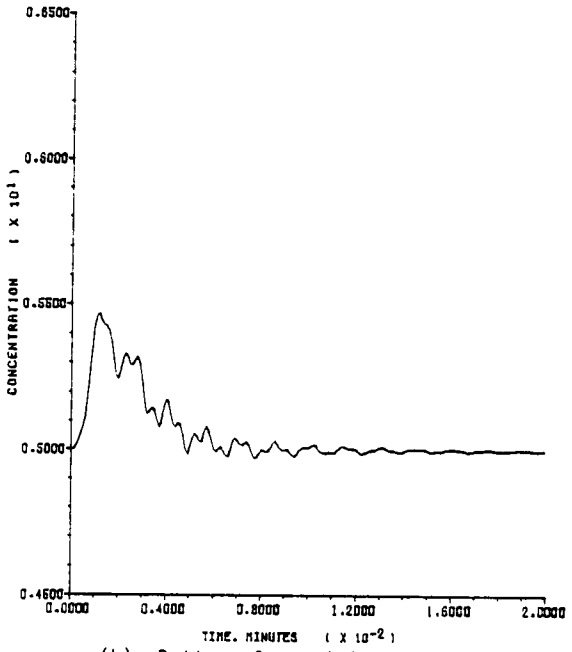

(b) Bottoms Composition.

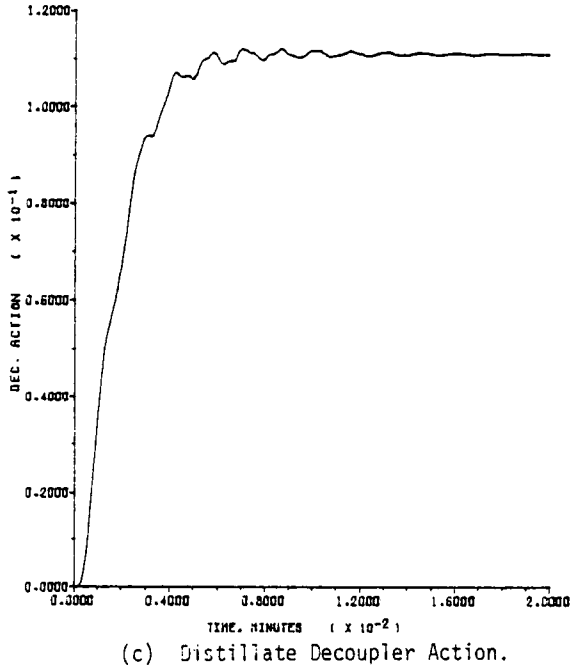

(c) Distillate Decoupler Action.

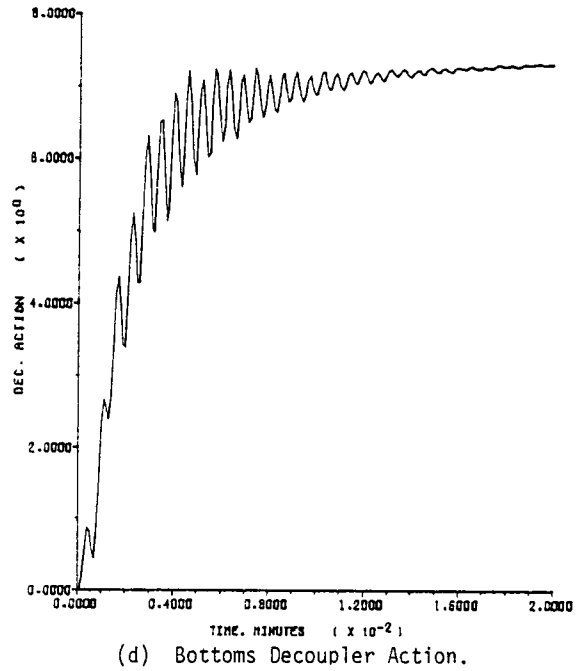

(d) Bottoms Decoupler Action.

FIGURE 31. CLOSED LOOP V-CANONICAL DECOUPLER WITH STEADY-STATE DERIVED ELEMENTS.

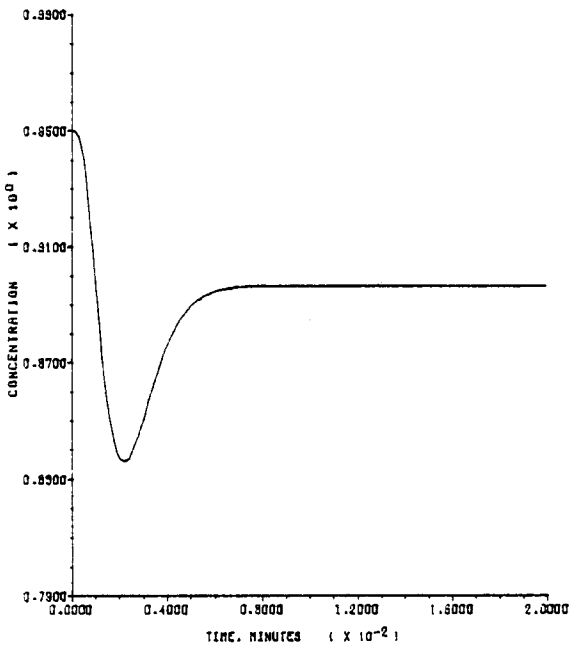

(a) Distillate Composition Response to a Step Increase in Distillate Controller Output.

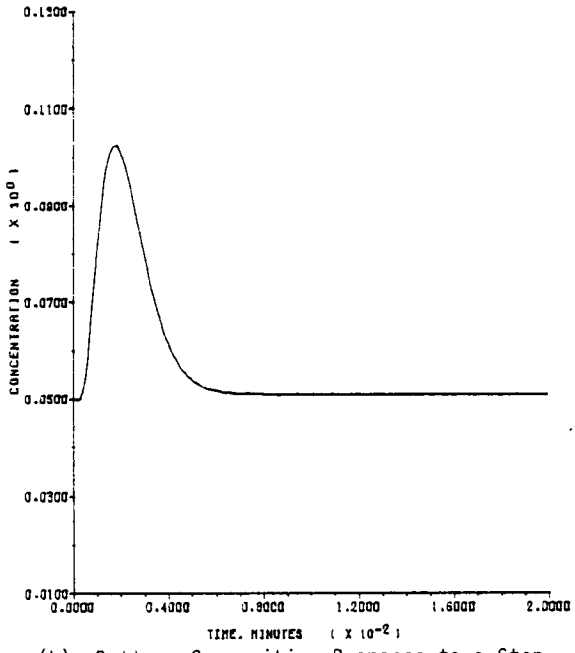

(b) Bottoms Composition Response to a Step Increase in Distillate Controller Output.

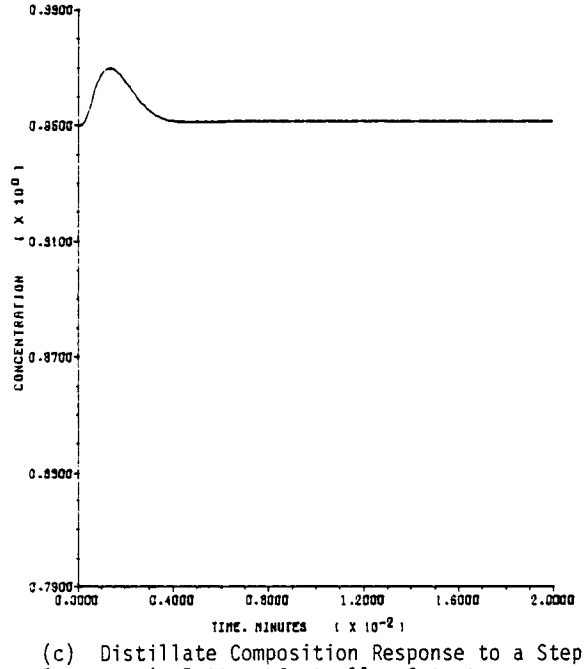

(c) Distillate Composition Response to a Step Increase in Bottoms Controller Output.

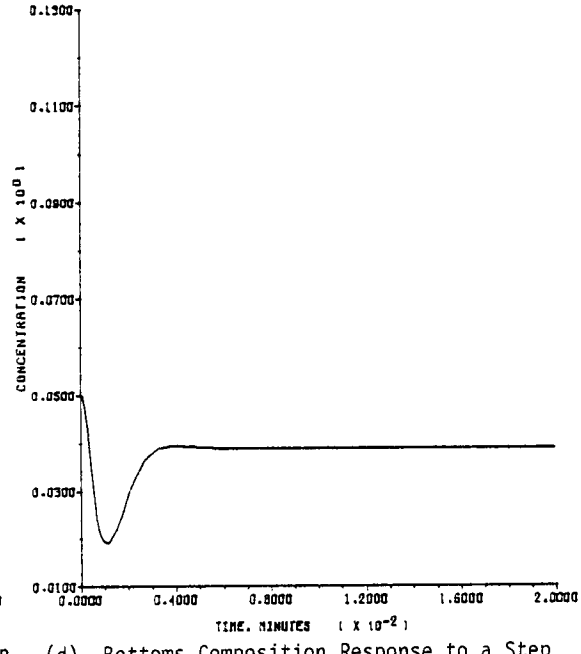

(d) Bottoms Composition Response to a Step Increase in Bottoms Controller Output.

FIGURE 32. OPEN LOOP V-CANONICAL DECOUPLER WITH FIRST ORDER LAG DERIVED ELEMENTS.

$P_D = 243.$ $P_B = 329.$

$I_D = 59.41$ $I_B = 30.92$

Figure 33 shows the closed loop response of this system to a feed composition disturbance. The IAE corresponding to these controller parameters was 0.7301 minutes.

In general, it can be concluded that the full v-canonical decoupler was stable for the system under consideration.

Partial Decouplers

If the full v-canonical decoupler had been unstable, one solution would have been to eliminate one decoupling element, leaving a partial decoupler. Practical considerations about which element to leave out were discussed in Chapter II. In the present study each was eliminated in turn.

First the distillate composition loop was decoupled from any interaction from the bottoms composition loop, leaving the bottoms loop to feel interaction from the distillate. The same element derived from the first order lag process model for the full v-canonical decoupler was used. The decoupler was attached to the column and open loop tests conducted to determine how effectively the system interaction was canceled. The test results are shown in Figure 34. Like the previous open loop figures, parts a and b were distillate and bottoms composition responses to a step change in distillate controller output, and parts c and d were distillate and bottoms composition responses to a step change in bottoms controller output.

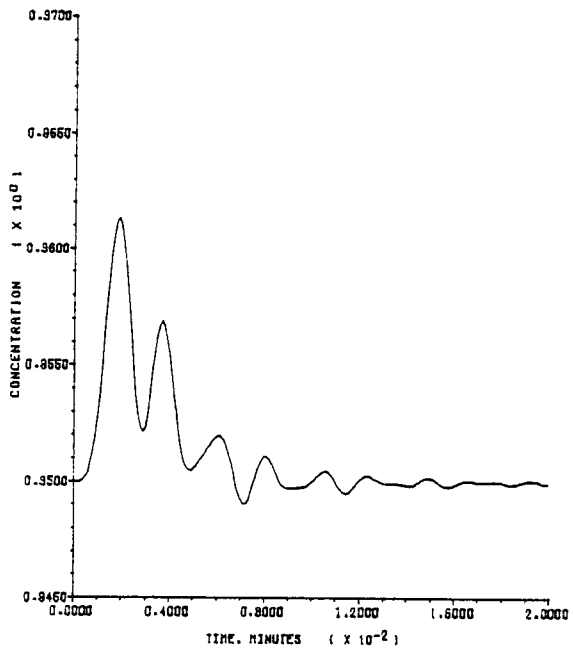

(a) Distillate Composition.

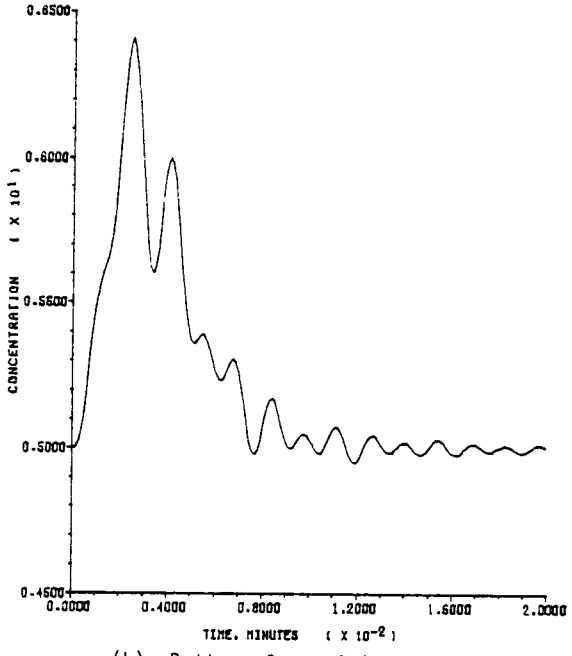

(b) Bottoms Composition.

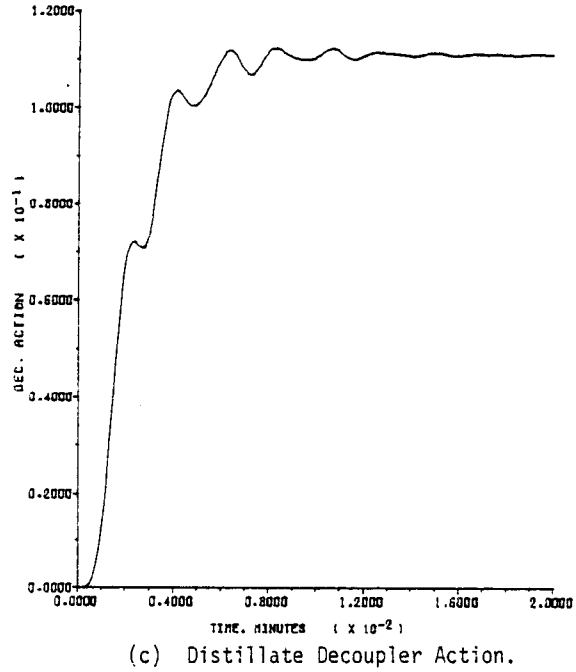

(c) Distillate Decoupler Action.

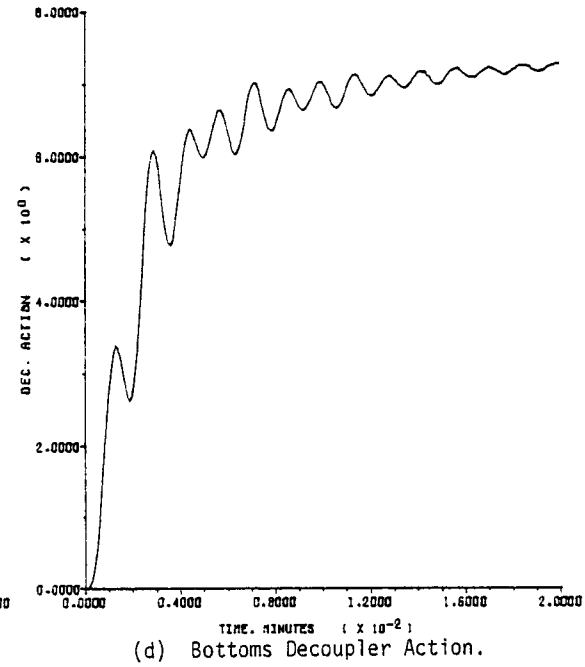

(d) Bottoms Decoupler Action.

FIGURE 33. CLOSED LOOP V-CANONICAL DECOUPLER WITH FIRST ORDER LAG DERIVED ELEMENTS.

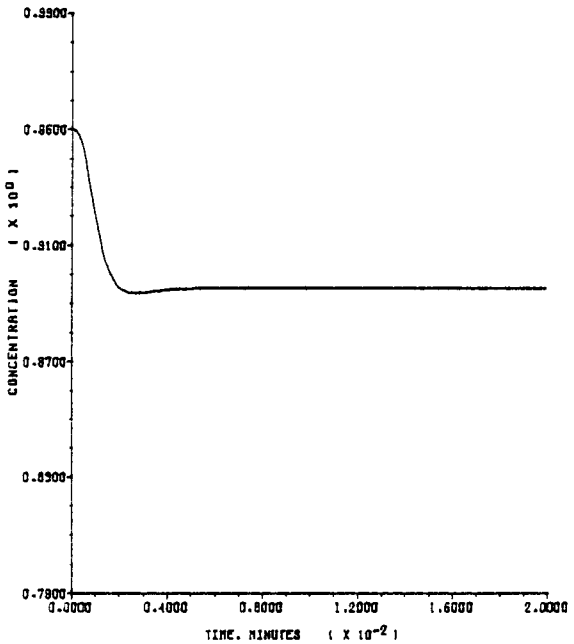

(a) Distillate Composition Response to a Step Increase in Distillate Controller Output.

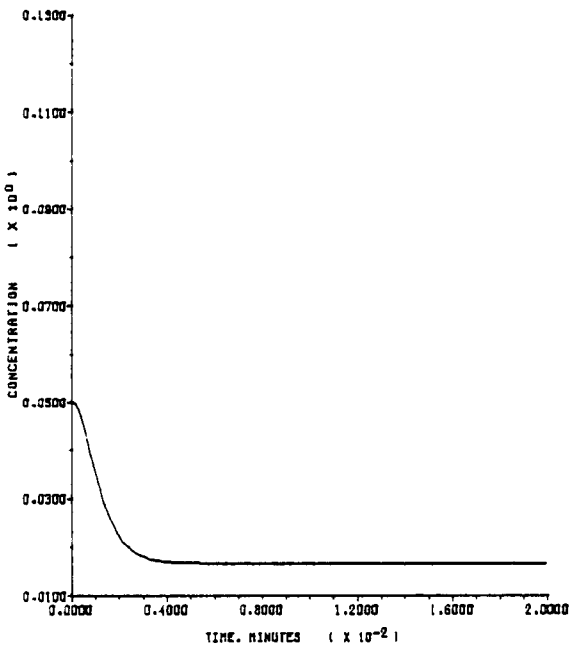

(b) Bottoms Composition Response to a Step Increase in Distillate Controller Output.

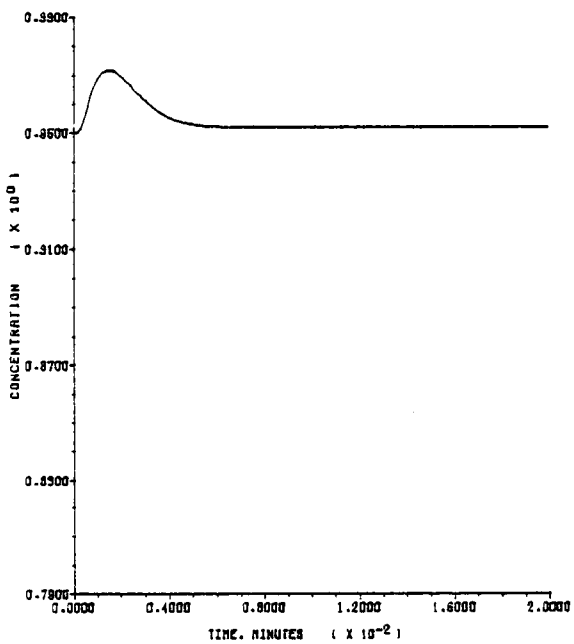

(c) Distillate Composition Response to a Step Increase in Bottoms Controller Output.

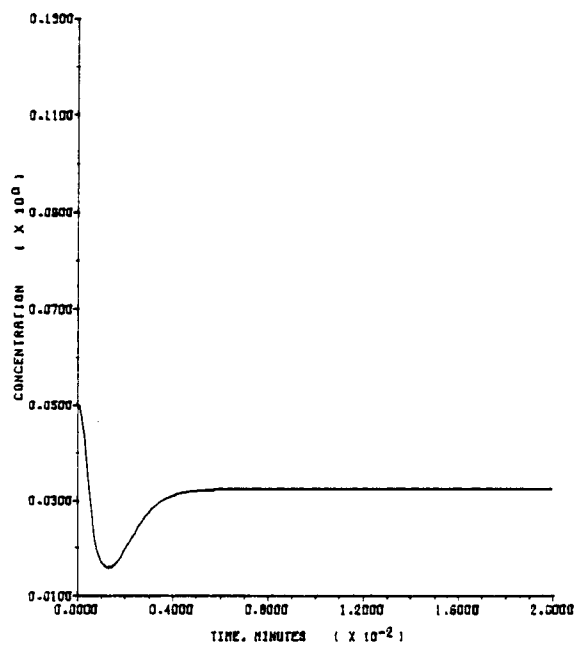

(d) Bottoms Composition Response to a Step Increase in Bottoms Controller Output.

FIGURE 34. OPEN LOOP PARTIAL DECOUPLER (DISTILLATE DECOUPLED) WITH FIRST ORDER LAG DERIVED ELEMENTS.

In this case, however, part b should show interaction and part c should not. From part c, it was determined that the peak distillate composition excursion was 0.022 and the final offset 0.002.

The loop was then closed around the column with distillate decoupling. The controller proportional gains and integral reset times were optimized using Pattern search and the results given.

$P_D = 605.$ $\quad P_B = 61.$

$I_D = 101.3$ min. $\quad I_B = 19.18$ min.

Figure 35 shows the closed loop response of this system to a feed composition disturbance. The IAE corresponding to these controller parameters was 0.433 minutes.

The bottoms composition loop was then decoupled from any interaction from the distillate loop, leaving the distillate loop to feel interaction from the bottoms. The same element derived for the full block diagram decoupler was used. The decoupler was attached to the column and open loop tests were conducted to determine how well the system interaction was canceled. The results are shown in Figure 36. In this case, part b should be decoupled, but part c should show interaction. From part b, it was determined that the peak bottoms composition excursion was 0.067 and the final offset 0.006.

The loop was then closed around the column with bottoms decoupling. The controller proportional gains and integral reset times were optimized using a Pattern search and the results given.

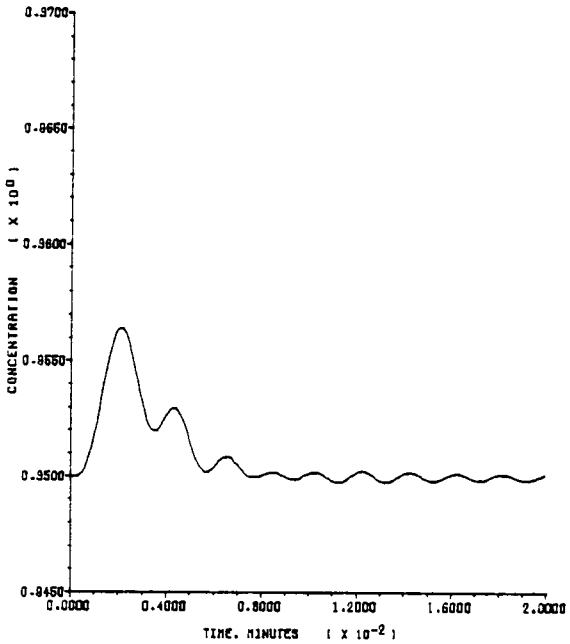

(a) Distillate Composition.

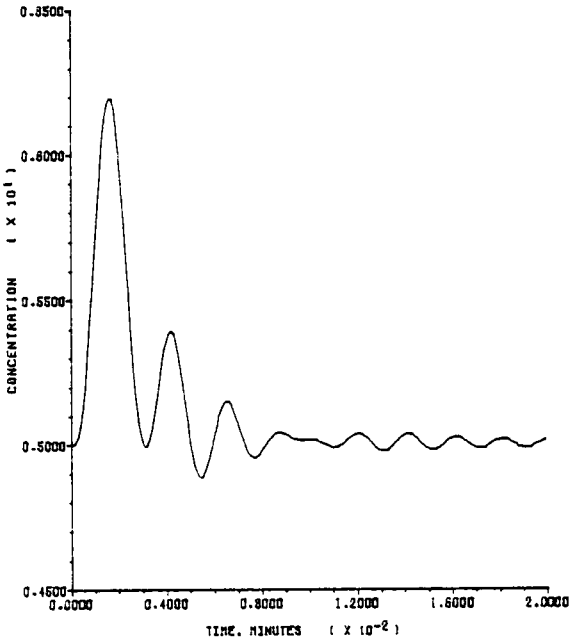

(b) Bottoms Composition.

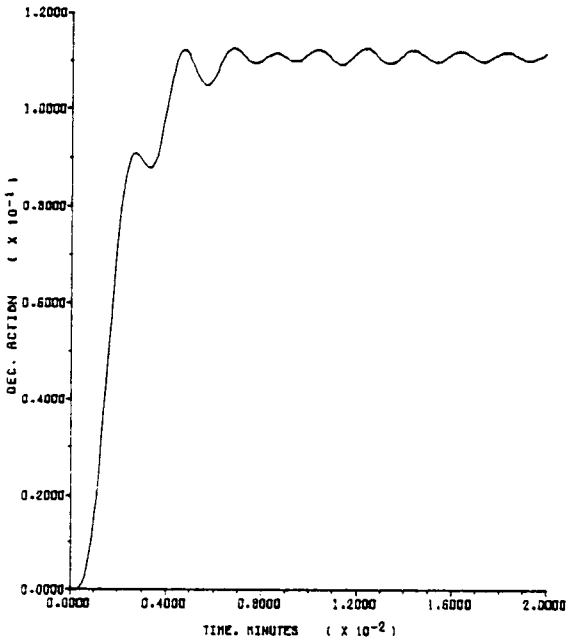

(c) Distillate Decoupler Action.

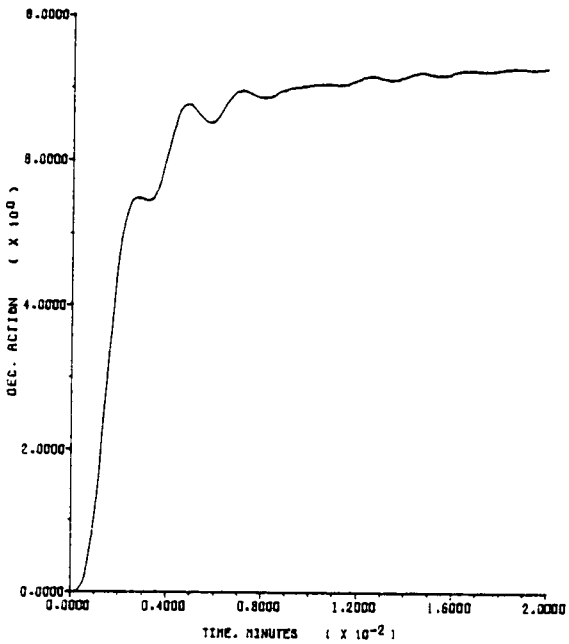

(d) Bottoms Decoupler Action.

FIGURE 35. CLOSED LOOP PARTIAL DECOUPLER (DISTILLATE DECOUPLED) WITH FIRST ORDER LAG DERIVED ELEMENTS.

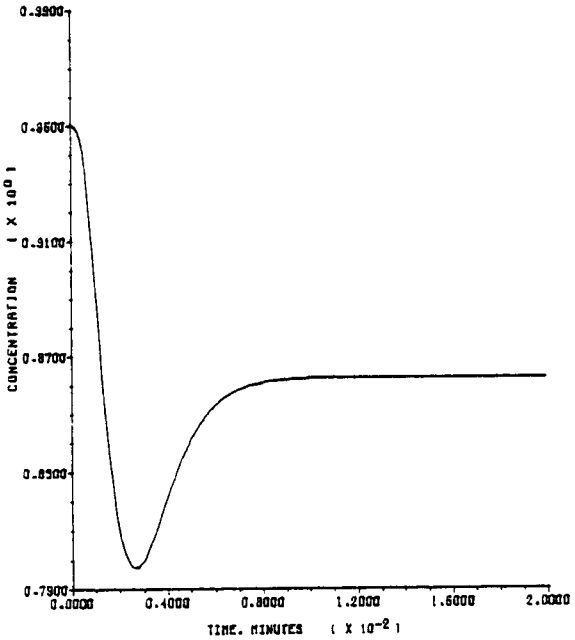

(a) Distillate Composition Response to a Step Increase in Distillate Controller Output.

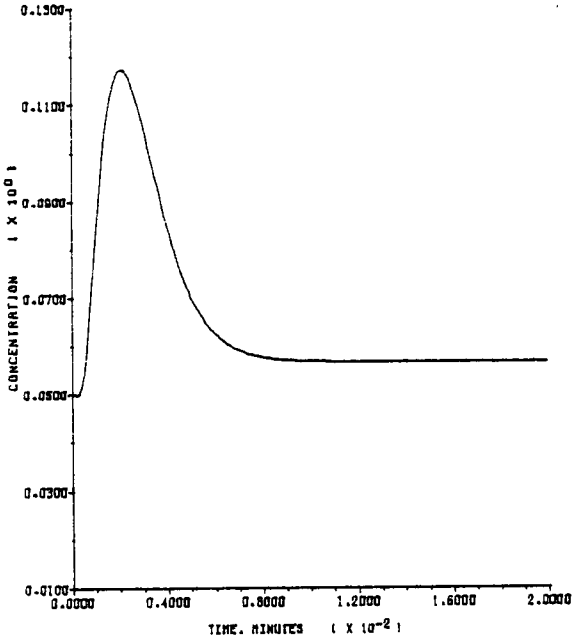

(b) Bottoms Composition Response to a Step Increase in Distillate Controller Output.

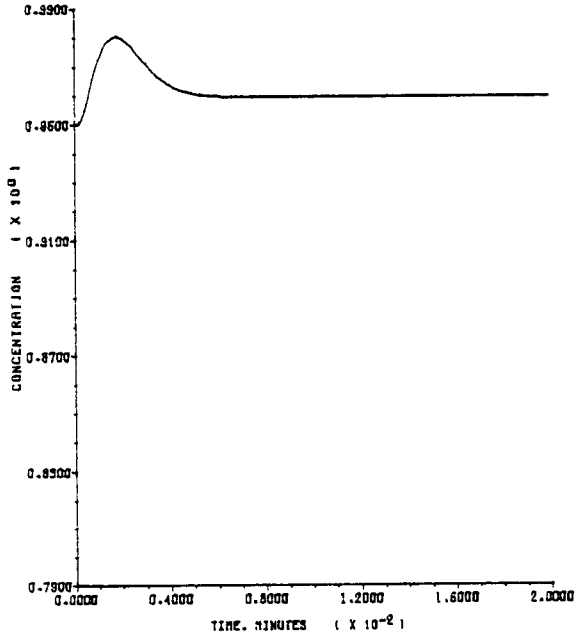

(c) Distillate Composition Response to a Step Increase in Bottoms Controller Action.

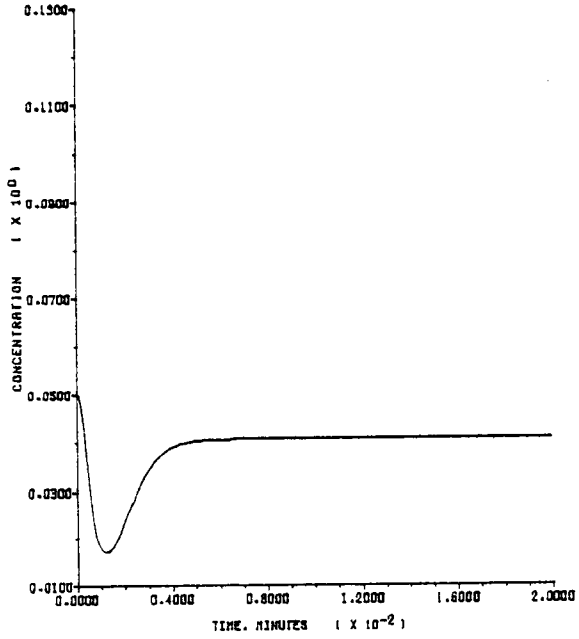

(d) Bottoms Composition Response to a Step Increase in Bottoms Controller Action.

FIGURE 36. OPEN LOOP PARTIAL DECOUPLER (BOTTOMS DECOUPLED) WITH FIRST ORDER LAG DERIVED ELEMENTS.

P_D = 187. P_B = 459.

I_D = 55.0 min. I_B = 36.7 min.

Figure 37 shows the closed loop response of this system to a feed composition disturbance. The IAE corresponding to the controller parameters was 0.764 minutes.

New Variable Methods

As described in Chapter II, two new-variable schemes were examined: one proposed by Ryskamp and one proposed by Waltz. As these methods manipulate and control, respectively, new variables, it makes little sense to examine the open loop systems.

Ryskamp's scheme of manipulating G and D/G to control x_B and x_D, respectively, was implemented on the column. The loop around the column was closed and the controller tuning parameters optimized. The results are given.

P_D = 1.235 P_B = 932

I_D = 6.432 min. I_B = 4.50 min.

The IAE corresponding to these controller parameters was 0.223 minutes.

Waltz's scheme of manipulating D to control x_D and G to control the separation factor, S, was implemented on the column. The loop around the column was closed and the controller tuning parameters optimized. The results were:

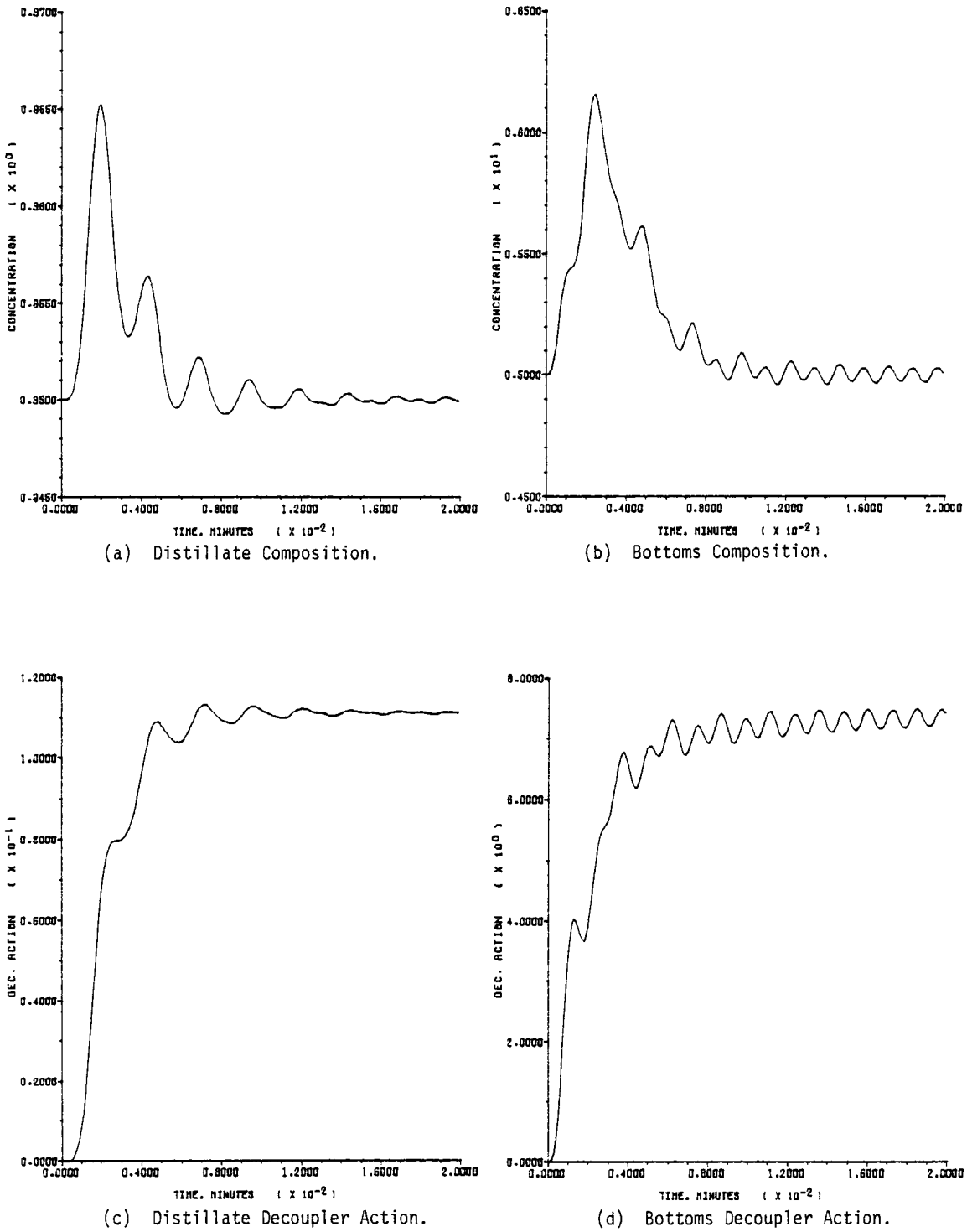

(a) Distillate Composition.

(b) Bottoms Composition.

(c) Distillate Decoupler Action.

(d) Bottoms Decoupler Action.

FIGURE 37. CLOSED LOOP PARTIAL DECOUPLER (BOTTOMS DECOUPLED) WITH FIRST ORDER LAG DERIVED ELEMENTS.

P_D = 655. P_S = -0.048

I_D = 5.40 min. I_S = 3.29 min.

where the subscript S corresponds to controlling the separation factor. The error corresponding to these controller parameters was 0.281 minutes. Figure 38 shows the closed loop response of both systems to a feed composition disturbance.

SVD Controller

The SVD controller described in Chapter 2 was implemented on the column. An "open loop" system of sorts could be examined by including the feedback loop and the V and U^T matricies of Figure 9, page 20, with the controllers in manual. If the structured variables are examined, they should be decoupled in the steady state. (No dynamics are included in the singular value decomposition.) A step increase was made in the bottoms controller action which is a structured input to the system. The resulting real inputs to the column are shown along with the structured outputs in Figure 39. Part c of Figure 39 was the structured distillate composition error which should be unaffected in the steady state. Examining part c reveals that the maximum excursion was 0.142 and the final offset 0.068. This seemed high and was probably due to the column nonlinearities as the real inputs to the column were of opposite sign from those used to find the steady-state gains.

The loop was then "closed" around the column and SVD controller (the controllers were put on automatic) and a step disturbance of the

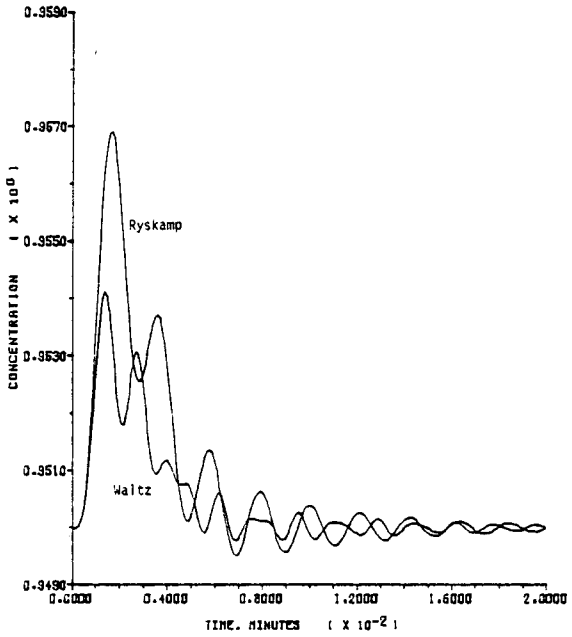

(a) Distillate Composition.

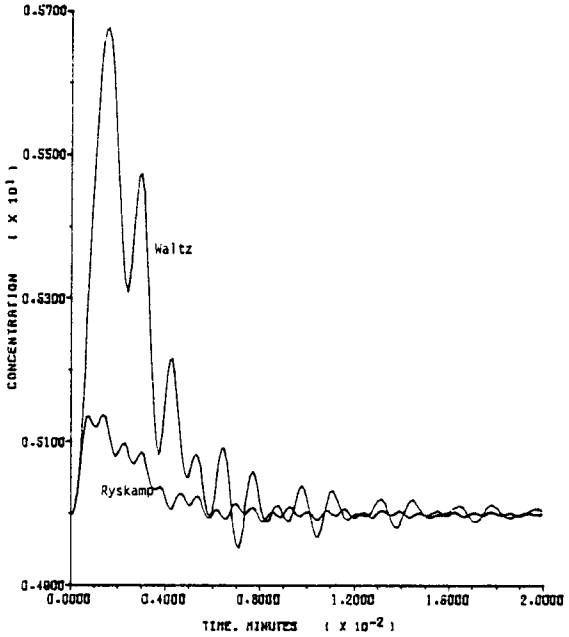

(b) Bottoms Composition.

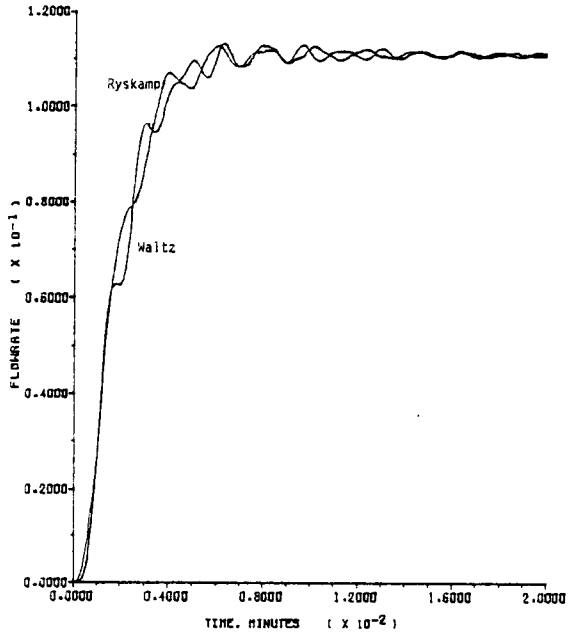

(c) Distillate Controller Action.

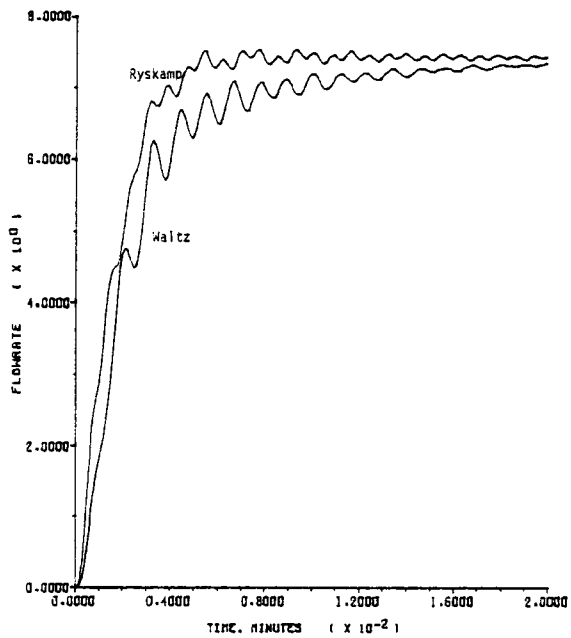

(d) Bottoms Controller Action.

FIGURE 38. CLOSED LOOP RESPONSE OF RYSKAMP AND WALTZ CONTROL STRATEGIES.

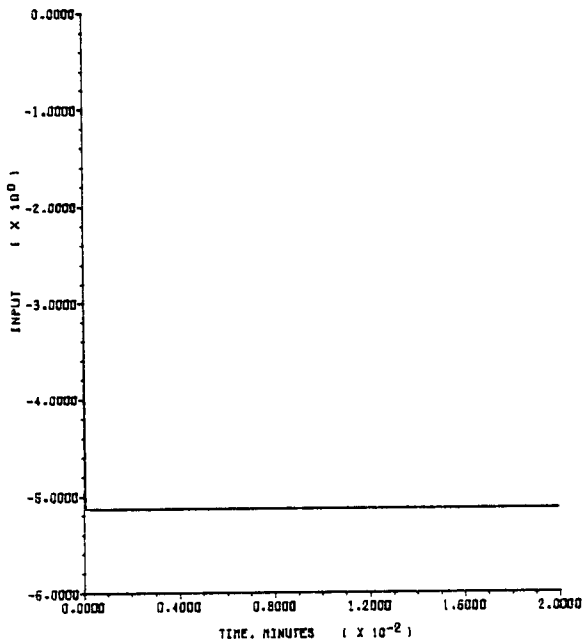

(a) Real Distillate Controller Action.

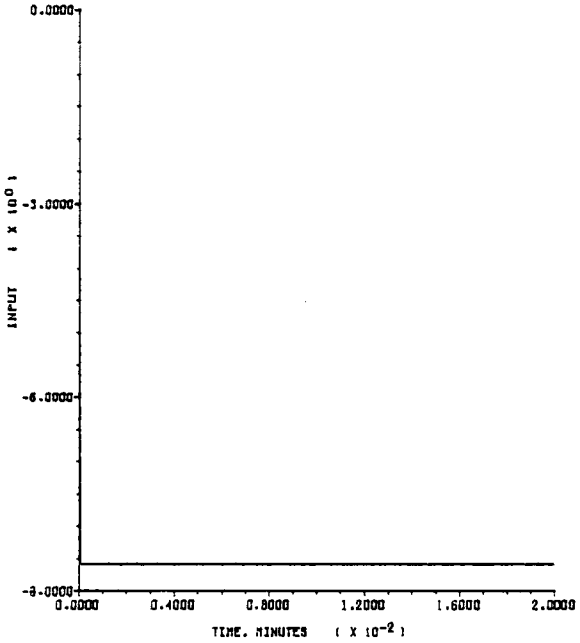

(b) Real Bottoms Controller Action.

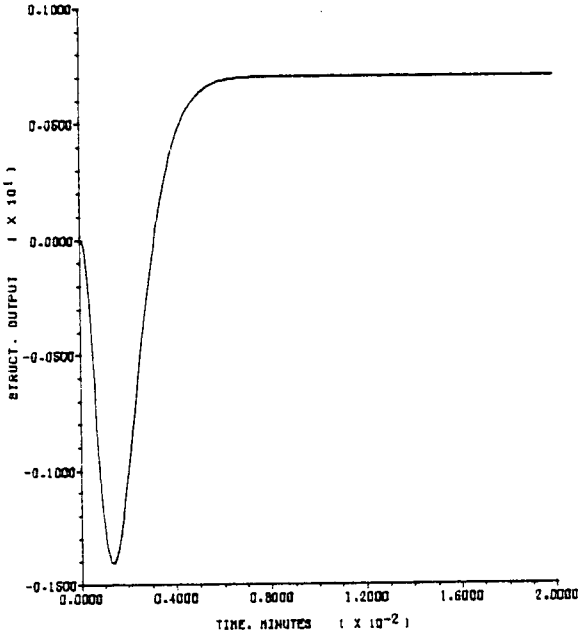

(c) Structured Distillate Composition Error

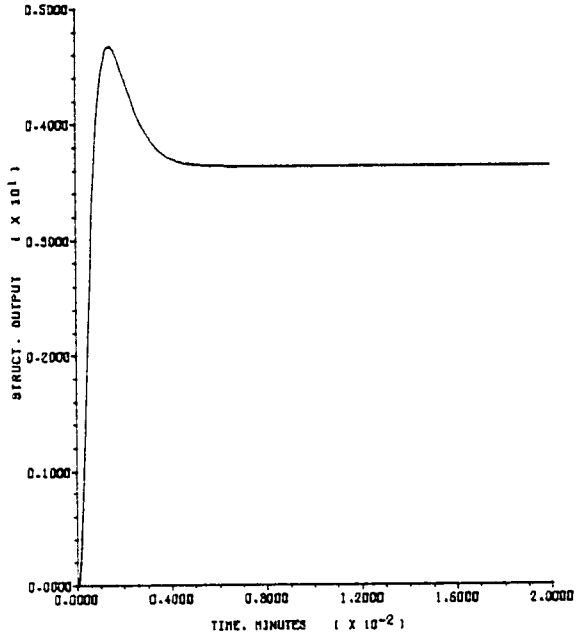

(d) Structured Bottoms Composition Error.

FIGURE 39. RESPONSE OF SVD SYSTEM TO A STEP INCREASE IN THE STRUCTURED BOTTOMS CONTROLLER ACTION.

feed composition was made. The controller proportional gains and integral reset times were optimized using a Pattern search and the results given.

$P_D = 730.$ $\quad\quad$ $P_B = 221.$

$I_D = 9.25$ min. $\quad\quad$ $I_B = 2.13$ min.

Figure 40 shows the response of the system. Parts a and b are the distillate and bottoms compositions (real process outputs), parts c and d the structured distillate and bottoms composition errors (inputs to the controllers), parts e and f the outputs from the distillate and bottoms controllers (structured process inputs), and parts g and h are the real distillate and steam rate changes to the column. The error for the SVD controller with optimum parameters was 0.209 minutes.

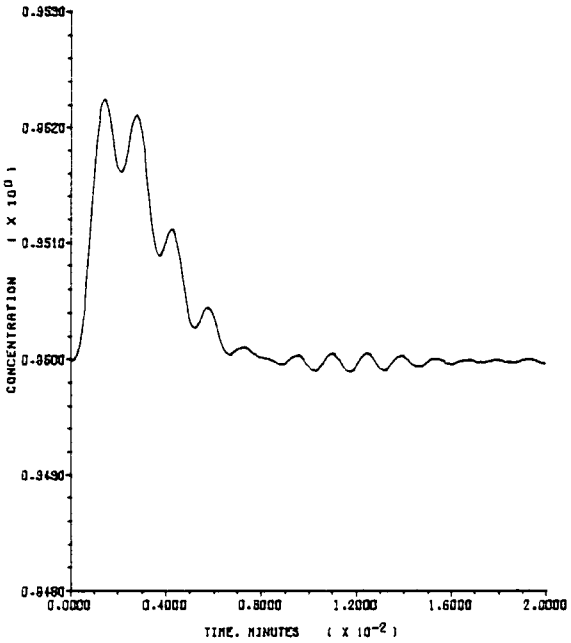

(a) Distillate Composition.

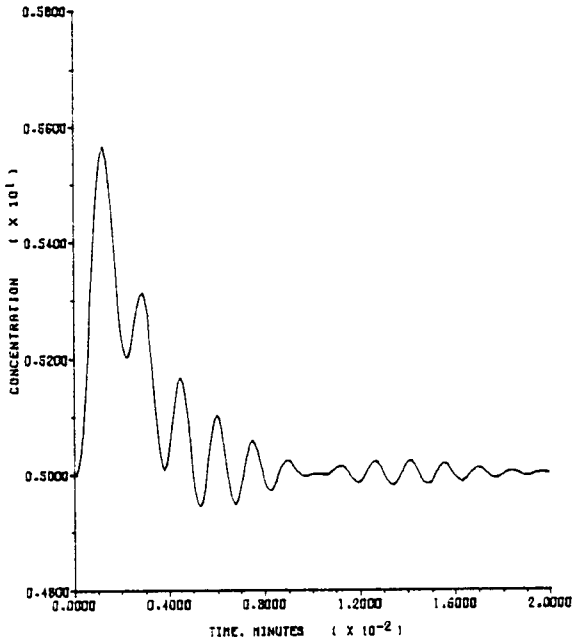

(b) Bottoms Composition.

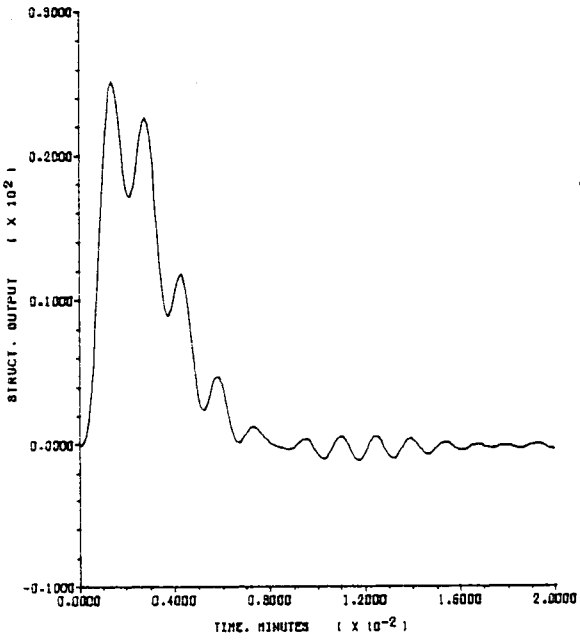

(c) Structured Distillate Composition Error

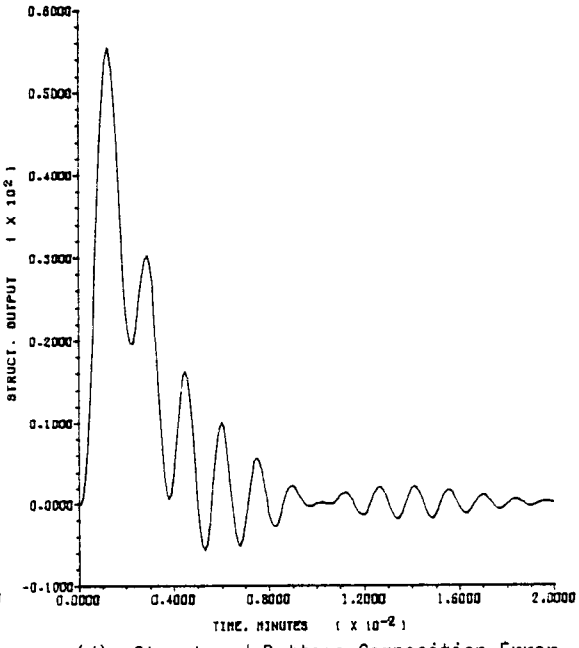

(d) Structured Bottoms Composition Error.

FIGURE 40. RESPONSE OF SVD SYSTEM TO A FEED COMPOSITION DISTURBANCE.

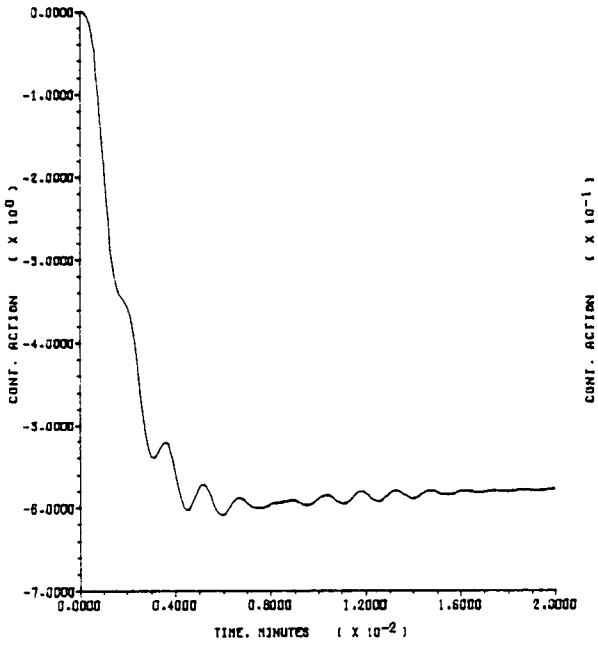

(e) Structured Distillate Controller Action

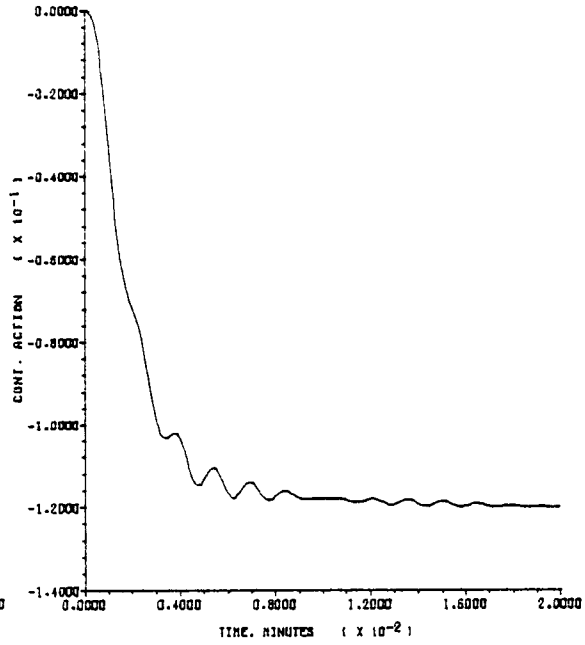

(f) Structured Bottoms Controller Action.

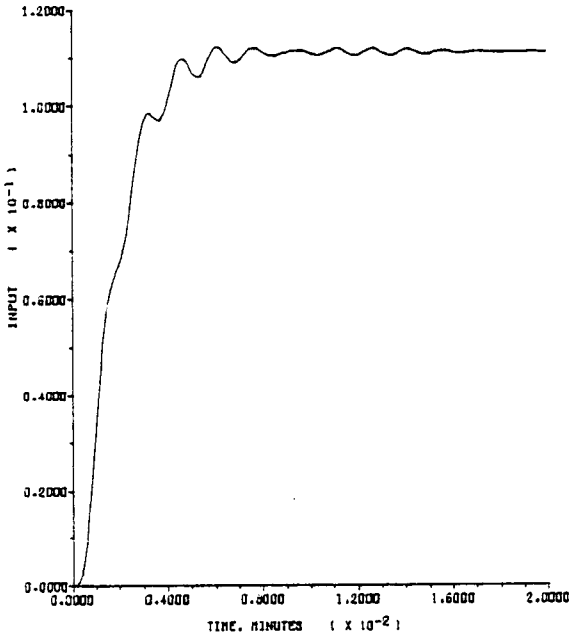

(g) Real Distillate Controller Action.

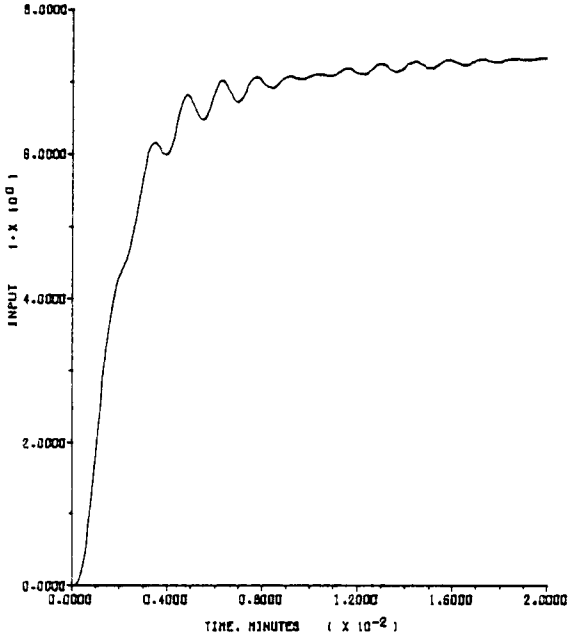

(h) Real Bottoms Controller Action.

FIGURE 40. (CONTINUED)

CHAPTER IV

SUMMARY AND CONCLUSIONS

To test the many methods of control for the distillation column simulation used in this study a single scenario was employed. At steady-state initially with feed composition at 0.50, the distillate at 0.95, and the bottoms at 0.05, a step disturbance of +0.05 was made in the feed composition and the system response observed for 200 minutes. The control schemes could then be compared on a common basis.

For analysis of the column and control strategy design, the system was modeled by transfer functions with increasing levels of complexity. The most interesting in terms of good fit with little complexity seemed to be steady-state, first order lag, and under-damped second order lag. These models are given in equations 48-50.

Steady-state: $$G = \begin{bmatrix} -0.0054537 & 0.00091622 \\ -0.0033343 & -0.00091622 \end{bmatrix} \qquad \text{Eq. 48}$$

First order lag: $$G = \begin{bmatrix} \frac{-0.005454}{1+8.038s} & \frac{0.000917}{1+2.96s} \\ \frac{-0.003335}{1+11.07s} & \frac{-0.000916}{1+1.82s} \end{bmatrix} \qquad \text{Eq. 49}$$

Under-damped second order lag:

$$G = \begin{bmatrix} \dfrac{-0.005454}{1+2(0.727)s/0.1668+s^2/(0.1668)^2} & \dfrac{0.000919}{1+2(0.2117)s/0.2816+s^2/(0.2816)^2} \\ \dfrac{-0.003334}{1+2(0.9421)s/0.1554+s^2/(0.1554)^2} & \dfrac{-0.000917}{1+2(0.1702)s/0.4335+s^2/(0.4335)^2} \end{bmatrix} \quad \text{Eq. 50}$$

These models were developed using the distillate flowrate and the steam rate to the reboiler as the first and second manipulated variables and the distillate and bottoms compositions as the first and second controlled variables.

The open loop column did show a considerable amount of interaction. Bristol's relative gain array, which gives some indication of the steady-state interaction, was calculated.

	x_D	x_B
D	0.62058	0.37942
G	0.37942	0.62058

This array indicated that, for a non-decoupled scheme, the best loop pairing would be D-x_D and G-x_B. This did indeed turn out to be the case.

P-canonical decoupling schemes were examined and, in general, it was found that first order lag derived elements gave the best

open loop responses. When the loop was closed, however, the steady-state derived elements provided the better control.

Using Routh Stability Criterion, the full v-canonical decoupler was predicted to be stable and this proved to be the case. Again, the first order lag derived elements gave superior decoupling in the open loop. But, when the loop was closed, it was the steady-state decoupler which provided better control. Partial decouplers were also examined by eliminating each leg, in turn, of the full v-canonical decoupler.

Two new-variable schemes, which try to take into account the physical realities of the system, were attached to the column. When the controllers had been fully tuned it appeared that Ryskamp's scheme had been superior. This was predicted by McAvoy, who said Waltz's scheme does well for columns separating components with low relative volatilities. (The relative volatility for the n-octane, n-pentane system used was 2.17.)

The singular value decomposition of the steady-state process matrix was calculated and is given in Equation 45. The SVD controller was attached to the column and very good results achieved. This control strategy deserves more work and attention to develop it to the stage of introduction to the engineer in the field.

Table 6 is a summary of the control methods attempted, the IAE associated with the optimum tuning parameters, and the figure number of the system response to a step feed composition disturbance. The error figures should not be the only judge of how well a control

TABLE 6

CLOSED LOOP RESULTS SUMMARY

Control Method	Associated Error (min)	Response Figure Number
Non-Decoupled		
Forward	0.307	20
Backward	2.72	20
P-Canonical Decoupler		
Simplified		
steady-state	0.305	24
first order lag	0.5803	25
Ideal		
first order lag	0.757	27
Alternate simplified		
first order lag	0.6111	29
V-Canonical Decoupler		
Steady-state	0.173	31
First order lag	0.7301	33
Partial Decoupler		
Distillate loop	0.433	35
Bottoms loop	0.764	37

TABLE 6 (Continued)

Control Method	Associated Error (min)	Response Figure Number
New-Variable Techniques		
Ryskamp's method	0.223	38
Waltz's method	0.281	38
SVD Controller	0.209	40

system performed. Rather, an examination of the response curves should also be used. Unfortunately, the IAE was all that was available to the Pattern routine for optimizing the parameters. As a result, some less than favorable adjustments could have been made which reduced the COST but, for instance, increased the system oscillation. One possibility would have been to use a different COST criteria, such as ITAE (integral of time times absolute error) which would have sacrificed some control during the transient response in favor of a smooth steady state at long times. In practice an operator would like to avoid excessive oscillation. In this respect, plus the fact that an operator would not explore the response surface so thoroughly, the Pattern search is unrealisitc. It cannot be shown what tuning parameters a given operator would use. There is a chance that if the system were not tuned down so tight, control strategies which did not compare well here might prove superior.

Another consideration is that the methods which did well attenuating this particular feed composition disturbance might not do so well when called upon to attenuate a different feed composition disturbance or to make a set point change.

Thus, the results presented here should not be used to make definitive statements about the particular control strategies. Rather they should be used to draw general conclusions about multivariable systems. For instance, it seems that increasing decoupling complexity does not pay off in terms of increased performance. This is true both in terms of the decoupler model (for example, the simplified p-canonical decoupler seems to perform better than the ideal) and the

process model (steady-state derived elements seemed to perform better than first order lag derived elements). If better model fits could be made (for instance, fit non-linear models to the column responses), then more complexity might be warranted and even better system response might be expected.

REFERENCES

REFERENCES

(1) Bristol, E. H., "On a New Measure of Interaction for Multivariable Process Control," IEEE Trans. Autom. Control, January 1966.

(2) Changlai, Yi-Shing and Thomas J. Ward, "Decoupling Control of a Distillation Column," AIChE Journal, Vol. 18, No. 1, January 1972.

(3) Downs, J. J. and C. F. Moore, "Steady-State Gain Analysis for Azeotropic Distillation," Joint Automatic Control Conference, Charlottesville, Virginia, June 1981.

(4) Finkelstein, L., Trans. Soc. of Instr. Tech., Vol. 16, No. 114, 1964.

(5) Freeman, H., "A Synthesis Method for Multivariable Control Systems," Trans. AIEE (Applied and Industrial), Vol. 7, pt. 2, pp. 28-31, March 1957.

(6) Freeman, H., "Stability and Physical Realizability Considerations in the Synthesis of Multiple Control Systems," Trans. AIEE (Applied and Industrial), Vol. 77, pt. 2, pp. 1-5, March 1958.

(7) Gilbert, E. G., "The Decoupling of Multivariable Systems by State Variable Feedback," preprints JACC, 1968, pp. 221-223, J. SIAM Control, Vol. 7, February 1969, pp. 50-63.

(8) Kavanagh, R. S., "Noninteracting Controls in Linear Multivariable Systems," Trans. AIEE (Applied and Industrial), Vol. 74, pp. 95-100, May 1957.

(9) Ibid., Vol. 77, pp. 425-429, November 1958.

(10) Kleinpeter, J. A. and R. E. C. Weaver, "Multivariate Control of a Phase Separation Process," AIChE Journal, Vol. 17, No. 3, May 1971.

(11) Klema, V. C. and A. J. Laub, "The Singular Value Decomposition: Its Computation and Some Applications," IEEE Trans. Autom. Control, Vol. 24, No. 2, pp. 164-176, April 1980.

(12) Koppel, L. B. and P. M. Aiken, "A General Process Controller," I & EC Process Design and Development, Vol. 8, No. 174, 1969.

(13) Latour, P. R., "The Time-Optimum Control of Chemical Processes," Ph.D. Thesis, Purdue University, 1966.

(14) Luyben, William L., "Distillation Decoupling," AIChE Journal, Vol. 16, No. 2, March 1970.

(15) Luyben, William L., "Steady-State Energy Conservation Aspects of Distillation Column Control System Design," I & EC Fundamentals, pp. 321-325, 1975.

(16) McAvoy, T., "Relative Gain Expressions for Dual Composition Control," Joint Automatic Control Conference, Charlottesville, Virginia, June 1981.

(17) Mesarovic, M., The Control of Multivariable Systems, Wiley and Sons, New York, 1960.

(18) Moczeck, J. S., R. E. Otto, and T. J. Williams, "Approximation Models for the Dynamic Response of Large Distillation Columns," Chemical Engineering Progress, Ser. 55, Vol. 61, No. 136, 1965.

(19) Niederlinski, Antoni, "Two-Variable Distillation Control: Decouple or Not Decouple," AIChE Journal, Vol. 17 No. 5, September 1971.

(20) Ogata, K., State Space Analysis of Control Systems, Prentice-Hall, Englewood Cliffs, New Jersey, 1967.

(21) PATERN, IBM Share Program Library, LSU-PATE SDA3552, 1965.

(22) Pierini, P. E., M. S. Thesis, The University of Tennessee.

(23) Rich, S. E., V. S. Law, and R. E. C. Weaver, "Simulation Model Characteristics and the Performance of Multivariate Control Schemes."

(24) Rekasius, X. V., "Decoupling of Multivariable Systems by Means of State Variable Feedback," Proc. 1965 Allerton Conf., Monticello, Illinois.

(25) Rosenbrock, H. H., Trans. Inst. Chem. Eng., Vol. 40, No. 35, 1962.

(26) Ryskamp, C., "New Stragety Improves Dual Composition Column Control," Hydrocarbon Processing, Vol. 59, pp. 51-59, June 1980.

(27) Shinskey, F. G., Process Control Systems, 2nd ed., McGraw Hill, New York, 1979.

(28) Slivinsky, C. R. and D. G. Schultz, "State Variable Feedback Decoupling and Design of Multivariable Systems," Preprints JACC, 1969, pp. 869-876.

(29) Smith, C. R., C. F. Moore, and D. D. Bruns, "A Structural Framework for Multivariable Control Applications," Joint Automatic Control Conference, Charlottesville, Virginia, June 17-19, 1981.

(30) Smith, C. R., "Multivariable Control Using Singular Valve Analysis Procedures," Ph.D. Thesis, University of Tennessee, 1981.

(31) Takahashi, Y., M. S. Robins, and D. M. Avslander, Controls and Dynamic Systems, Addison-Wesley, Reading, Massachusetts, pp. 137-143, 1972.

(32) Toijala, K. and K. Fagervik, "A Digital Simulation Study of Two-Point Feedback Control of Distillation Columns," Kem. Teollisvvs, January 1972.

(33) Waller, Kurt V. T., "Decoupling in Distillation," AIChE Journal, Vol. 20, No. 3, May 1974.

(34) Waltz, A. J., "Using Separation Factor for Dual Composition Control," Instrumentation Technology, Vol. 27, No. 8, pp. 41-44, August 1980.

(35) Weischedel, K. and T. J. McAvoy, "Feasibility of Decoupling Distillation Composition Control Loops," 72nd Annual AIChE Meeting, San Francisco, California, November 1979.

(36) Zalkind, C. S., "Practical Approach to Non-Interacting Control," Instruments Control Systems, Vol. 40, Nos. 89 and 111, 1967.

APPENDIXES

APPENDIX A

COMPUTER PROGRAMS AND COLUMN SIMULATION

The column simulation used in this study (COLMD) is a pseudo-dynamic simulation consisting of a nonlinear steady-state model which drives a simple linear dynamic model. This approach was chosen because in a relatively simple program both the nonlinear and dynamic problems of the n-octane and n-pentane separation could be accurately described. Alternatively, a more rigorous simulation (reference 3) would have been much more costly in terms of computer time but would have not added much in detail to the study.

Steady-State Simulation

The steady-state portion of the simulation is a tray-to-tray calculation assuming a constant molal overflow and assuming the binary equilibrium can be described by a constant relative volatilaty. The steady-state material balances on the column are determined by a trial and error search for the compositions at the top and bottom of the column which satisfy the material balance around the feed tray. (The trial and error logic is accomplished by ZEROUT, a one dimensional search routine with good nonlinear convergence properties.) The temperature profile for the column is calculated directly from the composition on each tray. The pressure is assumed to be constant at one atmosphere.

Dynamic Simulation

The dynamic simulation is shown schematically in Figure 41. It consists of a number of linear dynamic transfer functions which are driven by the steady-state material and energy balance routine. The location and nature of the dynamics was chosen to represent the data reported by Weischedel and McAvoy (35) for the n-octane/n-pentane column.

In each case the dynamic element was chosen to be a single parameter third order lag of the form

$$G(s) = \frac{1.0}{(1 + \tau s)^3}$$

(Note the steady-state gain of the element must be unity since the steady-state character is described in the nonlinear tray-to-tray calculation.) Form simplicity the third order lag was assumed to be three first order lags in series and were implemented numerically using an analytical solution which assumes the inputs are a series of steps.

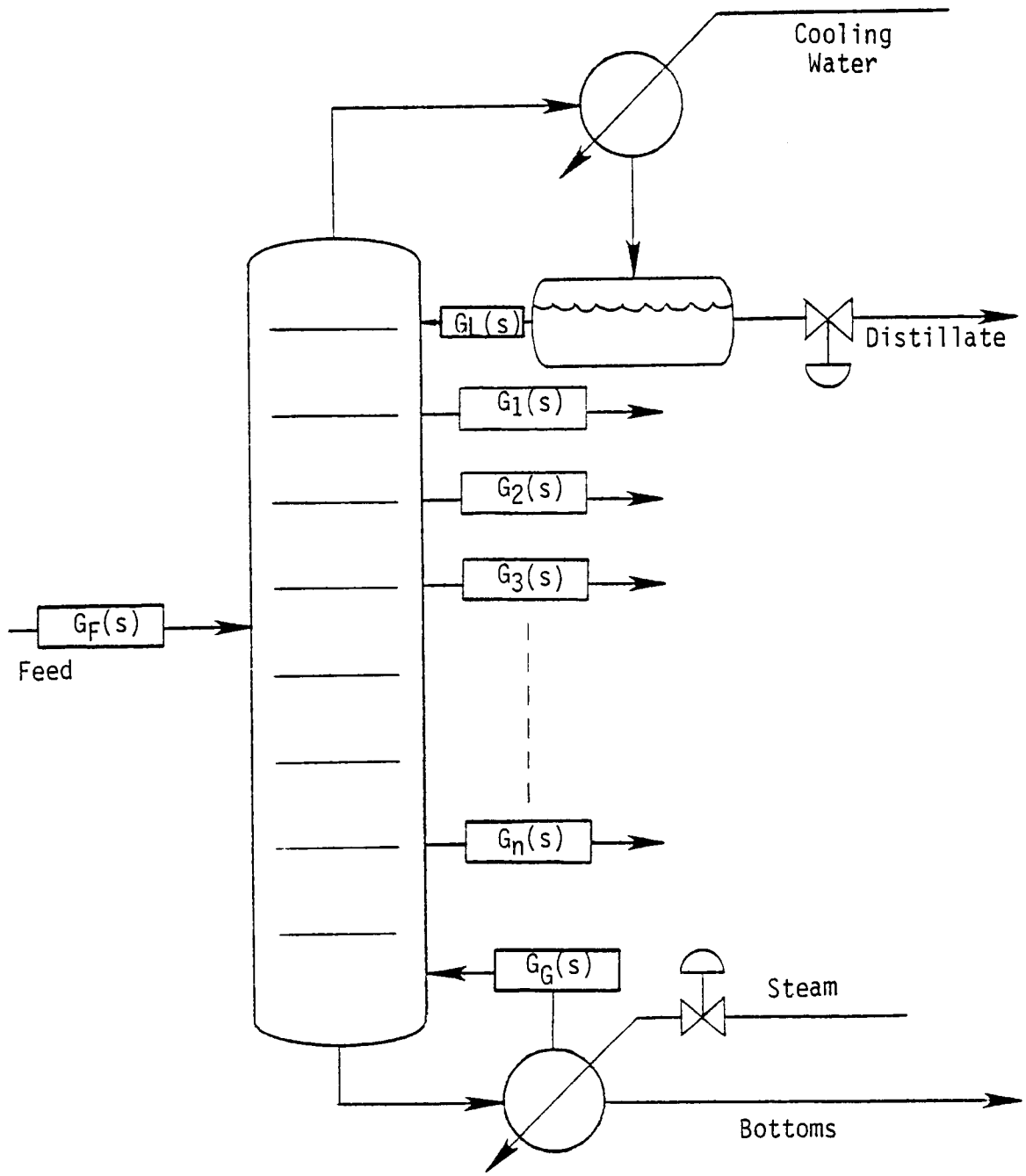

FIGURE 41. DYNAMIC MODEL SCHEMATIC.

Listing of the subroutine COLMD which is called by SS2.FOR.

```
      SUBROUTINE COLMD(FD,DD,GD,ZL,ZG,XFD,XD,XB,IC,IERR)
C-----PSEUDO-DYNAMIC COLUMN SIMULATION
      NAMELIST/DEBUG/IZZ,IFLAG,XDD,XBD,EX
      NAMELIST/BUG2/IZ,IFLAG,EXD,XDD,XBD,EX
      REAL L,LL,MF,MD,MB,MUP,MDOWN,L1,L2,LL1,LL2
      DIMENSION WORK(10)
      COMMON/PAR/NF,NB,RV,A0,A1,A2,A3
      COMMON/TAU/BL,BLL,BF,BG,BT,BD,BXS,BXR
      COMMON/XYSS/XSS(50),YSS(50),TSS(50)
      COMMON/XY/X(50),Y(50),T(50)
      COMMON/MBAL/L,LL,B,R,MF,MD,MB
      COMMON/ERR/IFLAG,EX
      IERR=0
5     IF(GD.LT.0)GD=0
      IF(DD.GT.GD)DD=GD
C-----LIQUID DYNAMICS
      IF(IC.GT.1)GOTO7
      L1=GD-DD
      L2=L1
      L=L1
      F1=FD
      F2=FD
      F=FD
      XF1=XFD
      XF2=XFD
      XF=XFD
      G=GD*(1.0+ZG)
      G1=G
      G2=G
      LL1=F+L
      LL2=LL1
      LL=LL1
      D1=DD
      D2=DD
      D=DD
      ZZL=ZL
7     CONTINUE
      F1=F1*BF+(1.-BF)*FD
      F2=F2*BF+(1.-BF)*F1
      F = F*BF+(1.-BF)*F2
      XF1=XF1*BF+(1.-BF)*XFD
      XF2=XF2*BF+(1.-BF)*XF1
      XF=XF*BF+(1.-BF)*XF2
      G1=G1*BG+(1.-BG)*(GD*(1.+ZG))
      G2=G2*BG+(1.-BG)*G1
```

```
        G = G*BG+(1.-BG)*G2
        D1=BD*D1+(1-BD)*DD
        D2=BD*D2+(1-BD)*D1
        D=BD*D+(1-BD)*D2
        L1=L1*BL+(1.-BL)*(G-DD)
        L2=L2+(ZL-ZZL)*L2
        ZZL=ZL
        L2=L2*BL+(1.-BL)*L1
        L = L*BL+(1.-BL)*L2
        LL1=LL1*BLL+(1.-BLL)*(F+L)
        LL2=LL2*BLL+(1.-BLL)*LL1
        LL=LL*BLL+(1.-BLL)*LL2
        B=LL-G
        R=L/G
        IF(B.LT.0)B=0
C-----TRIAL AND ERROR SEARCH FOR XD, CHECK IS MB AT FEED TRAY
        IPRINT=0
        XL=.05
        XH=.1
8       CONTINUE
        IFLAG=0
        EXL=ALOG(1./XL)
        EXH=ALOG(1./XH)
        WORK(1)=1.0E-8
        DO 500 IZ=1,40
        IZZ=IZ
        EXB=ZEROUT(IFLAG,EXL,EXH,EX,WORK)
        XB=EXP(-EXB)
        MF=F*XF
        MB=B*XB
        MD=MF-MB
        IF(MD.LT.0)MD=0
        XD=MD/D
        YSS(1)=XD
C-----RECTIFYING SECTION
        DO100 I=1,NF-1
        XSS(I)=YSS(I)/(RV*(1-YSS(I))+YSS(I))
        IF(XSS(I).GT.1)XSS(I)=1.0
        YSS(I+1)=(L/G)*XSS(I)+(D/G)*XD
        IF(YSS(I+1).GT.1)YSS(I+1)=1.0
100     CONTINUE
C-----MATERIAL BALANCE
160     CONTINUE
C-----STRIPPING SECTION
        XSS(NB)=XB
        DO200 J=1,(NB-NF)
        I=NB-J
        YSS(I+1)=RV*XSS(I+1)/(1.+XSS(I+1)*(RV-1.))
        IF(YSS(I+1).GT.1)YSS(I+1)=1.0
        XSS(I)=(G/LL)*YSS(I+1)+(B/LL)*XB
        IF(XSS(I).GT.1)XSS(I)=1.0
200     CONTINUE
```

```
      IF(IFLAG.EQ.1)GOTO550
      IF((IFLAG.LT.0).AND.(IPRINT.LT.10))GOTO540
      IF(IFLAG.LT.0)GOTO550
C-----CHECK EQUIL CONDITIONS ON FEED TRAY
      YNF=RV*XSS(NF)/(1.+XSS(NF)*(RV-1.))
      EX=YNF-YSS(NF)
      XDD=XD
      XBD=XB
C     WRITE(5,DEBUG)
      XDD=XD
      SBD=XB
      IF(IPRINT.EQ.0)GOTO500
500   CONTINUE
      GOTO550
540   CONTINUE
C     WRITE(5,DEBUG)
      IPRINT=IPRINT+1
      XL=XL+.01
      XH=XH+.01
      GOTO8
550   CONTINUE
      DO 600 I=1,NB
      IF(IC.GT.1)GOTO560
      X(I)=XSS(I)
      Y(I)=YSS(I)
      GOTO600
560   CONTINUE
      IF(XSS(I).GT.1.0)XSS(I)=1.0
      IF(XSS(I).LT.0.)XSS(I)=0.0
      IF(YSS(I).GT.1.0)YSS(I)=1.0
      IF(YSS(I).LT.0)YSS(I)=0.0
      IF(I.LT.NF)BXY=BXR
      IF(I.GE.NF)BXY=BXS
      X(I)=BXY*X(I)+(1-BXY)*XSS(I)
      Y(I)=BXY*Y(I)+(1-BXY)*YSS(I)
600   CONTINUE
C-----TEMPERATURE PROFILE
      DO 300 I=1,NB
      TSS(I)=A1*X(I)+A2*EXP(X(I))+A3*EXP(-X(I))+A0
300   CONTINUE
      DO 700 I=1,NB
      IF(IC.GT.1)GOTO650
      T(I)=TSS(I)
      GOTO700
650   T(I)=BT*T(I)+(1-BT)*TSS(I)
700   CONTINUE
      XD=Y(1)
      XB=X(NB)
      XBD=XB
      XDD=XD
      RETURN
      END
```

Listing of a program used to call subroutine PROC, the working routine in SS2.FOR.

```
      COMMON /ITES/ ITEST
      DIMENSION P(4)
      ITEST=2
      WRITE(5,100)
100   FORMAT(' INPUT AK1D,AK2D,AK1B,AK2B')
      READ(5,*) (P(I), I=1,4)
      CALL PROC(P,COST)
      WRITE(6,1000) COST
1000  FORMAT('   COST FOR THIS SYSTEM:   ',F9.5)
      STOP
      END
```

Listing of a program used to call PATERN, in this case to optimize the controller tuning parameters.

```
      COMMON /ITES/ ITEST
      DIMENSION P(4),STEP(4)
      ITEST=0
      P(1)=0.0
      P(2)=0.
      P(3)=0.0
      P(4)=0.0
      STEP(1)=1.
      STEP(2)=.1
      STEP(3)=100.
      STEP(4)=10.
      CALL PATERN(4,P,STEP,3,1,COST)
      ITEST=1
      CALL PROC(P,COST)
      STOP
      END
C-------------------
      SUBROUTINE BOUNDS(P,IOUT)
      DIMENSION P(4)
      IOUT=0
      RETURN
      END
```

Listing of SS2.FOR, a typical working routine with a controller and steady-state p-canonical decoupler.

```
        SUBROUTINE PROC(P,COST)
C-----PLOT STUDY FOR THE DYNAMIC COLUMN SIMULATION
C     FOR THE MATERIAL BALANCE SCHEME  (REBOILER LEVEL
C     CONTROLLED BY THE REFLUX TO THE COLUMN)
        REAL LL,L,MF,MD,MB
        DIMENSION TIME(500),TXD(500),TXB(500),P(4),
     C    ACAD(500),ACAB(500),ADAD(500),ADAB(500)
        COMMON /PAR/NF,NB,RV,A0,A1,A2,A3
        COMMON/TAU/BL,BLL,BF,BG,BT,BD,BXS,BXR
        COMMON /XYSS/XSS(50),YSS(50),TSS(50)
        COMMON /XY/X(50),Y(50),T(50)
        COMMON /MBAL/L,LL,B,R,MF,MD,MB
        COMMON/ERR/IFLAG,EX
        COMMON /ITES/ ITEST
        AK1D=P(1)
        AK2D=P(2)
        AK1B=P(3)
        AK2B=P(4)
C-----N-OCTANE & N-PENTANE SYSTEM
10      CONTINUE
        RV=2.17
        A0=119.56
        A1=-61.31
        A2=16.136
        A3=-10.1
C-----FEED CONDITIONS
        XF=.5
        F=200.
        ZL=0
        ZG=0
C-----COLUMN CONFIGURATION
        NF=10
        NB=20
        H=0.1
        TAUL=5.
        TAULL=1.0
        TAUG=2.
        TAUF=8.0
        TAUT=.5
        TAUXS=0.5
        TAUXR=5.0
        TAUD=2.5
        BL=EXP(-H/TAUL)
        BLL=EXP(-H/TAULL)
        BG=EXP(-H/TAUG)
        BF=EXP(-H/TAUF)
        BT=EXP(-H/TAUT)
```

```
        BXS=EXP(-H/TAUXS)
        BXR=EXP(-H/TAUXR)
        BD=EXP(-H/TAUD)
C-----TEST CONDITIONS
        D=100.
        G=258.28
        XB=.05
        XD=.95
        TIME(1)=0
        TXD(1)=0.95
        TXB(1)=0.05
        WRITE(8,*) TIME(1),TXD(1),TXB(1),ACAD(1),ACAB(1),ADAD(1),ADAB(1)
        DO100 I=1,2000
        ICOU=ICOU+1
        IF(ICOU.EQ.10) ICOU=0
        IF(ICOU.NE.0) GO TO 22
        TIME(I/10)=I*H
22      CONTINUE
        IC=I
        IF(I.GT.1) XF=0.55
        CALL COLMD(F,D,G,ZL,ZG,XF,XD,XB,IC,IERR)
C------------CONTROLLER BEGIN
        IF(IC.GT.1) GO TO 20
        XX1D=0.0
        XX1B=0.0
        COST=0.0
        DO=D
        GO=G
        CAB=0.0
        CAD=0.0
        DAD=0.0
        DAB=0.0
20      CONTINUE
        XX2D=0.95-XD
        XX2B=0.05-XB
        AD=AK1D*(XX1D-XX2D)+AK2D*(-XX2D)
        AB=AK1B*(XX1B-XX2B)+AK2B*(-XX2B)
        CAB=CAB+AB
        CAD=CAD+AD
        CAD=0.0
        CAB=10.0
        IF(ICOU.NE.0) GO TO 23
        ACAD(I/10)=CAD
        ACAB(I/10)=CAB
23      CONTINUE
        XX1B=XX2B
        XX1D=XX2D
C--------------CONTROLLER END
C--------------DECOUPLER BEGIN
        AH11=1.
        AH12=0.168
```

```
        AH21=-3.63919
        AH22=1.
        DAD=AH11*CAD+AH12*CAB
        DAB=AH21*CAD+AH22*CAB
        D=DO+DAD
        G=GO+DAB
        IF(D.LT.0.) D=0.
        IF(D.GT.F) D=F
        IF(G.LT.0.) G=0.
        IF(G.GT.(20.*F)) G=20.*F
        DAD=D-DO
        DAB=G-GO
        IF(ICOU.NE.0) GO TO 24
        ADAD(I/10)=DAD
        ADAB(I/10)=DAB
24      CONTINUE
C-----------------DECOUPLER END
        COST=COST+ABS(0.95-XD)+ABS(0.05-XB)
        IF(ICOU.NE.0) GO TO 100
        TXD(I/10)=XD
        TXB(I/10)=XB
        WRITE(8,*) TIME(I/10),TXD(I/10),TXB(I/10),ACAD(I/10),ACAB(I/10),
     C     ADAD(I/10),ADAB(I/10)
100     CONTINUE
        COST=COST/10.
        IF(ITEST.GT.0) CALL PLTR(TIME,TXD,200)
        IF(ITEST.GT.0) CALL PLTR(TIME,TXB,200)
        IF(ITEST.GT.1) CALL PLTR(TIME,ACAD,200)
        IF(ITEST.GT.1) CALL PLTR(TIME,ACAB,200)
        IF(ITEST.GT.1) CALL PLTR(TIME,ADAD,200)
        IF(ITEST.GT.1) CALL PLTR(TIME,ADAB,200)
        RETURN
        END
```

Listing of the decoupling section which was inserted into SS2.FOR for the ideal p-canonical decoupler with first order lag derived elements.

```
C--------------DECOUPLER BEGIN
        UI1=CAB
        UI2=CAD
        UI3=UI2
        UI4=UI1
        XI3=.7856*UIM13-1.5381*UIM23+.7528*UIM33+1.9527*XIM13-.9531*XIM23
        XI4=.7856*UIM14-1.5381*UIM24+.7528*UIM34+1.9527*XIM14-.9531*XIM24
        XI1=.3585*UIM11-.7094*UIM21+.3509*UIM31+1.9527*XIM11-.953*XIM21
        XI2=-.4701*UIM12+.899*UIM22-.4298*UIM32+1.9527*XIM12-.9531*XIM22
        XIM23=XIM13
        XIM13=XI3
        XIM24=XIM14
        XIM14=XI4
        UIM33=UIM23
        UIM23=UIM13
        UIM13=UI3
        UIM34=UIM24
        UIM24=UIM14
        UIM14=UI4
        XIM21=XIM11
        XIM22=XIM12
        UIM31=UIM21
        UIM21=UIM11
        UIM32=UIM22
        UIM22=UIM12
        XIM11=XI1
        XIM12=XI2
        UIM11=UI1
        UIM12=UI2
        DAD=XI1+XI3
        DAB=XI2+XI4
        D=DO+DAD
        G=GO+DAB
        IF(D.LT.0.) D=0.
        IF(D.GT.F) D=F
        IF(G.LT.0.) G=0.
        IF(G.GT.(20.*F)) G=20.*F
        DAD=D-DO
        DAB=G-GO
        IF(ICOU.NE.0) GO TO 24
        ADAD(I/10)=DAD
        ADAB(I/10)=DAB
24      CONTINUE
C----------------DECOUPLER END
```

Listing of the decoupling section which was inserted into SS2.FOR for the simplified p-canonical decoupler with first order lag derived elements.

```
C--------------DECOUPLER BEGIN
        UI1=CAB
        UI2=CAD
        UI3=UI2
        UI4=UI1
        XI3=UI3
        XI4=UI4
        XI1=0.4469*UIM11-0.4413*UIM21+0.9668*XIM11
        XI2=-0.626*UIM12+0.5932*UIM22+0.991*XIM12
        XIM23=XIM13
        XIM13=XI3
        XIM24=XIM14
        XIM14=XI4
        UIM33=UIM23
        UIM23=UIM13
        UIM13=UI3
        UIM34=UIM24
        UIM24=UIM14
        UIM14=UI4
        XIM21=XIM11
        XIM22=XIM12
        UIM31=UIM21
        UIM21=UIM11
        UIM32=UIM22
        UIM22=UIM12
        XIM11=XI1
        XIM12=XI2
        UIM11=UI1
        UIM12=UI2
        DAD=XI1+XI3
        DAB=XI2+XI4
        D=DO+DAD
        G=GO+DAB
        IF(D.LT.0.) D=0.
        IF(D.GT.F) D=F
        IF(G.LT.0.) G=0.
        IF(G.GT.(20.*F)) G=20.*F
        DAD=D-DO
        DAB=G-GO
        IF(ICOU.NE.0) GO TO 24
        ADAD(I/10)=DAD
        ADAB(I/10)=DAB
24      CONTINUE
C----------------DECOUPLER END
```

Listing of the controller section used in SS2.FOR for the Ryskamp control strategy.

```
C------------CONTROLLER BEGIN
         IF(IC.GT.1) GO TO 20
         XX1D=0.0
         XX1B=0.0
         COST=0.0
         DO=D
         GO=G
         DOGO=DO/GO
         CAB=0.0
         CAD=0.0
20       CONTINUE
         XX2D=0.95-XD
         XX2B=0.05-XB
         AD=AK1D*(XX1D-XX2D)+AK2D*(-XX2D)
         AB=AK1B*(XX1B-XX2B)+AK2B*(-XX2B)
         CAB=CAB+AB
         CAD=CAD+AD
         DOG=DOGO+CAD
         G=GO+CAB
         D=DOG*G
         IF(D.LT.0.0) D=0.0
         IF(D.GT.F) D=F
         IF(G.LT.0.0) G=0.0
         XYZ=20.0*F
         IF(G.GT.XYZ) G=XYZ
         CAD=D/G-DOGO
         CAB=G-GO
         ACAD(I)=D-DO
         ACAB(I)=CAB
         XX1B=XX2B
         XX1D=XX2D
C--------------CONTROLLER END
```

Listing of the controller section used in SS2.FOR for Waltz's control strategy.

```
C------------CONTROLLER BEGIN
         IF(IC.GT.1) GO TO 20
         XX1D=0.0
         XX1B=0.0
         COST=0.0
         DO=D
         GO=G
         CAB=0.0
         CAD=0.0
20       CONTINUE
         XX2D=0.95-XD
         S=XD/(1.-XD)*(1.-XB)/XB
         XX2B=361.-S
         AD=AK1D*(XX1D-XX2D)+AK2D*(-XX2D)
         AB=AK1B*(XX1B-XX2B)+AK2B*(-XX2B)
         CAB=CAB+AB
         CAD=CAD+AD
         D=DO+CAD
         G=GO+CAB
         IF(D.LT.0.0) D=0.0
         IF(D.GT.F) D=F
         IF(G.LT.0.0) G=0.0
         XYZ=20.0*F
         IF(G.GT.XYZ) G=XYZ
         CAD=D-DO
         CAB=G-GO
         ACAD(I)=CAD
         ACAB(I)=CAB
         XX1B=XX2B
         XX1D=XX2D
C---------------CONTROLLER END
```

Listing of the controller section inserted into SS2.FOR for the SVD controller.

```
C------------CONTROLLER BEGIN
         IF(IC.GT.1) GO TO 20
         DO=D
         GO=G
         XXDP1=0.0
         XXBP1=0.0
         CADP=0.0
         CABP=0.0
         COST=0.0
20       CONTINUE
         XXD=XD-0.95
         XXB=XB-0.05
         XXDP=0.9987796*XXD+0.04938975*XXB
         XXBP=-0.04938975*XXD+0.9987796*XXB
         AD=AK1D*(XXDP1-XXDP)+AK2D*(-XXDP)
         AB=AK1B*(XXBP1-XXBP)+AK2B*(-XXBP)
         XXDP1=XXDP
         XXBP1=XXBP
         CADP=CADP+AD
         CABP=CABP+AB
         CAD=-0.8582418*CADP-0.5132456*CABP
         CAB=0.5132456*CADP-0.8582418*CABP
         D=DO+CAD
         G=GO+CAB
```

APPENDIX B

SAMPLE Z - TRANSFORM CALCULATION

To illustrate the difference equation coefficient calculation using z-transforms, the H_{11} element of the ideal matrix decoupler will be derived using first order lag models (see Table 4).

To find the difference equation coefficients the Laplace transform must first be multiplied by a zero-order hold, given by

$$\frac{1-e^{-s\Delta t}}{s}$$

then the z-transform taken. So, if this is done with the H_{11} element,

$$Z\left[\frac{1-e^{-s\Delta t}}{s}\ H_{11}\right]$$

the $(1-e^{-s\Delta t})$ term can be taken out as $(1-z^{-1})$ leaving

$$(1-z^{-1})\ Z\left[\frac{H_{11}}{s}\right]$$

According to equation 40, the H_{11} element of an ideal matrix decoupler looks like

$$H_{11} = \frac{G_{11}\ G_{22}}{(G_{11}\ G_{22} - G_{12}\ G_{21})}$$

The following is an expression for the first order lag process model:

$$G = \begin{bmatrix} \frac{-0.005454}{1+8.038s} & \frac{0.000917}{1+2.96s} \\ \frac{-0.003335}{1+11.07s} & \frac{-0.000916}{1+1.82s} \end{bmatrix}$$

First, examining the denominator:

$$G_{11}\,G_{22} - G_{12}\,G_{21} = \frac{(0.005454)(0.000916)}{(1+8.038s)(1+1.82s)} + \frac{(0.003335)(0.000917)}{(1+11.07s)(1+2.96s)}$$

Finding a common denominator,

$$\frac{(0.005454)(0.000916)(1+11.07s)(1+2.96s) + (0.003335)(0.000917)(1+8.038s)(1+1.82s)}{(1+8.038s)(1+1.82s)(1+11.07s)(1+2.96s)}$$

Multiplying the numerator out, and adding common terms,

$$= \frac{8.054\cdot10^{-6} + 1.002\cdot10^{-4}s + 2.084\cdot10^{-4}s^2}{(1+8.038s)(1+1.82s)(1+11.07s)(1+2.96s)}$$

Factoring the numerator,

$$= \frac{8.054\cdot10^{-6}\,(1+9.804s)(1+2.64s)}{(1+8.038s)(1+1.82s)(1+11.07s)(1+2.96s)}$$

Now,

$$H_{11} = \frac{G_{11}\,G_{22}}{G_{11}\,G_{22} - G_{12}\,G_{21}}$$

$$= \frac{4.996\cdot10^{-6}}{(1+8.038s)(1+1.82s)} \quad \frac{(1+8.038s)(1+1.82s)(1+11.07s)(1+2.96s)}{8.054\cdot10^{-6}\,(1+9.804s)(1+2.64s)}$$

$$= 0.6205\,\frac{(1+11.07s)(1+2.96s)}{(1+9.804s)(1+2.64s)}$$

For now, take the constant term (0.6205) out. Divide by s and perform partial fraction expansion.

$$\frac{H_{11}}{s} = \frac{(1+11.07s)(1+2.96s)}{s(1+9.804s)(1+2.64s)} = \frac{A}{s} + \frac{B}{(1+9.804s)} + \frac{C}{(1+2.64s)}$$

To solve for A, multiply through by s, and set s=0.

$$A = \frac{(1)(1)}{(1)(1)} - 0 - 0 = 1$$

To solve for B, multiply through by (1+9.804s) and set s = -1/9.804.

$$B = \frac{-9.804\ (1-11.07/9.804)(1-2.96/9.804)}{(1-2.64/9.804)}$$

$$= 1.2095$$

To solve for C, multiply through by (1+2.64s) and set s = -1/2.64.

$$C = \frac{-2.64\ (1-11.07/2.64)(1-2.96/2.64)}{(1-9.804/2.64)}$$

$$= 0.3765$$

So, putting the constant term (0.6205) back in,

$$\frac{H_{11}}{s} = 0.6205\left[\frac{1}{s} + \frac{1.2095}{(1+9.804s)} + \frac{0.3765}{(1+2.64s)}\right]$$

From a table of z-transform pairs,

$$Z\left[\frac{1}{s}\right] = \frac{1}{1-z^{-1}} \quad \text{and} \quad Z\left[\frac{1}{s+a}\right] = \frac{1}{1-e^{-a\Delta t}z^{-1}}$$

Using the principle that the transform of a sum is the sum of the transforms,

$$(1-z^{-1})\ Z\left[\frac{H_{11}}{s}\right] = (1-z^{-1})\ 0.6205\left[\frac{1}{1-z^{-1}} + \frac{0.1234}{1-e^{-0.0102}z^{-1}} + \frac{0.1426}{1-e^{-0.03788}z^{-1}}\right]$$

After much algebraic manipulation, the final result is

$$= \frac{0.7856 - 1.5381z^{-1} + 0.7528z^{-2}}{1-1.9527z^{-1} + 0.9531z^{-2}}$$

This, then, is an expression for $\frac{x(z)}{u(z)}$. Multiplying through,

$$x(z) - 1.9527z^{-1}x(z) + 0.9531z^{-2}x(z) =$$
$$0.7856u(z) - 1.5381z^{-1}u(z) + 0.7528z^{-2}u(z)$$

Which, upon transforming to a discrete time domain, looks like

$$x_i - 1.9527x_{i-1} + 0.9531x_{i-2} = 0.7856u_i - 1.5381u_{i-1} + 0.7528u_{i-2}$$

Solving for x_i,

$$x_i = 0.7856u_i - 1.5381u_{i-1} + 0.7528u_{i-2} + 1.9527x_{i-1} - 0.9531x_{i-2}$$

which is the required difference equation.

VITA

Joe Mark Keeton was born in Paducah, Kentucky. He attended elementary schools in Oak Ridge, Tennessee, San Jose, California, and Chattanooga, Tennessee. He was graduated from Naperville Central High School in Naperville, Illinois, near Chicago. He received a Bachelor of Science degree in Chemical Engineering from The University of Tennessee in 1979, and a Master's degree in 1981.